



Deliverable D2.5

DELIVERABLE D2.5
REPORT ON
END-TO-END SYSTEM INTEGRATION

29TH NOVEMBER 2012

Editor: David Gómez-Barquero

iTEAM, Polytechnic University of Valencia, Spain

EXECUTIVE SUMMARY

In ENGINES work package two (WP2), individual system architecture components were studied, and the results from these studies have been forwarded to standardization work (DVB-T2 Lite, DVB-NGH). The outcome of WP2 work is collected in five deliverables. Deliverable 2.1 focuses on system architectural work performed by ENGINES partners. Deliverable 2.2 deals with DVB-NGH receiver implementation related issues. Devised advanced component techniques for DVB-NGH are presented in deliverable 2.3. Additionally there is work on overall architectures, including issues not covered by direct standardization that are novel access technologies (deliverable 2.4) and end-to-end system integration (deliverable 2.5).

This Deliverable aims to show the main advances achieved within the ENGINES project related to the upper layers above the physical layer that have a direct impact on the end-to-end performance.

First of all, DVB-NGH Task Force - System and Upper Layers (TF-SUL) main outcomes have been explained. Regarding this, it should be noted the Future Extension Frame (FEF) Bundling which sets a structure to include DVB-NGH services within DVB-T2 FEFs. In addition, Transport Stream (TS) and Internet Protocol (IP) profiles have been optimized according to their specific features, including OMA-BCAST to facilitate the interoperability with cellular networks. RoHC methods have been developed in order to reduce overheads introduced in the IP Profile.

On the other hand, SVC analysis has been developed for DVB-T2 and DVB-NGH. In DVB-T2 have been introduced methods to take advantage of Multiple PLP (MPLP) configuration to improve the SVC performance and in DVB-NGH has been shown the more recent researches in terms of MPLP encapsulation, synchronization and signalling.

Finally, an Upper Layer- Forward Error Correction (UL-FEC) research has been performed both for DVB-T2 and DVB-NGH. The studies have been focused on Expanding Window Fountain (EWF) Coded Scalable Video Broadcasting, on Receiver-Controlled Parallel Fountain Codes (RCPF) and a Fading Margin Reduction due to Inter-Burst Upper Layer FEC in Terrestrial Mobile Broadcast.

TABLE OF CONTENTS

1	DVB-NGH Upper Layers	5
1.1	Overview SUL	5
1.2	Frame Building in DVB-NGH	7
1.3	Transport Stream (TS) Profile	13
1.4	Internet Protocol (IP) Profile	20
1.5	Robust Header Compression (ROHC)	25
1.6	L1 Signalling	33
2	Scalable Video Coding in DVB-T2 and DVB-NGH	43
2.1	SVC in Mobile Broadcasting DVB Systems	43
2.2	SVC Delivery in DVB-T2	46
2.3	SVC Delivery in DVB-NGH	56
3	Upper Layer FEC in DVB-T2 and DVB-NGH	60
3.1	Expanding Window Fountain Coded Scalable Video Broadcasting	60
3.2	Receiver-Controlled Parallel Fountain Codes	65
3.3	Fading Margin Reduction due to Inter-Burst Upper Layer FEC in Terrestrial Mobile Broadcast Systems	69
4	References	82

LIST OF CONTRIBUTORS

- **Teracom**
Erik Stare

- **iTEAM, Polytechnic University of Valencia**
David Gómez-Barquero, Jordi Puig, Carlos Romero, Jose Llorca, and David Vargas

- **Åbo Akademi**
Kristian Nybom

- **Nokia**
Jani Vare, Lukasz Kondrad

- **Integrasys**
José Manuel Sanchez

1 DVB-NGH UPPER LAYERS

1.1 Overview SUL

DVB-NGH (Digital Video Broadcasting – Next Generation Handheld) is a transmission system for broadcasting multimedia contents to handheld devices, which allows for user interaction via the return channel of mobile broadband communication systems. The inter-operation between DVB-NGH and mobile broadband networks to create an effective interactive user experience requires a fully end-to-end IP (Internet Protocol) system, such that it becomes possible to deliver the same audio/visual content over the two networks in a bearer agnostic way. Therefore, DVB-NGH includes full support of an IP transport layer, in addition to the most common transport protocol used in broadcast systems: MPEG-2 TS (Transport Stream). DVB-NGH supports two independent transport protocol profiles, one for TS and another one for IP, each with a dedicated protocol stack. The profiles have been designed as mutually transparent in order to improve bandwidth utilization. It should be noted that this approach is possible in DVB-NGH thanks to a physical layer packet unit, known as base band frame (BB frame), which is independent of the transport layer (i.e. TS or IP). This is a major difference compared to the first generation mobile broadcasting DVB standards DVB-H (Handheld) and DVB-SH (Satellite to Handheld), where the physical layer unit in both is MPEG-2 TS packets. Hence, to transmit IP over DVB-H and DVB-SH it is necessary to introduce an additional encapsulation protocol known as MPE (Multi Protocol Encapsulation). However in DVB-NGH, this is no longer needed, and IP can be delivered directly over a generic encapsulation protocol known as GSE (Generic Stream Encapsulation), reducing the packet encapsulation overhead compared to MPE over TS by up to 70%.

Currently the only available upper layer solution for the IP profile of DVB-NGH is based on OMA-BCAST (Open Mobile Alliance Mobile Broadcast Services Enabler Suite). However, it should be noted that the specification allows also possibility to use any other upper layer solution, which may be defined in the future. OMA BCAST is an open global specification for mobile TV and on-demand video services which can be adapted to any IP-based mobile delivery technology. OMA BCAST specifies a variety of features including: content delivery protocols for streaming and file download services, electronic service guide for service discovery, service and content purchase and protection, terminal and service provisioning (e.g. firmware updates), interactivity, notifications, etc, as shown in Figure 1.

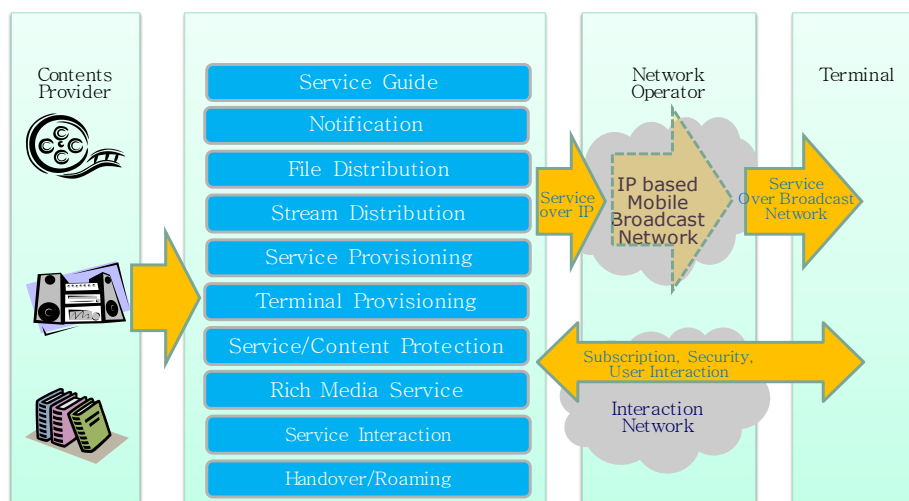


Figure 1: OMA BCAST overview: end-to-end hybrid cellular and broadcasting system.

OMA BCAST is thus an interworking platform that enables the convergence of services from broadcast and cellular domains, combining the strengths of broadcast networks to efficiently deliver very popular content with the personalization, interaction and billing features of cellular networks. In this sense, the mobile broadcasting network is a complement of the cellular system. It should be pointed out that there is no convergence in networks, since both broadcasting and cellular networks are used separately and

independently. Convergence is realized in services, platforms and multi-mode terminals which support both radio access technologies. OMA-BCAST specifies separate set of adaptation specifications for different physical layer bearers, such as 3GGP, DVB-H and, now DVB-NGH. The set of specifications consist of OMA-BCAST specification and the Adaptation specification(s), which are typically developed jointly with the standardization organization, which develops the specifications for the transmission bearer.

Both TS and IP profiles in DVB-NGH have been designed with the commercial requirement of minimizing the overall signaling overhead and increasing the bandwidth efficiency [1]. Also the latency in the service reception and hence the end user experience is emphasized in the commercial requirements. In order to minimize the redundancy and latency on the signaling, and hence also the complexity and signaling overhead, the OMA-BCAST adaptation for DVB-NGH has taken a radical approach to split the majority of the signaling between physical layer and on the top of IP, more specifically for the latter inside the OMA-BCAST SG structures. Only minimal signaling is defined at the link layer (L2), for optimizing the receiver latency and power saving. One of most important conclusions of the study item performed prior to the development of DVB-NGH was that a significant data net throughput is today wasted in signaling overheads such as packet headers and metadata, and that the optimization of the signaling and packet encapsulation could yield to important throughput improvements without losing any functionality [2]. In DVB-NGH, two header compression mechanisms have been adopted for both TS and IP packets. For the TS profile, for PLPs that carry only one service component, the TS header can be reduced from three bytes to only one byte. For the IP profile, the unidirectional mode of the Robust Header Compression (ROCH) protocol [3] has been adopted alongside an external adaptation to allow for a more efficient compression without implication on the zapping time and latency. In addition to the new TS and IP packet header compression mechanisms, DVB-NGH has improved the physical layer signaling in terms of reduced signaling overhead.

The two transport protocol profiles of DVB-NGH have been also designed with the commercial requirement of transmitting layered video, such as Scalable Video Coding (SVC) [4], with multiple Physical Layer Pipes (PLPs). Layered video codecs allow for extracting different video representations from a single bit stream, where the different sub-streams are referred to as layers. SVC is the scalable video coding version of H.264/AVC (Advanced Video Coding). It provides efficient scalability on top of the high coding efficiency of H.264/AVC. SVC encodes the video information into a base layer, and one or several enhancement layers. The base layer constitutes the lowest quality, and it is a H.264/AVC compliant bit stream, which ensures backwards-compatibility with existing H.264/AVC receivers. Each additional enhancement layer improves the video quality in a certain dimension. SVC allows up to three different scalability dimensions: temporal, spatial, and quality scalability. SVC utilizes different temporal and inter-layer prediction methods for gaining coding efficiency while introducing dependencies between the different quality layers. Due to these dependencies, parts of the bit stream are more important than others. In particular, the enhancement layer cannot be decoded without the base layer due to missing references.

The combination of layered video codec such as SVC with multiple PLPs presents a great potential to achieve a very efficient and flexible provisioning of mobile TV services in DVB-NGH system [5]. By transmitting the SVC base layer using a heavily protected PLP and the enhancement layer in one PLP with moderate/high spectral efficiency, it is possible to cost-efficiently provide a reduced quality service with a very robust transmission, while providing a standard/high quality for users in good reception conditions.

The benefits of using SVC compared to simulcasting the same content with different video qualities in different PLPs with different robustness are twofold. First of all, SVC has reduced bandwidth requirements compared to simulcasting. Compared to single layer AVC coding, the SVC coding penalty for the enhancement layer can be as little as 10% [4]. Secondly, with SVC it is possible to provide a graceful degradation of the received service quality when suffering strong channel impairments with seamless switching between the different video qualities.

The DVB-T2 specification states that DVB-T2 receivers are only expected to decode one single data PLP at a time [6]. But they must be able to decode up to two PLPs simultaneously when receiving a single service: one data PLP and its associated common PLP, which is normally used to transmit the information shared by a group of data PLPs. This feature cannot be used to deliver SVC with multiple PLPs and differentiated protection in DVB-T2 because the behavior of the receivers when only one PLP is correctly received is not

specified [5]. In DVB-NGH, it is possible to receive up to four PLPs simultaneously [7]. Compared to DVB-T2, DVB-NGH has enhanced the handling of multiple PLPs belonging to the same service updating the receiver buffer model and the synchronization requirements, which determines the necessary time delays at the transmitter in order to avoid buffering overflow or underflow in the receivers, and defining a new signaling to provide mapping between service components and PLPs and the scheduling of the PLPs at the physical layer.

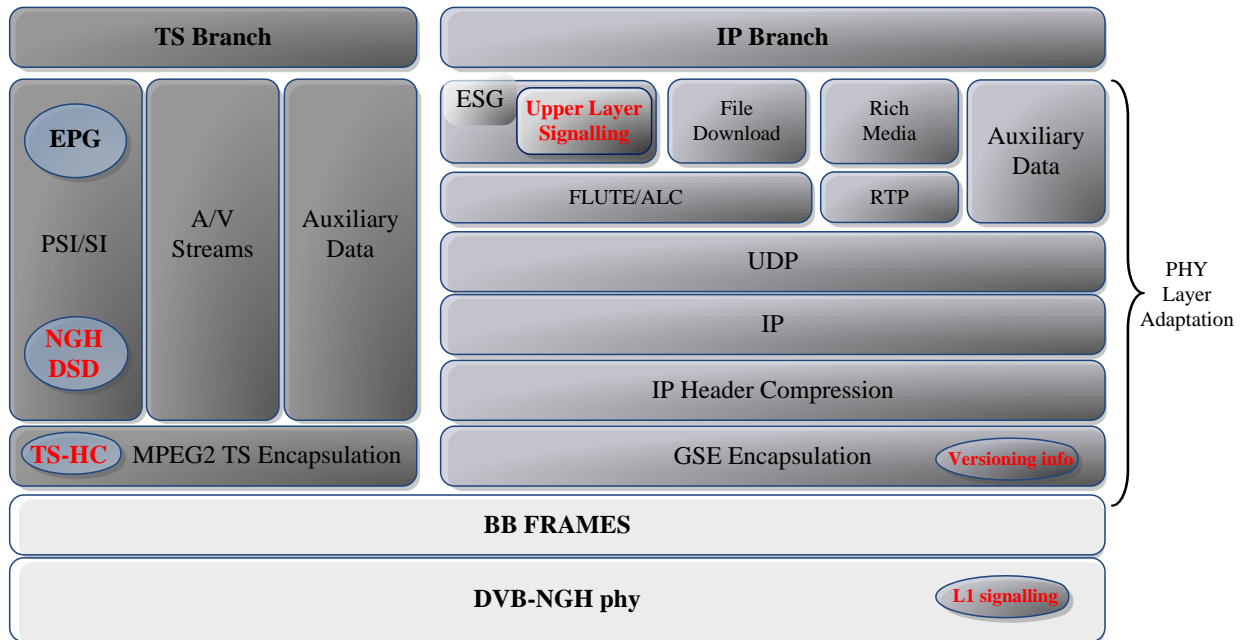


Figure 2: TS and IP profiles of DVB-NGH, including header compression mechanisms. Both profiles may co-exist in the same multiplex. The TS signaling and service discovery is based on the PSI/SI tables with a new NGH delivery system descriptor. The upper layers IP signaling is carried within the Electronic Service Guide (ESG) for better convergence with IP-based systems (cellular networks) and is compatible with OMA-BCAST.

1.2 Frame Building in DVB-NGH

1.2.1 Introduction

The widespread success of DVB-T2 has been a key stimulus for the development of DVB-NGH. A primary deployment scenario envisaged for DVB-NGH is in-band with DVB-T2, hence promoting the co-existence of DVB-NGH with DVB-T2 in the same RF channel, and allowing the reuse by DVB-NGH of the existing DVB-T2 network infrastructure. Along this line, the DVB Project has opted for an alignment of DVB-NGH with DVB-T2 (e.g. OFDM waveform, LDPC+BCH coding, Physical Layer Pipe (PLP) concept, etc). Furthermore, the DVB has set an important commercial requirement that it shall be possible to combine DVB-NGH and DVB-T2 signals in the same RF channel. Such a requirement can be fulfilled thanks to the Future Extension Frame (FEF) mechanism defined in DVB-T2.

Thanks to the FEF concept, DVB-T2 makes it possible to accommodate different technologies in the same multiplex in a time division manner. Each FEF starts with a preamble OFDM symbol known as P1 [8], which among other basic signaling information, it identifies the frame type. The positions of the FEFs in time and their duration are signaled in the physical Layer-1 (L1) signaling in the T2 frames. This way, DVB-T2 legacy receivers, not able to decode the FEFs, simply ignore the transmission during that time whilst still receiving the DVB-T2 signal. Terminals can switch-off their RF front-ends during the transmission of FEFs, saving power, like in a stand-alone DVB-T2 discontinuous transmission. Figure 3 illustrates the combined transmission of DVB-T2 with FEFs in the same multiplex. It should be pointed out that the FEF concept is relative to the system of focus, so that a system (e.g. DVB-NGH) sitting the FEF of DVB-T2 will see the T2 frames as their respective FEFs (e.g. of DVB-NGH).

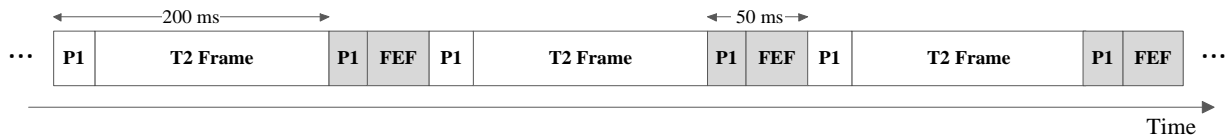


Figure 3: Co-existence of T2 frames and future extension frames (FEFs) in a single multiplex. Each T2 frame and FEF starts with a preamble P1 OFDM symbol which identifies the type of frame.

DVB-NGH is the third type of transmission specified in the FEF of DVB-T2. The first type of transmission is used for transmitter identification in Single Frequency Networks (SFN) [9], whilst the second type of transmission is used for the mobile profile of DVB-T2 known as T2-Lite. A typical deployment scenario for DVB-NGH or T2-Lite in a shared DVB-T2 multiplex is the one depicted in Figure 3: one FEF of reduced size (e.g., 50 ms duration) after every T2 frame with a considerably longer duration (e.g., 200 ms). This configuration devotes most of transmission time to DVB-T2 services, which are supposed to be the main services for the broadcast operator, but it allows introducing few mobile services (e.g., 4-6 multimedia services at 500 kbps, including video and audio). Moreover, since the FEFs are rather short, the zapping time of the DVB-T2 services is practically not affected by the introduction of any new technology in the FEF.

In the case of T2-Lite, there is a one-to-one relation between FEFs and T2-Lite frames. That is, each DVB-T2 FEF is a T2-Lite frame. DVB-NGH allows for a more flexible and efficient allocation between FEFs and NGH frames, and several FEFs can belong to the same NGH frame. DVB-NGH has defined a logical framing concept suited to the transmission of DVB-NGH signals in DVB-T2 FEFs. The logical framing concept has taken particular care to include Time-Frequency Slicing (TFS). TFS is a transmission technique adopted in DVB-T2 for transmitting one service across several RF channels with frequency hopping and time-slicing (i.e., discontinuous transmission). It can provide an important gain in coverage due to increased frequency diversity, and also a gain in capacity due to improved statistical multiplexing (StatMux) for variable bit rate (VBR) services. TFS also offers the possibility of finding spectrum more easily and in a more flexible way, since it is possible to combine different RF channels.

The new logical frame structure of DVB-NGH allows combining RF channels with different FEF sizes and transmission intervals, bandwidth, frequency band, transmission modes, etc., which can be seen as a generalization of TFS. Without the logical frame structure, it would be also required that the different DVB-T2 multiplexes are time synchronized to employ TFS in DVB-NGH. The logical frame structure also enables the possibility of hybrid satellite-terrestrial reception with a single demodulator (tuner).

Another important advantage of the logical frame structure of DVB-NGH is that there is no need to transmit all L1 signaling in each FEF, which reduces the signaling overhead compared to DVB-T2 and T2-Lite. In DVB-T2 (and T2-Lite), the physical layer L1 signaling is transmitted in every frame. In addition to the preamble P1 symbol, each frame has so-called preamble P2 symbols that carry the rest of the physical layer L1 signaling at the beginning of each frame. For very short FEFs, which may be the most representative use case for the initial transmission of DVB-NGH services (like the example shown in Figure 3 of 50 ms), the amount of physical layer signaling overhead could then become significant. The logical frame structure also avoids any limitation in the number of PLPs used in the system, as the L1 signaling capacity is no longer constrained to a fixed number of preamble P2 symbols.

1.2.2 NGH Frame Building

Frame building in DVB-NGH is performed in two stages: logical frame building and NGH frame building, as depicted in Figure 4. Logical frames are carried in NGH frames which represent the physical containers of the NGH system.

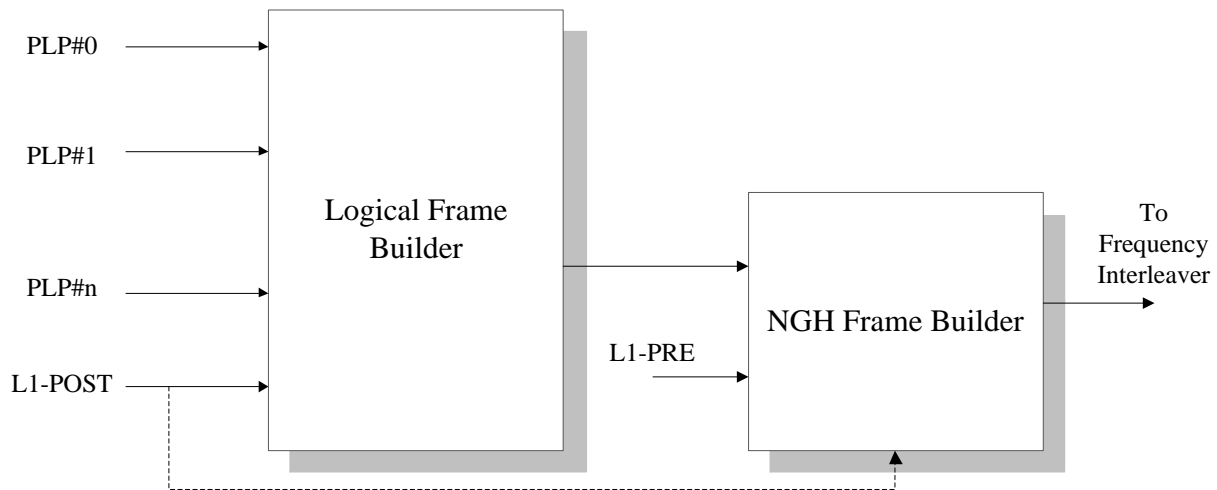


Figure 4: Two stages of DVB-NGH frame building.

NGH Frames

A (physical) NGH frame is composed of one preamble P1 OFDM symbol, which may be followed by one additional aP1 symbol for the MIMO and the hybrid profiles, one or more P2 symbols (the number of P2 symbols is given by the FFT size as in DVB-T2), and a configurable number of data symbols (the maximum frame size is as in DVB-T2 250 ms). According to the combination of the FFT size, guard interval and pilot pattern, the NGH frame may be closed by a frame closing symbol.

In addition to the aP1 symbol, the main difference compared to DVB-T2 is that not all L1 signaling information is necessarily transmitted in all NGH frames. The L1 signaling is divided into two fields, known as L1-pre and L1-post. The L1-pre is always transmitted in all NGH frames in the preamble P2 symbol(s). An NGH frame provides capacity for carrying the L1-pre signaling followed by the contents of the logical frames, which includes the L1-post signaling.

NGH Super-Frames

An NGH super-frame can carry NGH frames and also FEF parts. The maximum length of a super-frame without FEFs is 63.75 s as in DVB-T2, equivalent to 255 NGH frames of 250 ms. The only difference compared to DVB-T2 is that the maximum length of a FEF part in DVB-NGH is 1 s instead of 250 ms.

1.2.2.1 Logical Frame Structure in DVB-NGH

The logical frame structure of DVB-NGH defines how to carry NGH services into DVB-T2 FEFs. The FEFs can be transmitted in a single RF channel (time-domain bundling), or in multiple RF channels with TFS (time-frequency domain bundling). The logical frame structure provides a lot of flexibility to TFS, as it relaxes constraints such as having the same length for the FEFs in all RF channels, or synchronizing the different T2 multiplexes. Hence, a DVB-NGH network could be managed independently from the DVB-T2 network(s).

The logical frame structure defined in DVB-NGH is formed by the following elements:

- Logical frames.
- Logical super-frame.
- Logical channels.

- Logical channel group.

1.2.2.1.1 Logical Frames (LF)

A logical frame is a data container which also carries L1-post signaling. Each logical frame starts with L1-post signaling followed by the PLPs. The capacity of the logical frame is defined in terms of number of cells (constellation symbols), which comprises the L1-post cells, common and data PLP cells, auxiliary streams, and dummy cells.

The logical frame structure also avoids any limitation in the number of PLPs used in the system, since the L1-post signaling capacity is not constrained by a fixed number of preamble P2 symbols, as opposed to DVB-T2. The L1-post signaling must be transmitted after the L1-pre, but it does not have to follow immediately after. The L1-post may occupy any chunk of cells after L1-PRE in the NGH frame, see Figure 5.

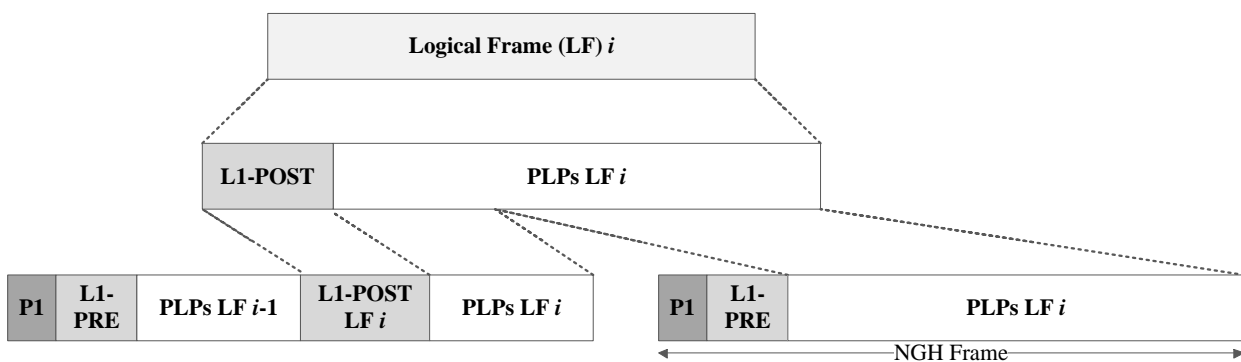


Figure 5: L1 signaling structure in DVB-NGH. The aP1 symbol is only transmitted in the MIMO and hybrid profiles.

1.2.2.1.2 Logical Super-Frames

Logical frames are grouped in logical super-frames. The maximum number of logical frames in a logical super-frame is 255. The number of logical frames in a logical super-frame must be chosen correctly in order that for every data PLP there is an integer number of interleaving frames in a logical super-frame.

1.2.2.1.3 Logical Channel (LC)

A logical channel is defined as a sequence of logical frames which are transmitted over 1 to N RF frequencies available in the NGH network. The logical NGH channels are introduced to account for the possibility that more than one FEF is simultaneously transmitted in different RF channels. Each logical channel is an independent entity with its own transmission mode (e.g. FFT, guard interval, pilot pattern, etc.) in which all the necessary signaling is being transmitted.

Depending how the logical frame is mapped into the NGH frames and the number of RF channels used, it is possible to distinguish four types of LCs. There may be different LCs in the same NGH network.

The basic LC Type A uses a single RF channel and the NGH frames contain cells from only one logical frame. That is, as in DVB-T2, there is a one-to-one relationship between logical frames and NGH frames, and the L1-post is transmitted in every NGH frame, see Figure 6.

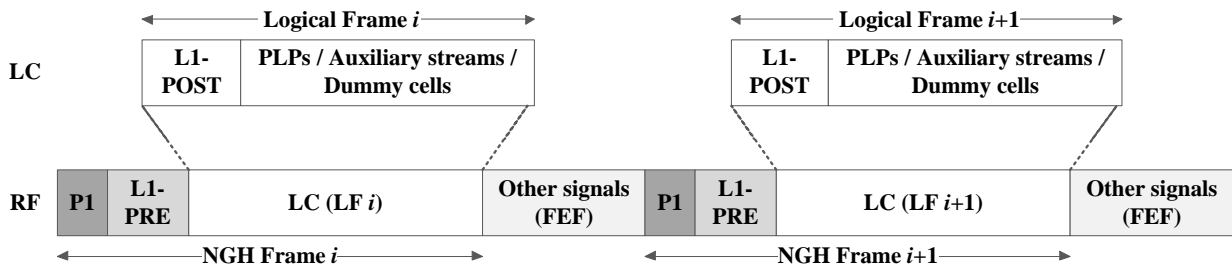


Figure 6: Logical channel Type A.

LC Type B uses a single RF channel but each logical frame is mapped to several NGH frames, see Figure 7. Thus, each NGH frame may contain cells from multiple logical frames. Compared to the reference LC Type A, this configuration has a reduced L1 signaling overhead since the L1-post is not transmitted in all NGH frames. It should be pointed out that LCs Type B do not degrade the zapping time provided that NGH frames are transmitted with a sufficient high rate.

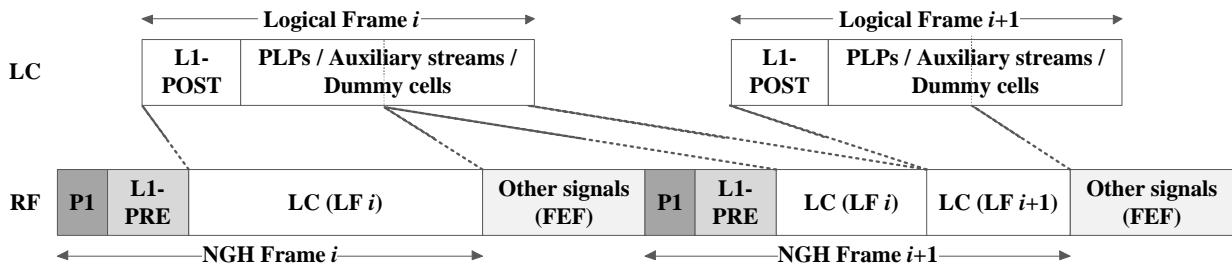


Figure 7: Logical channel Type B.

LCs of Type C and Type D employ multiple RF channels. An LC of Type C corresponds to the case where each logical frame is mapped onto multiple NGH frames which are transmitted over a set of RF channels, see Figure 8. Each NGH frame may carry cells from multiple logical frames. The NGH frames are separated from channel to channel in order to allow LC reception with a single tuner, and may be of different length.

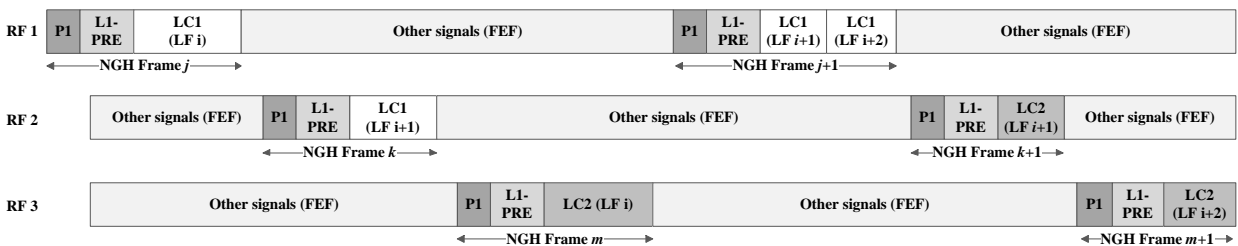


Figure 8: Logical channel Type C.

For LCs Type D, each logical frame is mapped one-to-one to multiple time-synchronized NGH frames of the same length which are transmitted in parallel over a set of RF channels (one NGH frame in each RF channel), see Figure 9. In this case, the different RF channels of the TFS multiplex shall be synchronized.

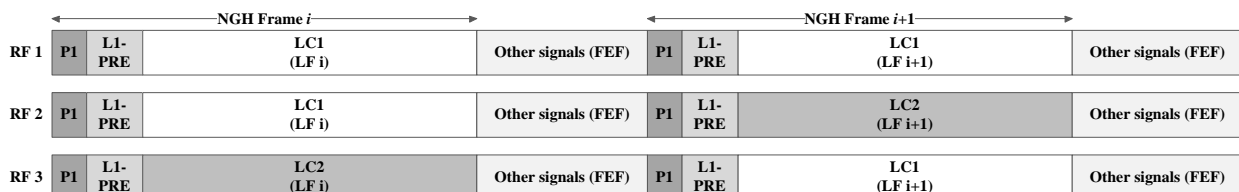


Figure 9: Logical channel type D.

Type C and Type D logical channels are also referred as intra-frame and inter-frame TFS, respectively. LC Type C with inter-frame TFS benefits of an improved frequency diversity and higher StatMux gain, with L1 overhead reduction thanks to the transmission of L1-POST in only one physical container (NGH frame) of the logical frame. This configuration is also very flexible, since it allows finding spectrum for DVB-NGH joining several independent T2 multiplexes without restriction on perfect alignment of all FEF parts available in the different T2 multiplexes. LC Type D with intra-frame TFS provides higher frequency diversity and higher StatMux gain than LC Type C, but it is not that flexible because the length of the FEFs has to be identical in all T2 multiplexes, and the multiplexes have to be time synchronized.

Table 1 compares the four types of LC in terms of overhead reduction, time and frequency diversity, statistical multiplexing gain and system flexibility. The reference configuration is LC Type A (without time-frequency bundling and without time-frequency slicing).

Table 1: Comparison between different types of logical channel.

Logical Channel	Description	Overhead Reduction	Time Diversity	Frequency Diversity	StatMux Gain	System Flexibility
Type A	No bundling no TFS	0	0	0	0	0
Type B	Time bundling no TFS	+	+	0	0	0
Type C	Time + Freq. bundling TFS inter-frame	++	+	+	+	+
Type D	Time + Freq. bundling TFS intra-frame	+	+	++	++	-

1.2.2.1.4 Logical Channel Group

Logical channels are grouped such that the NGH frames of one logical channel can be separated in time from the NGH frames that carry the information of another logical channel within the same group such that it shall be possible to receive all the logical channels of the same group with a single tuner. This concept was developed in order to allow parallel reception of terrestrial and satellite transmissions in hybrid Multi Frequency Networks (MFN) with a single demodulator. Figure 10 illustrates an example in which logical frames are mapped to the terrestrial and satellite transmissions.

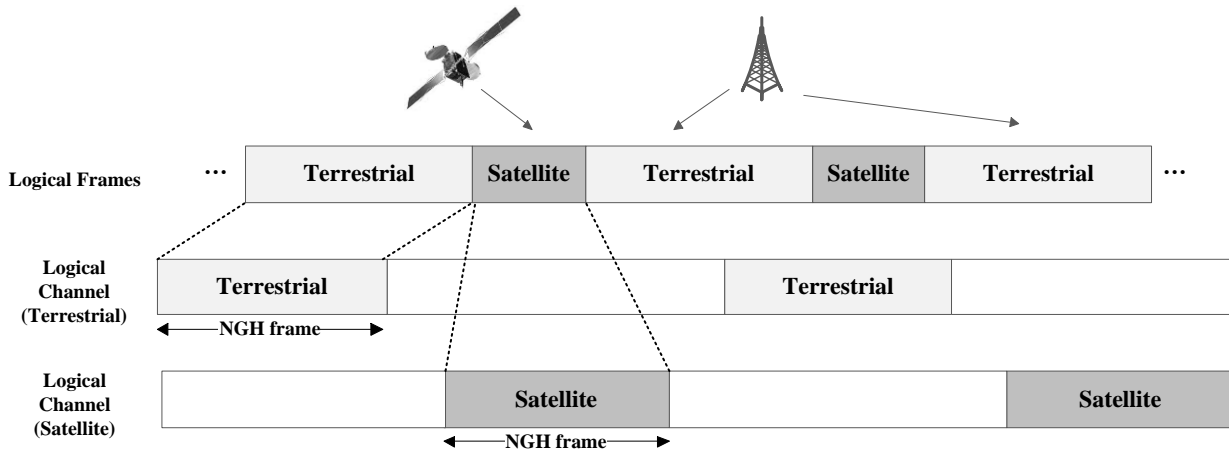


Figure 10: Logical frame mapping for hybrid terrestrial-satellite MFN networks. Parallel reception of both signals is possible for terminals with a single demodulator.

Figure 11 shows an example of two logical channels member of the same group, a first logical channel LC1 of type C over RF1 and RF2 and a second logical channel LC2 of type A over RF3.

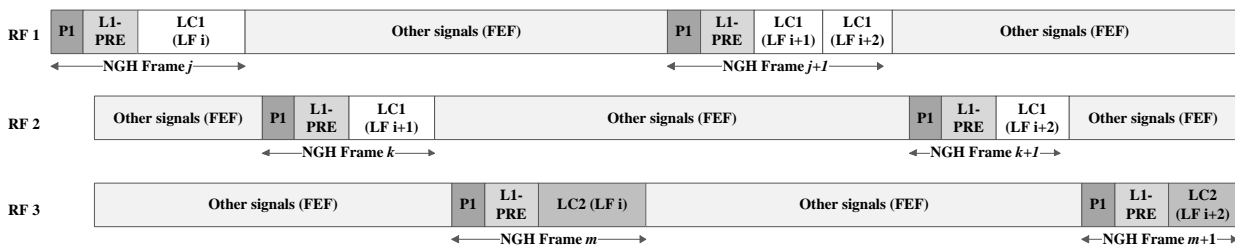


Figure 11: Logical channel groups with type C LC and type A LC transmitted in different RF channels.

1.2.3 Conclusions

DVB-NGH has defined a new logical frame structure in order to guarantee flexible and efficient exploitation of the FEFs of DVB-T2. In DVB-NGH, one logical frame can be transmitted across a number of physical frames or FEFs, with the possibility for the associated L1-POST signalling to appear in only one physical frame or FEF, yielding a significant overhead reduction especially in the context of multiple RF channels. The logical frame structure enables the combination of FEFs of different length, bandwidth, frequency band, etc., without tight restriction on perfect time alignment. Hence, it can be seen as a generalization of TFS known from DVB-T2, hence preserving the high frequency diversity and high statistical multiplexing gains achieved by TFS. This is in addition with the possibility to allow for TFS reception with one single tuner, enabling for example hybrid terrestrial-satellite reception with relatively low complexity receivers.

1.3 Transport Stream (TS) Profile

The transport stream profile of DVB-NGH is dedicated for the transmission of the TS multiplexes. The DVB-NGH TS profile is based on DVB-T2, and follows the same protocol stack structure, taking advantage of the methods to achieve an efficient transmission such as Null Packet Deletion (NPD). In addition, DVB-NGH includes novelties to increment the flexibility of the system and the efficiency, such as SVC delivery with multiple PLPs and TS header compression. In addition, an adaptation of the PSI/SI signaling has been performed by adding a new descriptor, the NGH delivery system descriptor, containing the new necessary information for DVB-NGH.

MPEG-2 imposes strict constant bit rate (CBR) requirements on a TS multiplex. However, a TS multiplex may contain a number of Variable Bit Rate (VBR) services with null TS packets that do not contain any useful data. Depending on the bit rate characteristic of the multiplexed services, it is possible that null packets may constitute a large percentage of the TS multiplex bitrate. On the other hand, statistical multiplexing algorithms can exploit the properties of the VBR video content by means of real-time analysis of the encoded content. This analysis allows the adaptation of the transmission to the set of services bit rates. Nevertheless, this improvement is not free. Statistical multiplexing requires a real-time analysis of the video content and processing to allocate appropriately the optimal amount of information of each service in each time interval. This processing complexity implies usually extra buffering in the transmitter, hence increasing the end-to-end delay.

In DVB-NGH, it is possible to transmit with different physical layer configuration by means of MPLPs. In this case, the services multiplexing needs to be performed by the scheduler at the physical layer in the stream adaptation, managing the cells number per PLP and allowing a most accurate mechanism to optimize the transmission. In any case, the benefits of statistical multiplexing are substantial in terms of bandwidth optimization allowing more services transmission per multiplex.

1.3.1 TS Protocol Stack Overview

The protocol stack of the TS profile keeps the same structure that the previous first generation of DVB standards, see Figure 12. The Elementary Streams (ES) containing audio and video information are encapsulated in Packetized Elementary Streams (PES) and at lower level to Transport Stream (TS) packets. Finally, this flow of TS packets undergoes both mode and stream adaptation to achieve BB frame flows, as described in the previous section.

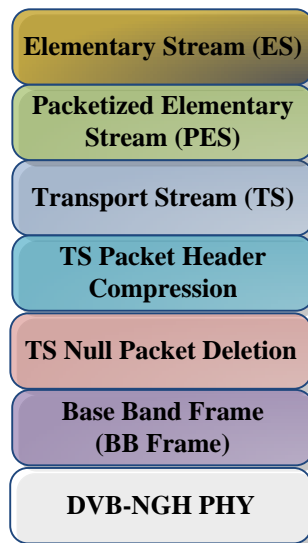


Figure 12: DVB-NGH TS profile protocol stack.

1.3.2 TS Null Packet Deletion

DVB-NGH adopts the TS null packet deletion mechanism of DVB-T2, which avoids the transmission over the air of null packets. The removal of null packets at the transmitter side is performed in a way that at the receiver side the removed null-packets can be re-inserted in the TS at their original positions, see Figure 13. NPD is optional, and when used, useful TS packets are transmitted, and null TS packets are removed. A Deleted Null Packets (DNP) counter of 1 byte is defined that is first reset and then incremented at each deleted null packet. This DNP counter is sent instead of the null packets allowing an overhead reduction.

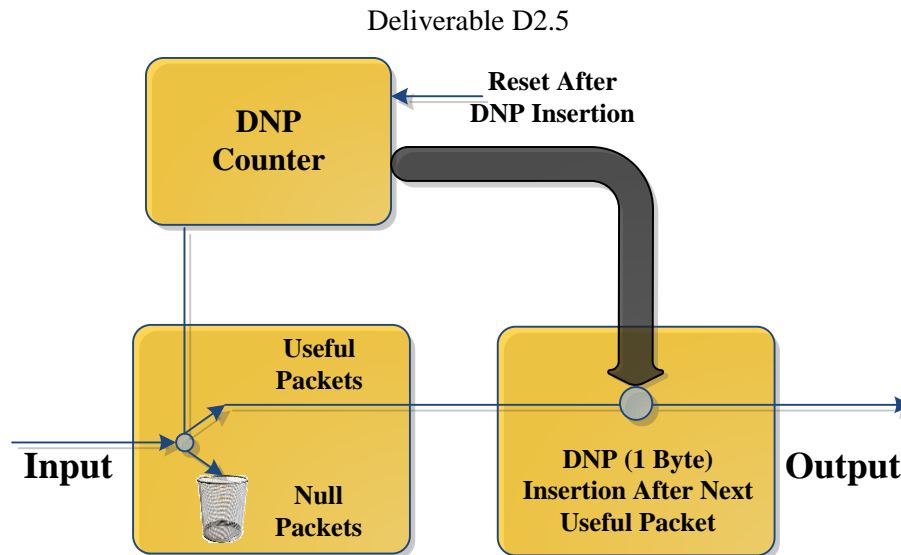


Figure 13: TS null-packet deletion process at the transmitter.

1.3.3 TS Packet Header Compression

TS Header Compression (TS-HC) is a new technique introduced in DVB-NGH that allows reducing the TS header signaling information for PLPs with only one Packet Identifier (PID), e.g. video. The TS/HC scheme assumes that the PID values can be transmitted by some other means such as L1 signaling or PSI/SI. TS packets that implement the compression have another structure of header that provides a more efficient transmission and, in addition, it is possible to perform TS decompression purely on L1 with negligible complexity. With this method it is possible to achieve overhead saving by about 1% within the overall system performance. However, it is not easy to manage contents with a dynamic PID where it is necessary to synchronize the changes with the PMT. To solve this complication, in DVB-NGH the PID value is transmitted in the BB header, and a new pointer (SYNCD-PID) is defined to indicate the TS packet where the PID changes. These new fields in the BB header, in combination with the new consistent signaling, represent an overhead saving of 4 bytes in the BB frame in comparison with DVB-T2, in addition to the TS header compression performed. With this solution, when a particular PLP uses TS-HC all the TS packets are compressed and have a constant length, and receivers can be correctly synchronized working with dynamic PID.

1.3.4 PSI/SI Signaling in TS profile

As in other previous TS-based DVB systems, the signaling of the upper layers within DVB-NGH TS profile is based on the PSI/SI tables. Traditionally, all network-related signaling is kept in the NIT, including in addition to network information everything related with the transmission characteristics. In a similar way, all PID mapping is done by the PMT. The system provides a demodulation mechanism at the receiver to output correct MPEG2-TS packets without first parsing PSI/SI tables.

The PSI/SI signaling consists of tables that are carried over transport streams. The main PSI/SI tables are: Network Information Table (NIT), Program Association Table (PAT), Program Map Table (PMT), Service Description Table (SDT), Event Information Table (EIT) and Time and Date Table (TDT). Each table, in turn, excluding PAT and TDT, carries a number of different descriptors that contain most of the actual information that is carried within the tables. The majority of the descriptors and PSI/SI tables are common for different DVB technologies. However, the *NGH_delivery_system_descriptor* is specific to the TS profile of NGH. This descriptor maps the services with the network information and PLPs, see Table 2.

Table 2: NGH delivery system descriptor.

Syntax	# of bits	Identifier
<pre> NGH_delivery_system_descriptor() { descriptor_tag descriptor_length descriptor_tag_extension ngh_system_id ngh_stream_id service_loop_length for (i=0;i<N,i++){ service_id component_loop_length for (j=0;j<N,j++){ component_tag plp_id anchor_flag SISO/MIMO reserved_for_future_use } } if (descriptor_length – service_loop_length > 5) { bandwidth reserved_future_use guard_interval transmission_mode other_frequency_flag tfs_flag common_clock_reference_id for (i=0;i<N,i++){ cell_id if (tfs_flag == 1){ frequency_loop_length for (j=0;j<N;j++){ centre_frequency } } else { centre_frequency } subcell_info_loop_length for (k=0;k<N;k++){ cell_id_extension transposer_frequency } } } } </pre>	<p>8</p> <p>8</p> <p>8</p> <p>16</p> <p>8</p> <p>8</p> <p>16</p> <p>8</p> <p>8</p> <p>8</p> <p>1</p> <p>2</p> <p>5</p> <p>4</p> <p>3</p> <p>4</p> <p>3</p> <p>1</p> <p>1</p> <p>4</p> <p>16</p> <p>8</p> <p>32</p> <p>32</p> <p>8</p> <p>8</p> <p>32</p>	<p>uimsbf</p> <p>uimsbf</p> <p>uimsbf</p> <p>uimsbf</p> <p>uimsbf</p> <p>uimsbf</p> <p>uimsbf</p> <p>uimsbf</p> <p>uimsbf</p> <p>uimsbf</p> <p>uimsbf</p> <p>uimsbf</p> <p>bslbf</p> <p>bslbf</p> <p>bslbf</p> <p>bslbf</p> <p>bslbf</p> <p>bslbf</p> <p>bslbf</p> <p>uimsbf</p> <p>uimsbf</p> <p>uimsbf</p> <p>uimsbf</p> <p>uimsbf</p> <p>uimsbf</p> <p>uimsbf</p> <p>uimsbf</p> <p>uimsbf</p> <p>uimsbf</p>

The descriptor follows the same philosophy adopted in DVB-T2, being used for one of the TS carried by a particular *network_id/ngh_system_id* combination. The other TSs of the same combination only carries the upper part in order to save overhead. With the same *network_id/ngh_system_id* combination it is possible to get a 1-to-1 mapping between *transport_stream_id* (16 bits) and *ngh_stream_id* (8 bits), the latter used in the L1 signaling. In addition, the PMT table also contains, as usual, the *service_id/component tag*, i.e. the PID for all service components. On the other hand, as opposed to DVB-T2, the MIMO/SISO field goes to the component loop because of the possibility of have different schemes per service component. Other fields in the lower part are assumed to be the same for a complete service.

Otherwise, it should be noted that there are two key differences in the receiver behavior for the TS profile of DVB-NGH, one in the initial scanning and the other one in the zapping case, as presented below.

1.3.4.1 Initial Scanning

Below is described the initial scanning procedure in the receiver.

- The receiver reads the configurable part of L1-post signaling (L1-config) and parses the *stream_id* loop. For each *stream_id* entry it will therefore see the collection of *plp_ids* carrying the TS (or other stream).
- Later, the receiver can demodulate the relevant PLPs and access the TS packets (or other packets) of each demodulated PLP.
- In the TS case the receiver can easily identify which TS packets are desired by checking the *stream_id* byte of the packets in the relevant PLPs.
- All packets having the same *stream_id* byte are merged and will together form a complete TS after replacement of *stream_id* with sync byte.
- When the common PLP is used, it is included in the merging. Packets in the common PLP do not use the *stream_id* feature (since the packets are merged into all TSs).
- The TS is output from the demodulator and parsed by the backend.
- Other TSs are output in the same way or via help from already parsed PSI/SI tables of so-far received TSs.

1.3.4.2 Zapping Case

Here is the receiver procedure in a zapping case.

- When a new service has been selected the receiver finds the *ts_id*, *service_id* and *component_tags* via the stored SDT.

- It then finds the access parameters of the relevant service components of the TS via the stored NIT, e.g. frequency, *stream_id* and relevant *plp_ids*.
- The receiver can then demodulate the relevant *plp_ids* and merge the TS packets having the right *stream_id* to form an output TS.
- The receiver then reads the PAT/PMT of the output TS and finds the PIDs for the selected service.

1.3.5 TS Signaling

Once the Layer 1 signaling has provided the required information to start the PLP decoding and has access to the TS flow, the receiver needs to identify which TS packets belong together to the desired TS by checking the *stream_id* byte (byte replacing the TS sync byte in transmission, see Figure 14) of the packets in the relevant PLPs. With this identification, all the packets with the same *stream_id* are merged and together form a complete TS stream after replacing the *stream_id* byte by the sync byte. It should be noted that this sync byte replacement is not performed in the common PLP as the packets here are merged into all TS flows.

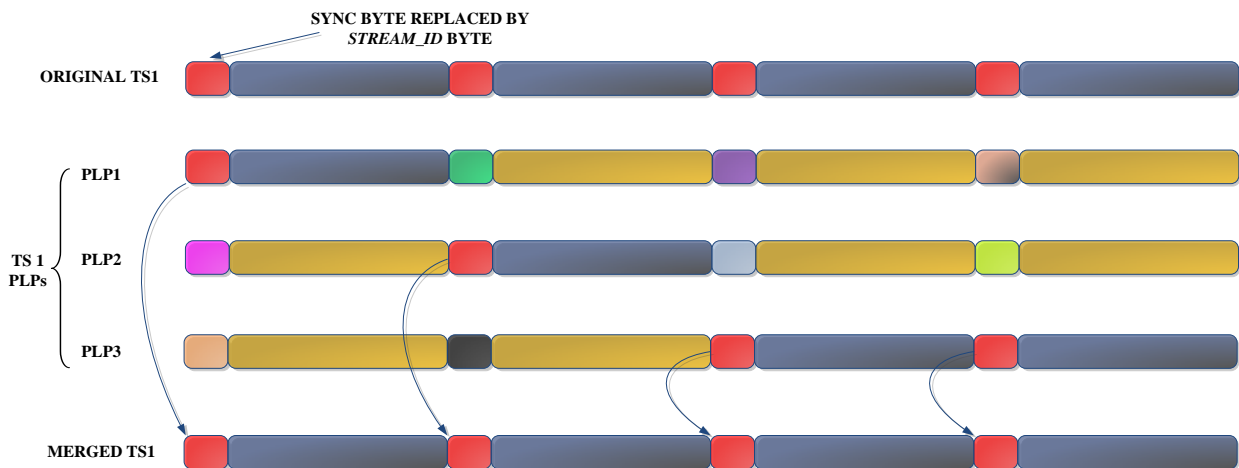


Figure 14: Stream_id byte utilization example for PLP splitting and merge.

1.3.6 SVC Delivery in the TS Profile

The synchronization between PLPs that carry the different layers of the same NGH service is a critical aspect. The synchronization depends on the chosen profile. Transport stream specifies a container format encapsulating packetized elementary streams (video, audio and other information), with error correction and stream synchronization features for maintaining transmission integrity when the signal is degraded. The synchronization mechanism used in TS profile is ISSY. The required signaling for SVC with multiple PLPs in DVB-NGH is based on the delivery system descriptor present in the NIT of the PSI/SI, where the different PLPs are signaled allowing in the receiver the corresponding selection, see Figure 15.

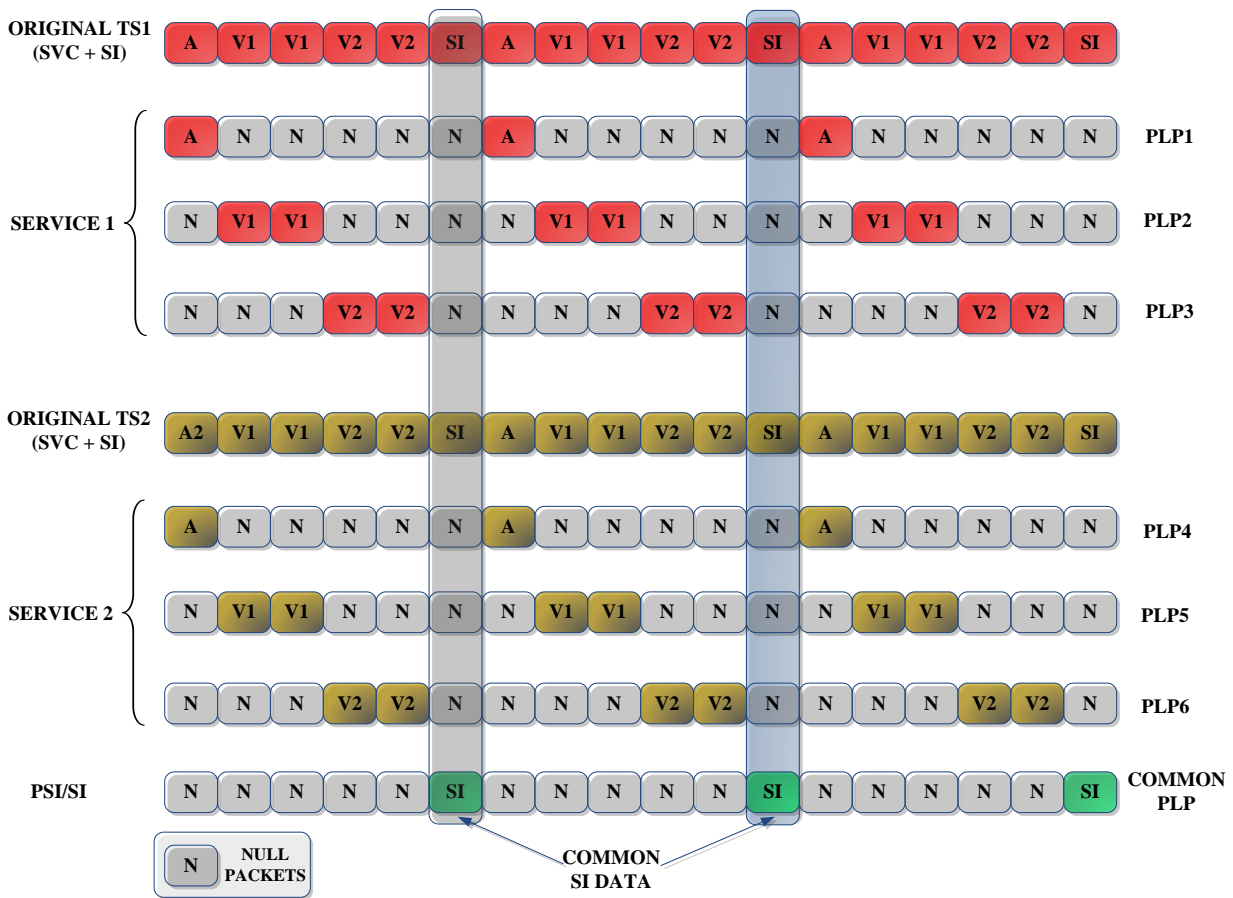


Figure 15: SVC delivery with multiple PLPs in the TS profile. The original TSs include audio (A), SVC video (base layer V1 and enhancement layer V2), and PSI/SI signaling information.

1.3.7 TS Profile Receiver Buffer Model

A typical DVB-NGH receiver should be composed of an RF input and followed by a number of physical layer stages in order to recover BB frames [10]. The data field bits of decoded BB frames belonging to a PLP are then converted to a canonical form, independent of the mode adaptation options in use. The resulting bits are written into a de-jitter buffer (DJB). Bits are read out from the buffer according to a read clock; removed sync bytes and deleted null packets are re-inserted at the output of the de-jitter buffer. When the receiver is decoding the data PLPs together with its associated common PLP, it shall be assumed that the time de-interleaver and de-jitter buffer are duplicated as shown in Figure 16. It should be noted that there is a single FEC HW chain, and that the TDI memory is shared among the data PLPs and the common PLP.

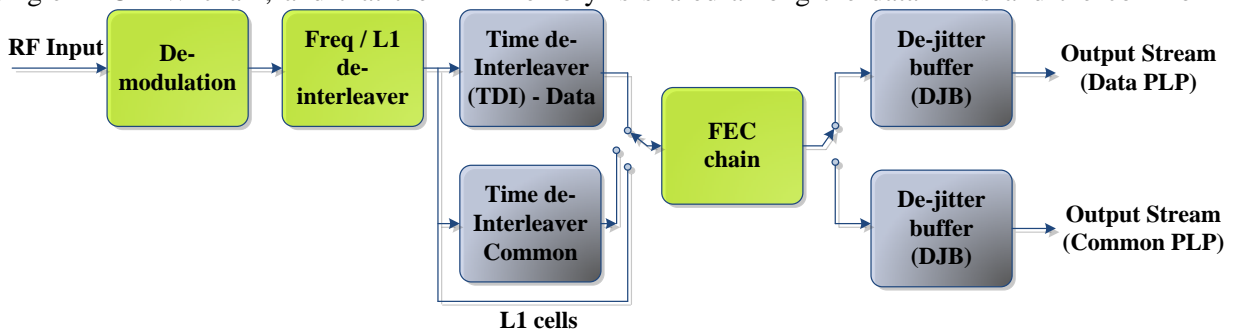


Figure 16: DVB-NGH receiver buffer model. DVB-NGH terminals are capable of simultaneously receiving up to four PLPs including the common PLP.

After this process, it is necessary to have a TS packet reconstruction mechanism in order to recover the original TS flow. Basically, this mechanism has to reverse partially the mode adaptation performed at the transmitter. This process includes sync bytes reinsertions, CRC-8 removals (if present) and DNP analysis in order to reinsert null packets deleted at the transmission side. All these processes make use of the synchronization mechanisms introduced by the gateway at the transmission side such as the SYNC-D, SYNC and UPL (to regenerate the user packets), the TTD (to set the initial occupancy of the DJB), the DNP (to reinsert the deleted null packets) and the ISCR (to calculate the output bit-rate and for fine adjustment of the relative timing of data and common PLPs).

1.4 Internet Protocol (IP) Profile

The IP profile of DVB-NGH is dedicated for the transmission of IP data flows. IP protocols, as part of the so-called Internet protocol suite, are designed to ensure reliable interchange of data over a communication channel with multiple hops, requiring routing. DVB-NGH is designed to deliver a wide range of multimedia services over its IP profile in a bearer agnostic way, so that these services can be made accessible through mobile cellular networks.

DVB-T2 is not optimized for the transmission of IP content delivery especially that it lacks a corresponding signaling to deliver properly the information. In addition, the amount of overhead present in DVB-T2 IP encapsulation chain is significantly high and not effective for consideration in DVB-NGH specification. In DVB-T2, the IP profile uses several protocols that are not specifically designed for broadcasting so they introduce big amounts of overhead through the added headers. In DVB-NGH, the bandwidth usage has been improved by means of an overhead reduction module based on the ROHC specification [3], which allows reducing the overhead connected with RTP, UDP and IP headers.

1.4.1 Protocol Stack Overview

In the IP profile of DVB-NGH, see Figure 17, the Service Guide (SG) together with the upper layer signaling is carried on the top. On the same level with the SG, audio and video streams and files are provided as contents. FLUTE/ALC is used for the encapsulation of the SG and files, while RTP/RTSP is used for the delivery of audio and video streams on the top of User Datagram Protocol (UDP). Below UDP, there is IP, which can be compressed by using ROHC, which follows after the IP. Next, GSE is used as encapsulation protocol for ROHC and/or IP streams. The LLC signaling element inside the GSE carries also the versioning information of the upper layer signaling. The BB frames are next used for presenting the GSE streams into frames, which are then encoded into the DVB-NGH physical layer as NGH-frames. The DVB-NGH physical layer contains also the L1 signaling.

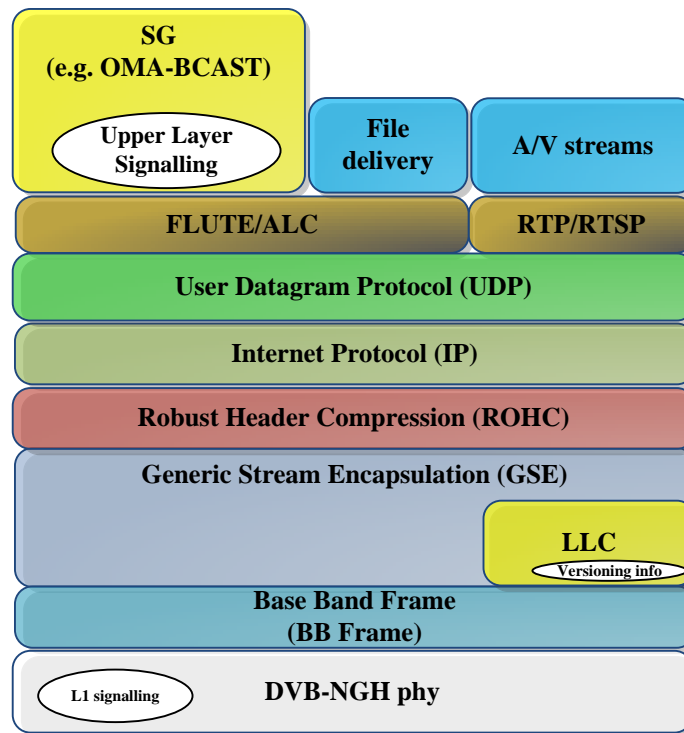


Figure 17: DVB-NGH IP profile protocol stack, where the signaling elements are marked as ellipsoids.

1.4.2 ROHC

In DVB-NGH IP profile the useful data is encapsulated over several protocols such as RTP, UDP, or IP. All these protocols were not designed for broadcasting contents delivery as they include a number of header information that is not relevant for the broadcasting use case. In addition, most of these headers' fields have a static behavior or change in a more or less predictable way. A method to optimize the transmission of headers over DVB-NGH was deemed necessary in order to improve the transmission efficiency. DVB-NGH has thus considered methods such as RObust Header Compression for unidirectional transmission (ROHC-U). ROHC aims to provide a RTP/UDP/IP header compression that allows overhead reductions about 1% of the total transmission capacity.

Basically, ROHC algorithms use the inter-dependencies between packets to determine a correct static and dynamic context on the receiver side. However, standard ROHC algorithms introduce undesirable effects in terms of zapping delay and error propagation due the inter-dependency utilization. To solve that, DVB-NGH adds an adaptation module to the conventional ROHC-U standard module in order to reduce or avoid the mentioned problems, forming the Overhead Reduction Module (ORM), see Figure 18.

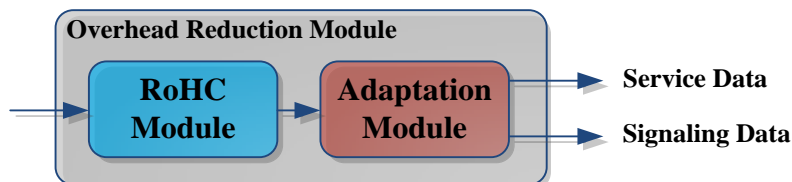


Figure 18: IP overhead reduction module in DVB-NGH.

With this structure, the ROHC module of the ORM is responsible of the IP flow overhead reduction, whereas the Adaptation Module is in charge of mitigating the effects of zapping delay and error propagation. Thanks to this scheme, backwards compatibility with the standalone ROHC framework is guaranteed, whilst minimizing the impact on zapping delay and error propagation.

The way that ROHC provides compression is an algorithm based on state machines in transmission and reception that establish different packet type deliveries depending on the context, see Figure 19. The state machine determines if it is necessary to send all the information (static and dynamic) or simply a set of modified fields (only dynamic information).

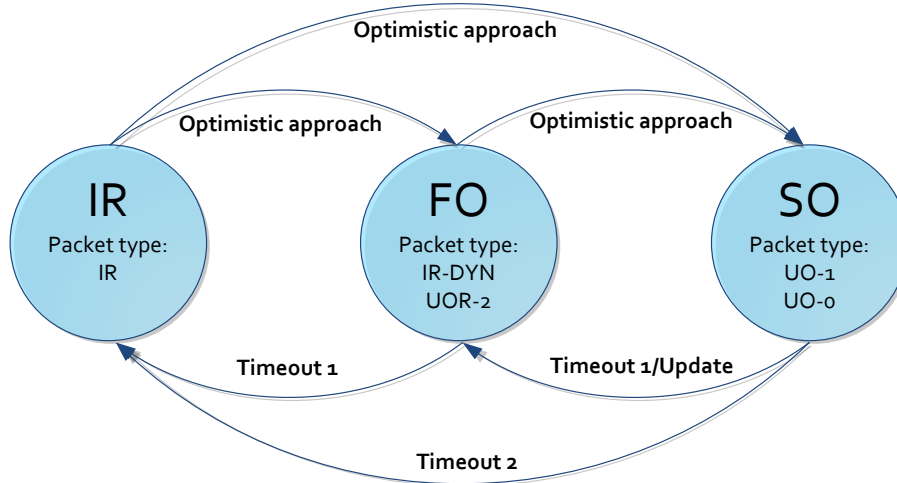


Figure 19: ROHC compressor states and transition between states.

The ORM block is introduced in the DVB-NGH system to be transparent for the rest of the components as it is shown in Figure 20. It should be noted that the adaptation module sends the essential headers fields of the ROHC process in a common PLP. This improves the zapping delay and error propagation.

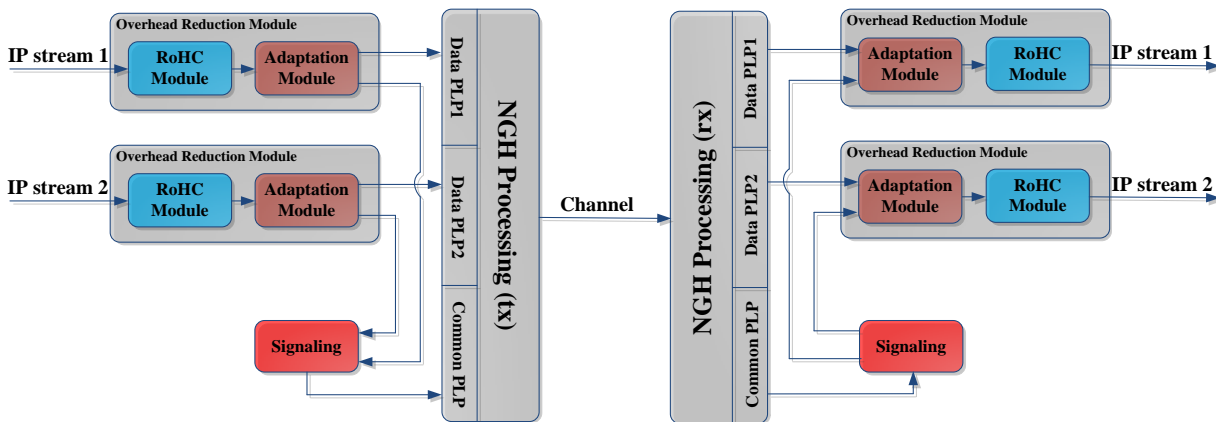


Figure 20: IP overhead reduction method in DVB-NGH transmission-reception chain.

1.4.3 Signaling in the DVB-NGH IP Profile

The upper layer signaling in the DVB-NGH IP profile consists of the network information together with signaling information for mapping services and service components onto PLPs, and related versioning information. The upper layer signaling is carried inside the service guide delivery descriptor in OMA-BCAST and it contains the mapping between the services and PLPs, ROHC context information as well as the mapping between the services available within the current frequency/multiplex and within the neighboring multiplexes. The versioning information, however, is a dedicated descriptor defined within the LLC information at the link layer (L2) and it contains versioning information of the upper layer signaling tables, service guide, and possible bootstrap information. Finally, it also provides information of the upper layer type that is being used, even though OMA-BCAST is currently the only upper layer defined so far.

1.4.4 OMA BCAST Service Guide

OMA BCAST is the “default” upper layer solution considered for the delivery of the service guide over the DVB-NGH bearer, see Figure 21. As opposed to the previous generation of mobile DVB standards, DVB-H, so far only OMA BCAST solution has been adopted in DVB-NGH as upper layer solution. However, as stated before, the versioning information within the LLC signaling enables future additions of other upper layer solutions as well.

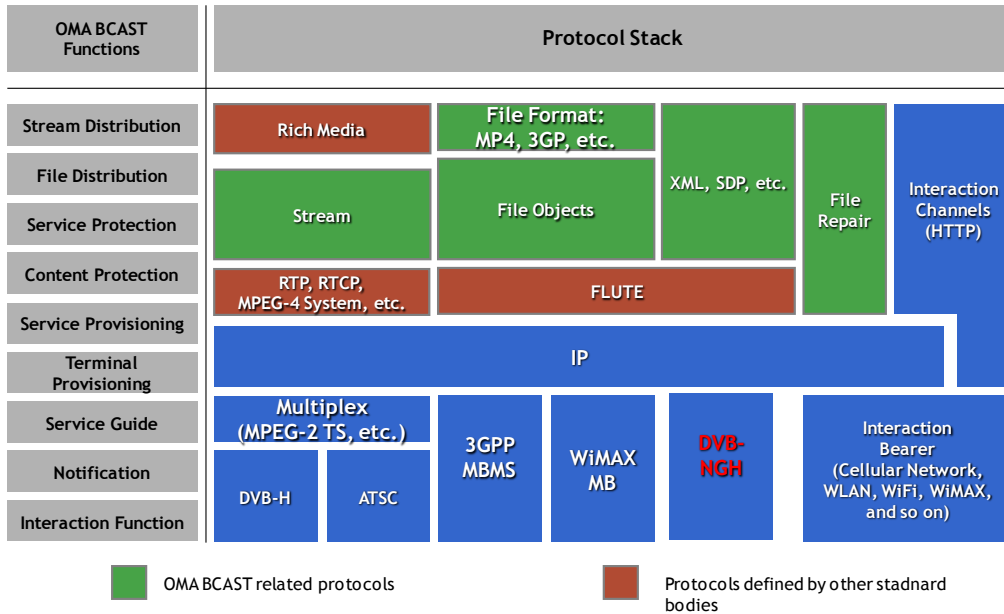


Figure 21: OMA BCAST protocol stack.

In OMA-BCAST, the Service Guide Delivery Descriptor (SGDD) plays a very important role to deliver efficiently the Service Guide. SGDD is transported on the Service Guide Announcement Channel, and informs the terminal about the availability, metadata and grouping of the fragments of the SG in the service guide discovery process. This allows for a quick identification of the service guide fragments that are either cached in the terminal or being transmitted. For that reason, the SGDD is preferably repeated for distribution over a broadcast channel. In addition, the SGDD also provides the grouping of related service guide fragments and thus a means to determine completeness of such a grouping.

The SGDD is especially useful if the terminal moves from one service coverage area to another. In this case, the SGDD can be used to quickly check which of the service guide fragments that have been received in the previous service coverage area are still valid in the current service coverage area, and therefore do not have to be re-parsed and re-processed.

This solution reports benefits as the BCAST SG delivery protocol was tested, implemented and commercialized, and so it is a stable solution. In addition, BCAST SGDD can deliver BDS specific entry information with the element “*BDSSpecificEntryPointInfo*”. This element is used in OMA BCAST adaptation specification to DVB-H for the provision of DVB-H network information such as network ID, frequency, etc. It is also adapted and used in OMA adaptation specification to DVB-NGH for the transport of bearer specific upper layer signaling.

1.4.5 Service Discovery

The service discovery process in DVB-NGH starts from the search of P1 symbol while the receiver is trying to synchronize to signals available within the frequency range. This so-called signal scan is a traditional procedure in all other broadcast systems. Once, the P1 symbol is found, the receiver can detect whether the found signal is desirable, i.e. if it is a DVB-NGH signal the receiver is capable to decode. Once the P1 phase has been completed, the receiver utilizes additional tuning information, particularly FFT and GI information,

which it can use for fast reception of the next signaling element, P2 symbol. The P2 symbol carries the L1 signaling information which the receiver needs in order to find out the necessary parameters needed to decode L1-post signaling and desired PLPs from the physical layer frames. Prior to the start of the decoding process of desired PLPs, the receiver needs to resolve which services are available on which PLPs. This can be done by accessing the common PLP, which carries all signaling information. The terminal checks whether there is an IP stream with an IP multicast address 224.0.23.14 or FF0X:0:0:0:0:12D available within the data streams carried in the common PLP defined in [7]. If either or both of the IP addresses are available, then the entry point for one or more OMA-BCAST SGs can be found through SGDD according to [10]. The upper layer signaling of DVB-NGH is carried on the top of IP layer, inside the SGDD. Hence, the upper layer signaling can be discovered by using “*BDSSpecificEntryPointInfo*”. The encapsulation and the signaling parameters for the upper layer signaling elements of the BCAST 1.2 are defined in [11] and in [8]. In addition, the LLC information contains versioning information of the upper layer signaling, which may also be used for checking whether the signaling information needs to be updated.

1.4.6 SVC Delivery in the IP Profile

The main critical issue for SVC delivery is the synchronization of the multiple streams carrying multiple associated PLPs. The IP profile takes advantage of the protocol stack defined, where the RTP protocol is able to synchronize different multimedia streams by means of the timestamp, a field designed for this purpose. Furthermore, the IP profile also uses the ISSY field in the same way as in the TS profile for the synchronization of the multiple associated PLPs delivering the SVC components.

1.4.7 IP Profile Receiver Buffer Model

The mission of the Receiver Buffer Model (RBM) is to ensure continuous reception of RTP stream packets of an RTP stream that is delivered over DVB-NGH [9]. This model is designed to avoid buffer underflows or overflows at the receiver for a specific service component. This receiver model is implemented at the sender side, in order to mimic the receiver behavior when handling the receiver service component. The sender signals required minimum buffering time to correctly and continuously receive and decode the corresponding service component. In this manner, the receiver buffers are sized according to this minimal buffering times, taking into account that the consumptions of the corresponding service will not result in buffer over or underflows.

The RBM is composed of: Physical Layer Pipe Buffer (PLPB), GSE De-capsulation Buffer (GDB), RTP De-capsulation Buffer (RTPDB), Re-Multiplexing Buffer (RMB), Media Decoding Module (MDM), and Decoded Data Buffer (DDB), see Figure 22. The RBM takes also into account the operations of Overhead Reduction Module (ORM), if present. It should be noted that there is one PLPB and GDB per each receiving PLP, one ORM and RTPDB per each transport flow, one RMB, one MDM, and one DDB per each service component.

In a first term, the PLPB extracts the generic stream carrying GSE packets. Then, the GDB output gives one or more transport flows or one or more compressed transport flows. If the GDB output flows are compressed the next block has to be the ORM, otherwise the flows are directly passed to the corresponding RTPDB. The ORM uses De-Adaptation Module and the ROHC Decoding Module to extract the datagram of the transport flow to the block output. Later, the RTPDB model extracts from the datagrams at its input the RTP packets that are passed to the RMB. If needed, a re-multiplexing is performed to join different service components transmitted in different PLPs (e.g. SVC with multiple PLPs), and then passed to the MDM to be decoded. The MDM is a decoding module which includes buffering of both coded and decoded data. Finally, the DDB aims to smooth out differences in the buffering delays of different service components until the DDB.

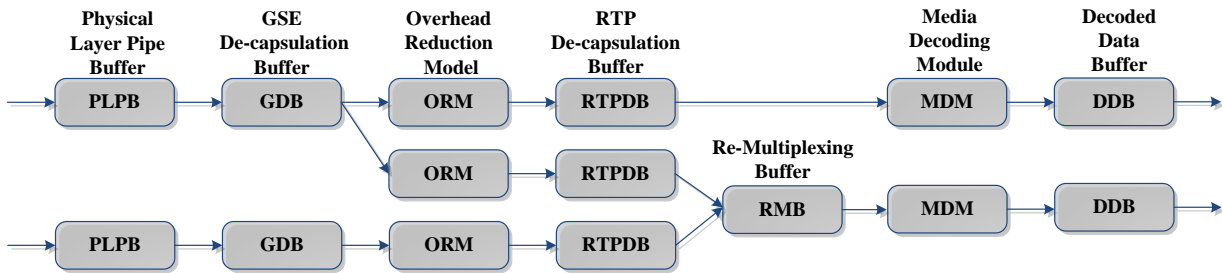


Figure 22: IP profile Receiver Buffer Model example. Service with one audio and two video flows (Base Layer and Upper Layer). Base Layer and audio are allocated in the same PLP.

1.5 Robust Header Compression (ROHC)

In an IP when the transmission occurs over point-to-point medium such as DVB-NGH, some of the protocol fields, which are required in traditional Internet, serve no useful purpose. Also, some of the headers' fields do not vary randomly from packet to packet during transmission. Some of the fields exhibit static behaviour or change in a more or less predictable way. Moreover, some of the field can be obsolete by information extracted from lower layers protocols. For example, length of the IP packet could be inferred from Generic Stream Encapsulation (GSE) protocol [11], which is employed in the DVB-NGH system to transport IP flows.

In IP Profile the overhead of transmitted multimedia service typically comprises 12 bytes of RTP [12], 8 bytes of UDP [13], and 20 (40) bytes of IPv4 (IPv6) headers. If the average protocol data unit (PDU), size is assumed to be 1000 bytes, the overhead would constitute around 4% (6%) of the transmitted data. One of the main new features of DVB-NGH is the use of Robust Header Compression (ROHC) protocol [14] as mechanism to reduce overhead caused by RTP/UDP/IP protocols. By employing ROHC protocol the overhead can be reduce to approximately 1% of the transmitted data [3].

The ROHC protocol uses inter-packet dependencies by relying on the establishment of a correct static and dynamic context on the receiver side. However, due to the large number of receivers targeted by the DVB-NGH system, it is highly unlikely that all receivers will be synchronized to the context refresh rate. Consequently, the zapping time to a service may be increased. Moreover, the error propagation caused by the inter-packet dependencies is likely to happen at any time for a set of receivers. Hence, when using ROHC, the frequency of transition between the compressor states must be balanced between minimizing the zapping time and error propagation after failure and maximizing the overhead reduction efficiency. Therefore, in order to reduce a zapping time to a service and the probability of error propagation, while maximizing the overhead reduction efficiency of ROHC, DVB-NGH introduces so-called adaptation module.

In DVB-NGH ROHC module together with Adaptation module compose Overhead Reduction Module (ORM), presented in Figure 23.

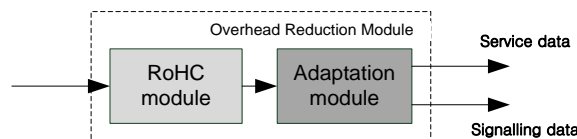


Figure 23: Overhead Reduction Module in IP profile

In ORM, the ROHC module is responsible for overhead reduction in IP flow while the adaptation module is introduced to loosen constraints of ROHC module in regard to zapping delay and error propagation. Consequently, the overhead reduction performance of ORM may be increased without impact on the zapping and error propagation, when compare to standalone ROHC operation. Moreover, ORM is designed to

guarantee backward compatibility to standalone ROHC framework, which allows the reuse of exiting software implementations of the ROHC protocol.

The ROHC header compression algorithm [12, 14] was created to reduce the overhead in IP streams. The algorithm classifies the header fields into: a) inferred, b) static, and c) dynamic. The classification is based on how the values of the header fields change in the consecutive packets. Inferred are these fields that contain values that can be concluded from other lower protocols information (e.g. IP length and UDP length). These values are removed from compressed header and are not transmitted by the compression flow. Static are these fields that are: a) expected to be constant throughout the lifetime of the packet flow (e.g. IP destination address) and therefore must be communicated to receiver only once or b) expected to have well-known values (e.g. IP version) and therefore do not need to be communicated at all. Dynamic are these fields that are expected to vary during the transmission of the packet flow (e.g. IP Hope Limit, UDP checksum, etc.).

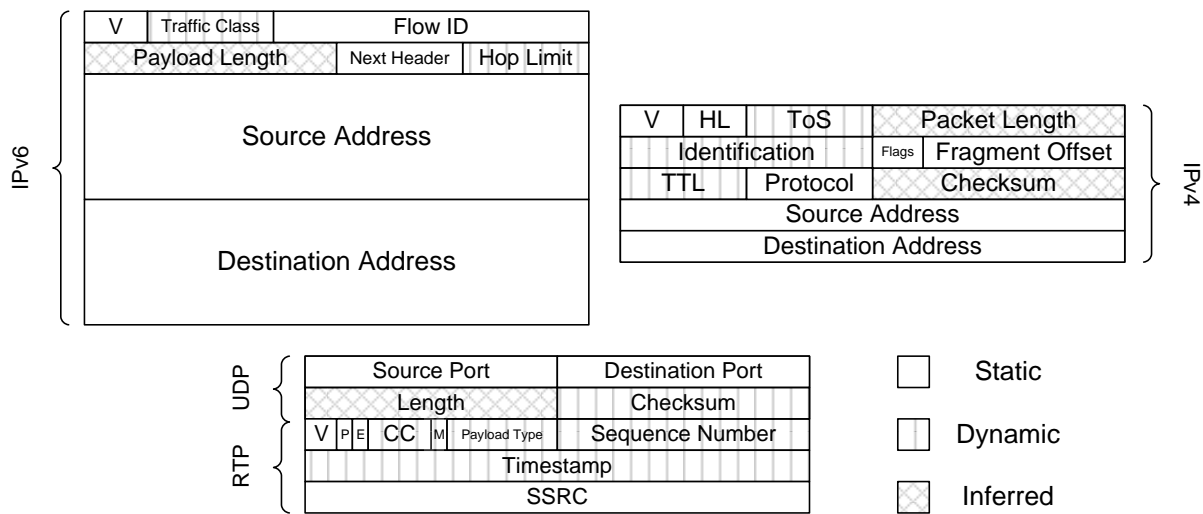


Figure 24: Split of header fields into Static, Dynamic, and Inferred fields according to ROHC framework [12]

Header compression with ROHC is characterized as an interaction between two state machines, one compressor machine and one decompressor machine, each instantiated once per context. The compressor and the decompressor poses three states each, which in many ways are related to each other even if the meanings of the states are slightly different for the two parties. Both machines start in the lowest compression state and transit gradually to higher states. Transitions do not have to be synchronized between the two machines. In normal operation, it is only the compressor that temporarily transits back to lower states. Decisions about transitions between the various compression states are taken by the compressor on the basis of periodic timeouts or variations in packet headers. In the decompressor, transition between states happen when context damage is detected.

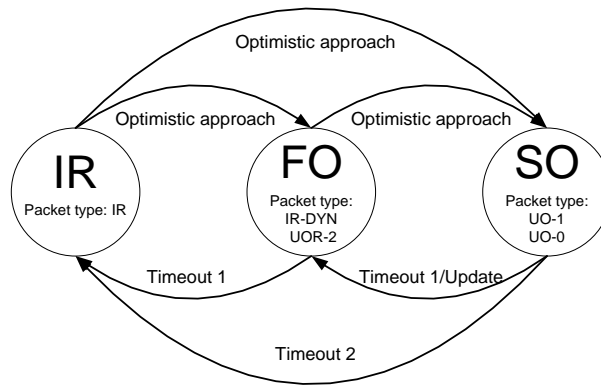


Figure 25: ROHC compressor states and transition between states in U-mode

In compressor, the three states are: a) Initialization and Refresh (IR), b) First Order (FO), and c) Second Order (SO) states. The compressor in each state create different packets format to establish the information in the decompressor, see Figure 26. IR state is to initialize the static parts and dynamic parts of the context at the decompressor, or to recover after failure. In this state, the compressor sends complete header information. This includes all static and non-static fields in uncompressed form plus ROHC header bytes. The purpose of the FO state is to efficiently communicate irregularities in the packet stream. When operating in this state, the compressor rarely sends information about all dynamic fields, and the information sent is usually compressed at least partially. The compressor enters the FO state from the IR state and from the SO state whenever the headers of the packet stream do not conform to their previous pattern. It stays in the FO state until it is confident that the decompressor has acquired all the parameters of the new pattern. The compressor enters the SO state when the header to be compressed is completely predictable. The compressor leaves this state and goes back to the FO state when the header no longer conforms to the uniform pattern and cannot be independently compressed on the basis of previous context information. When operating in U-mode, transitions between compressor states are performed only on account of periodic timeouts and irregularities in the header field change patterns in the compressed packet stream.

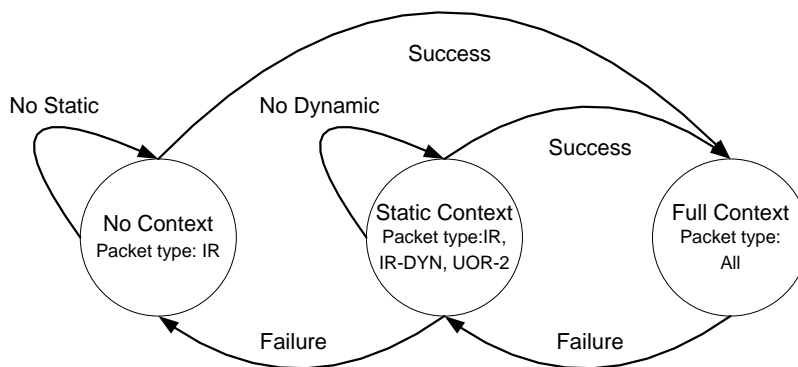


Figure 26: ROHC decompressor states and transition between states in U-mode

The decompressor starts in its lowest compression state, "No Context" and gradually transits to higher states. Initially, while working in the "No Context" state, the decompressor has not yet successfully decompressed a packet. Once a packet has been decompressed correctly (after receiving IR packet) the decompressor can transit all the way to the "Full Context" state.

The decompressor state machine normally never leaves the "Full Context" state once it has entered this state. Only upon failure, it transits back to lower states. However, when this happens, the decompressor first transits back to the "Static Context" state. In this state, reception of any packet generated in the IR or FO state of the compressor (IR, IR-DYN, UOR-2) is sufficient to enable transition back to the "Full Context" state. When

decompression of packets generated in the FO state of the compressor fails in the "Static Context" state, the decompressor goes all the way back to the "No Context" state.

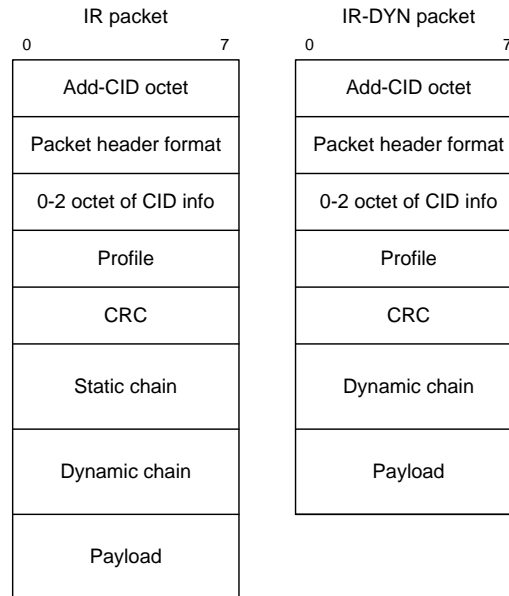


Figure 27: Example of the generic format of some of ROHC packets

1.5.1 Adaptation Module

DVB-NGH introduce adaptation module, to minimize inter-packet dependencies which could cause the error propagation and increased zapping time.

The channel zapping time is defined as the amount of time elapsed from the moment the user decides to consume a service to the moment when the rendering of the service starts. The channel zapping time can be considering as a cumulative sum of the many components. In DVB-NGH these components may be: time to synchronize to NGH frame, time to acquire the L1 signalling, time to acquire the L2 signalling, time until media decoders are refreshed to produce correct output samples, time to compensate the varying bitrates of media (e.g. video buffering), time to synchronize associated media streams (e.g. audio and video). The ROHC may introduce an additional delay, caused by the time needed for the decompressor to initialize; in ROHC it would be time to receive the IR packet.

Mobile data delivery over DVB-NGH is prone to errors at it may happen that some of the ROHC compress packet may be received corrupted. If any of these packets would be IR packet then all packets received subsequently, even when not corrupted, would be typically marked as unusable till the next received IR packet.

Therefore, from zapping time and error propagation perspective it would be desirable to maximize the IR packet transmission frequency. On the other hand from compression efficiency perspective it is desirable to make the refresh as seldom as possible.

The adaptation module allows to loosen the trade-off by providing the full refresh with frequency transmission of IR-DYN packet, which may be transmitted more frequent than refresh of IR packet with smaller impact on the compression efficiency. To achieve that the adaptation module splits transmission of static and dynamic information fields of ROHC compressed stream into two logical channels. The dynamic header information is sent without any modification over in-band channel together with the payload data, while the static header information are sent out-of-band.

The adaptation module extracts the static chain information (as defined in [12]) from IR packets and converts the IR packets to IR-DYN packets by changing the corresponding header fields accordingly and recalculating the CRC value of the IR-DYN packet. The extracted static chain data is then transmitted over

designated signalling bytes. The newly created IR-DYN packet is transmitted together with the rest of compressed data flow.

Due to the splitting transmission to two logical channels, the receiver possesses all static information for all available services as soon as the signalling data is processed. Due to this, a receiver is able to convert any received IR-DYN packet to IR packet on account of early received static chain data. The conversion can be done by adding the static chain information to IR-DYN packet, and changing the corresponding header fields accordingly and recalculating the CRC value of the packet. As a result, ROCH de-compressor may start the decompression of the ROHC flow not only with the reception of IR packet but also IR-DYN packet.

1.5.2 Overhead Reduction Module in DVB-NGH

The Overhead Reduction Module is optional in DVB-NGH and, if used, is applied to IP streams carrying service data. An example deployment of the module in the DVB-NGH system is depicted in Figure 28.

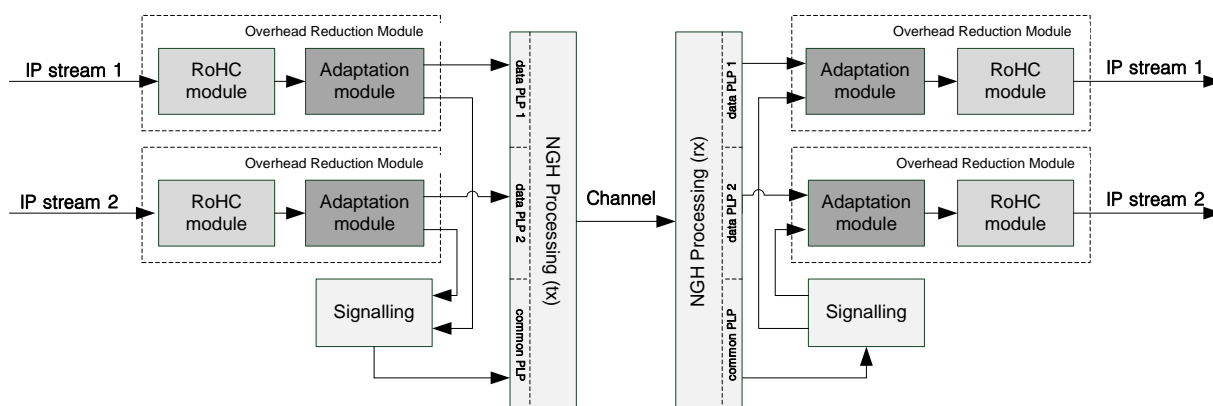


Figure 28: Block diagram of the DVB-NGH system employing Overhead Reduction Module

1.5.2.1 ROHC module

The ROHC module is responsible for reduction of overhead in IP flow. The detailed operation of the ROHC module is specified in [12, 14].

1.5.2.1.1 Supported profiles

ROHC framework defines multiple header compression algorithms, called profiles. Each profile is specific to the particular network layer, transport layer or upper layer protocol combination. The profiles presented in Table 3 must be supported.

Table 3: ROHC Profiles supported in DVB-NGH

Profile Identifier	Usage:	Reference
0x0001	RTP/UDP/IP	RFC 3095, RFC 4815
0x0002	UDP/IP	RFC 3095, RFC 4815
0x0003	ESP/IP	RFC 3095, RFC 4815
0x0004	IP	RFC 3843, RFC 4815

1.5.2.1.2 ROHC module parameters

The ROHC framework has configuration parameters that are mandatory and that must be configured between compressor and decompressor peers [12, section 5.1.1].

The usage and definition of the parameters in DVB-NGH shall be as specified below.

- MAX_CID: This is the maximum CID value that can be used. The parameter MAX_CID is delivered in L2 signalling.
- LARGE_CIDS: This value is inferred from the configured value of MAX_CID according to the following rule:

If MAX_CID > 15 then LARGE_CIDS = TRUE else LARGE_CIDS = FALSE.

- PROFILES: Profiles are used to define which profiles are allowed to be used by the UE. The parameter PROFILES is delivered in L2 signalling.
- FEEDBACK_FOR – not used
- MRRU – segmentation not used

1.5.2.1.3 ROHC module restriction

DVB-NGH imposes additional restriction to the operation of ROHC framework.

- If any change in the static fields of the input IP stream is detected by the ROHC compressor, then the ROHC compressor must perform context re-initialization (CONTEXT_REINITIALIZATION signal is triggered as described in [12, section 6.3.1] and the new value of the Context ID (CID) must be assigned to the compressed IP stream. The new value should be unique for the system and be not used by any other instance of ROHC compressors operated in the system.
- ROHC compressor and decompressor, employed in DVB-NGH, must always operate in unidirectional mode as described in [12].

1.5.2.1.4 Example output from the ROHC module

The example output of ROHC module is presented on Figure 29. The output corresponds to the DVB-NGH setup presented on Figure 28.



Figure 29: An example output of from the ROHC module on TX side

1.5.3 Adaptation module

The adaptation module allows to: a) minimize the impact of header compression mechanism on zapping delay and b) improve error robustness of compressed flow. Consequently, by deploying the adaption module the compression efficiency of ORM can be increased, due to the loosen constrains imposed on the ROHC compressor.

1.5.3.1 TX side

The adaptation module shall extract the static chain bytes from the each IR packets transmitted in the ROHC compressed data flow. After extracting the static chain bytes, each IR packet shall be converted to IR-DYN packet type by the Adaptation module.

Note: ROHC module may be configured to produce only one IR packet at the beginning of the compression process. Consequently, the operation of extraction of the static bytes and conversion of the packet type may be performed only once.

1.5.3.2 RX side

The Adaptation module shall detect IR-DYN type packets in the ROHC compressed data flow. At least one IR-DYN packet from the received data flow shall be converted by the Adaptation module to IR packet type, using the static chain bytes received through signalling. The conversion ensures that initialization of ROHC decompressor (i.e. transition to Full Context) is possible.

1.5.3.3 Example output from the Adaptation module

The example output of the Adaptation module is presented on Figure 30. The output corresponds to the DVB-NGH setup presented on Figure 28 and input to the Adaptation module as presented on Figure 29.

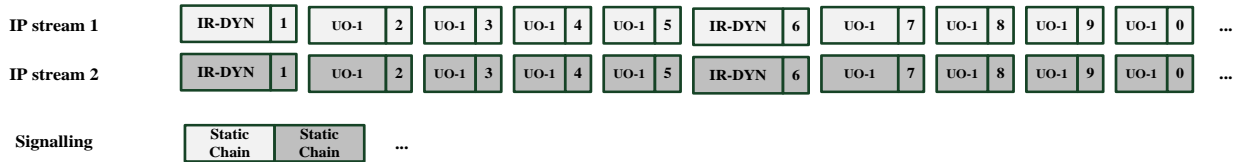


Figure 30: An example output of from the Adaptation module on Tx side

1.5.4 Mapping to GSE

Protocol carried by GSE stream is identified by Protocol Type/Extension field included in GSE header. The Protocol Type field is mandatory when GSE is carried over DVB-NGH and its value shall be set as presented in Table 4.

Table 4

Protocol Type value	Protocol
0x22F1	ROHC
0x0800	IPv4
0x86DD	IPv6

1.5.5 Signalling

Signalling for the IP profile of the DVB-NGH is still under discussion. The DVB TM-H SUL Task Force has been progressing with the specification of NGH upper layer signalling for the IP profile, based on an initial proposal from Nokia. The proposal defines an equivalent structure of the PSI/SI [15] in the TS profile, featuring three elements: ULI (Upper Layer Information), LMI (Local Multiplex Information), and OMI (Other Multiplex Information). ULI and LMI elements will be used for the ESG and service/components mapping to PLPs (equivalent role of EPG and PAT/PMT tables in PSI/SI). OMI element will include all network related information in the local and other multiplexes (equivalent to INT/NIT tables in PSI/SI). The structure of ULI/LMI/OMI contents is still open for further refinement before the DVB TM-H SUL Task Force comes to decision.

The Overhead Reduction Module related data is carried in the ULI element. More precisely, in service association section, which is responsible for mapping the URI with PLP id and also provide ROHC related information for each data stream.

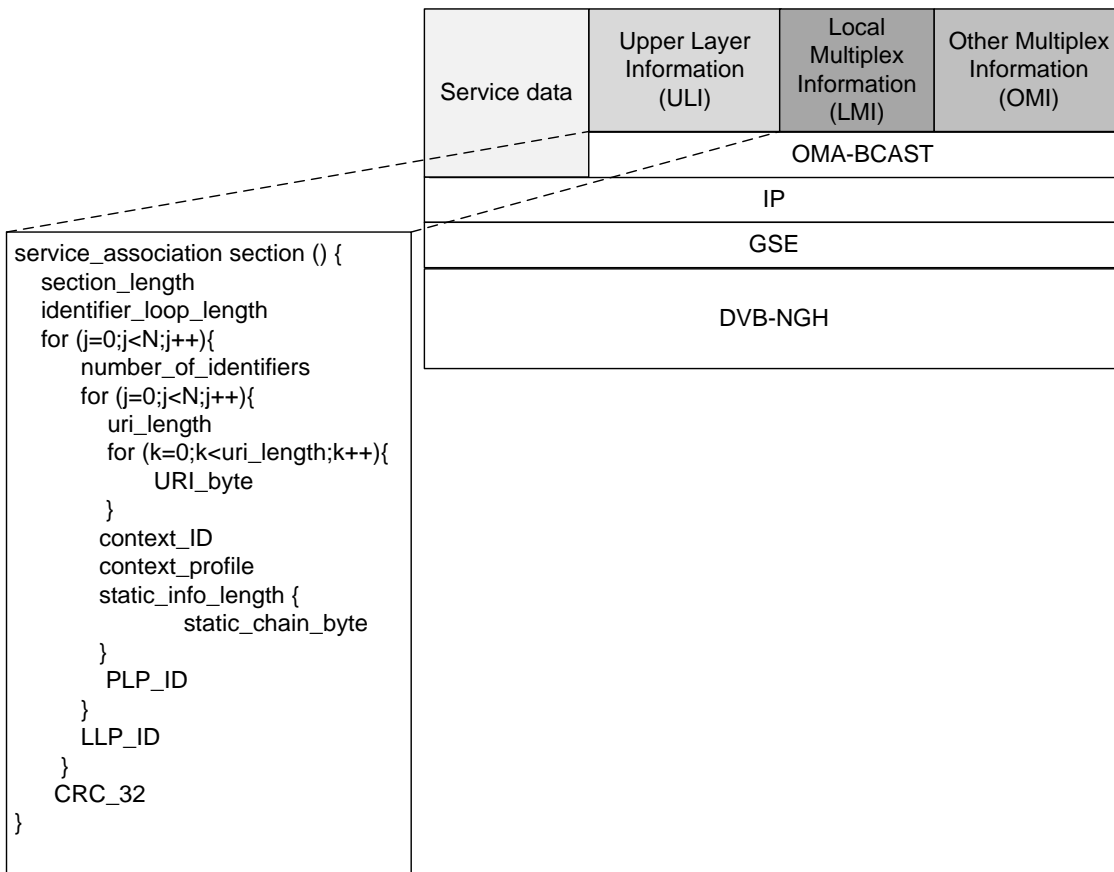


Figure 31: Protocol stack and an example service association section carrying ROHC related information

The ULO/LMI/OMI tables will utilize OMA BCASST service guide channels as the conveyors.

1.5.6 Results

1.5.6.1 Overhead Reduction Module (IP Profile)

1.5.6.1.1 Compression Efficiency

The compression efficiency of the ORM depends on the incoming IP flow and characteristics of payload it carries.

Use Case 1:

Two video sequences (Ice, City), in 4CIF format and with 30 fps frame rate, were compressed using H.264/AVC codec. The resulted compressed bitstream bit rate was 1500 kbps with an average NAL unit size of 1150 bytes. The bitstream was encapsulated into RTP, UDP, IP packets. In RTP protocol packetization mode 0 was used. The timestamp field of RTP header was monotonically increasing over time. Timestamp delta between two consecutive packets was not constant value. The ROHC used TS_STRIDE value equal to 90 and refresh packet was inserted every 62nd packet, i.e. every 380 ms.

Table 5: Use Case 1

	ORM	Uncompressed
Ice	10.10 bytes (0.918%)	40.00 bytes (3.47%)
City	10.08 bytes (0.925%)	40.00 bytes (3.47%)

Use Case 2:

Two video sequences (Ice, City), in 4CIF format and with 30 fps frame rate, were compressed using H.264/AVC codec. The resulted compressed bitstream bit rate was 1500 kbps and average NAL unit size was 800 bytes. The bitstream was encapsulated into RTP, UDP, IP packets. In RTP protocol packetization mode 1 was used. The timestamp field of RTP header was not monotonically increasing over time. Timestamp delta between two consecutive packets was constant value. The ROHC used TS_STRIDE value equal to 3600 and refresh packet was inserted every 62nd packet, i.e. every 270 ms.

Table 6: Use Case 2

	ORM	Uncompressed
Ice	9.91 bytes (1.267%)	40.00 bytes (5.00%)
City	9.67 bytes (1.385%)	40.00 bytes (5.00%)

Use Case 3:

Live video content in VGA format and with 30 fps frame rate, were compressed using H.264/AVC codec. The resulted compressed bitstream bit rate was 800 kbps and average NAL unit size was 900 bytes. The bitstream was encapsulated into RTP, UDP, IP packets. In RTP protocol packetization mode 0 was used. The timestamp field of RTP header was monotonically increasing over time. Timestamp delta between two consecutive packets was not constant value. The ROHC used TS_STRIDE value equal to 1 and refresh packet was inserted every 62nd packet, i.e. every 550 ms.

Table 7: Use Case 3

	ORM	Uncompressed
Live	10.65 bytes (1.249%)	40.00 bytes (4.40%)

1.5.6.1.2 Error Propagation

To present how the error propagation may degrade the video quality, a simple scenario is assumed where a BB frame carrying IR packet is corrupted during transmission. Transmission of two sequences, Ice and City, were simulated. Both sequences were in 4CIF resolution and with frame rate 30 fps. The frequency of IR packet in the compressed ROHC stream was every 250ms and the frequency of IR-DYN packet was every 50 ms. Thus, with at a frame rate of 30 fps, 8 video frames are affected in standalone ROHC and 2 frames in ORM. Table 8 shows the impact of the loss of one IR packet on the video quality.

Table 8: PSNR

	Ice	City
ROHC	37.191	32.859
ORM	39.706 (38.600)	34.131(33.751)
Error Free	40.346	34.509

1.6 L1 Signalling

DVB-NGH (Next Generation Handheld) has enhanced the physical layer signaling of DVB-T2 in three different aspects:

- Reduced overhead.
- Higher capacity.
- Improved robustness.

DVB-NGH has restructured the L1 signaling structure of DVB-T2 in order to reduce the signaling overhead. Instead of signaling the configuration of each PLP (MODCODTI, modulation, code rate, and time

interleaving configuration), PLPs' configurations are classified into categories with the same settings, hence reducing the required signaling information when a number of PLPs have the same configuration (i.e. belong to the same category). Furthermore, DVB-NGH makes it possible to split across a number of frames some signaling information which is in practice static, as opposed to DVB-T2, where all signaling information is always transmitted in every frame. DVB-NGH has also introduced a new concept of logical framing where the L1 signaling is further split into logical and physical parts, with the logical part (typically dominant) transmitted only once within the logical frame and so may appear in only one of the sequence of physical frames carrying the logical frame.

On the other side, the new logical frame structure avoids any limitation on the maximum number of PLPs that can be used in the system due to signaling constraints. For the preamble P1, DVB-NGH has also increased the signaling capacity. In DVB-T2, the preamble P1 symbol provides seven signaling bits. In DVB-NGH, for the terrestrial MIMO (Multiple Input Multiple Output) profile and the hybrid terrestrial-satellite profiles of DVB-NGH, an additional preamble P1 (aP1) symbol has been introduced in order to cope with the required amount of signaling capacity of the P1 symbol. The P1 symbol signals the presence of the aP1 symbol through an escape code.

The improvement in the signaling robustness is also particularly relevant, because DVB-NGH adopts for the data path code rates more robust than in DVB-T2 (i.e., $1/5$ instead of $1/2$). DVB-NGH adopts for L1 signaling new mini LDPC codes of size 4320 bits (4k) with a code rate $1/2$. Although 4k LDPC codes have in general a worse performance than 16k LDPC codes, the 4k LDPC codes turn out to outperform 16k LDPC for L1 signaling thanks to the reduced amount of shortening and puncturing. In DVB-T2, LDPC codewords with L1 signaling are shortened (i.e. padded with zeros to fulfill the LDPC information codeword) and punctured (i.e. not all the generated parity bits are transmitted), which decreases the LDPC decoding performance. The adopted 4k LDPC codes have similar parity check matrix structure than the 16k LDPC codes used for data protection. This allows for efficient hardware implementations at the transmitter and receiver side efficiently sharing the same logic.

DVB-NGH has also adopted two new mechanisms to improve the robustness of the L1 signaling known as Additional Parity (AP) and Incremental Redundancy (IR). The additional parity mechanism consists in transmitting punctured bits in the previous frame. When all punctured bits have been transmitted and there is still a need for more parity bits to be added, the incremental redundancy mechanism extends the original 4k LDPC code into an 8k LDPC code of 8640 bits. The overall code rate is thus reduced from $1/2$ down to $1/4$. L1-repetition can be used to further improve the robustness of the L1 signaling as a complementary tool to AP and IR. It should be pointed out that the robustness improvement of the L1 signaling in DVB-NGH can be translated into a reduction of the signaling overhead for the same coverage.

Another improvement of the physical layer signaling in DVB-NGH compared to the first two releases of DVB-T2 (v.1.1.1 and v.1.2.1) is related to a reduction of the peak-to-average power ratio (PAPR) of the L1 signaling. After the first transmitters were manufactured, it was observed that large numbers of data PLPs resulted in peaks in the time domain signal during the P2 symbols. The reason was the lack of energy dispersal scrambling for the L1 signaling data. In the second release, several improvements were done to overcome this situation, based on a combination of the PAPR reduction mechanism of DVB-T2 ACE (Active constellation Extension) and TR (Tone Reservation), and using reserved bits for future use and additional bias balancing cells [16]. DVB-NGH, as well as the third release of DVB-T2 (v.1.3.1, whose main novelty is the profile T2-Lite), simply scrambles the L1 signaling based on the mechanism employed to scramble the data.

1.6.1 L1 Signaling Overhead Reduction in DVB-NGH

The L1 signaling overhead in DVB-T2 is usually at reasonable values around 1-5% [16]. However, in DVB-NGH, the overhead make become significant, as it increases with the higher number of PLPs, the higher robustness required for the signaling, and the shorter frame length. Further analysis of the L1 signaling in DVB-T2 shows that the configurable signalling (L1-config) represents the dominant part of the amount of signaling information, though it does not bring any useful information once the receiver is in its steady state

(i.e., semi-static). In DVB-T2, all L1 signaling fields, i.e., L1-pre, L1-config, and L1-dynamic, are transmitted in every frame. The values of the L1-dynamic can change frame by frame, whereas the L1-pre and L1-config may only change on a super frame basis. In practice however, they only change when the multiplex of the RF channel is reconfigured, which occurs rather seldom. For these reasons, DVB-NGH allows the transmission of the L1-pre and L1-config signaling fields to be split into several frames (n-periodic L1-pre signaling, and self-decodable L1-config partitioning). The drawback is that the channel scanning time increases when the receiver is switched on for the very first time because the signaling information is not completed after the reception of the first frame.

The different techniques adopted in DVB-NGH to reduce the L1 signaling overhead can achieve an increase in the total system capacity higher than 1% (up to 1.5% in realistic settings). Nevertheless, the actual saving depends on the number of PLPs, the number of different PLPs configurations, the actual PLP settings and system features used, and finally the number of frames used to transmit the n-periodic L1-pre and the self-decodable L1-config partitions.

Next, the different mechanisms to reduce the signaling overhead of the L1-pre and L1-config are briefly described.

1.6.1.1 L1-Pre Overhead Reduction

The L1-pre signaling field can be divided into n blocks of the same size, such that the signaling overhead is reduced by a factor of n . This is known as n-periodic transmission of L1-pre. The selection of the parameter n represents a trade-off between channel scanning time and signaling overhead. A superposed correlation sequence is used to detect the value of n and the order of the portions. The detection is very robust, being possible even at negative SNR. N-periodic transmission of L1-pre cannot be used with Time-Frequency Slicing (TFS).

1.6.1.2 L1-Post Overhead Reduction

DVB-NGH has introduced a new logical frame structure compared to DVB-T2 specially suited to the transmission of DVB-NGH in DVB-T2 Future Extension Frames (FEFs), see Figure 32.

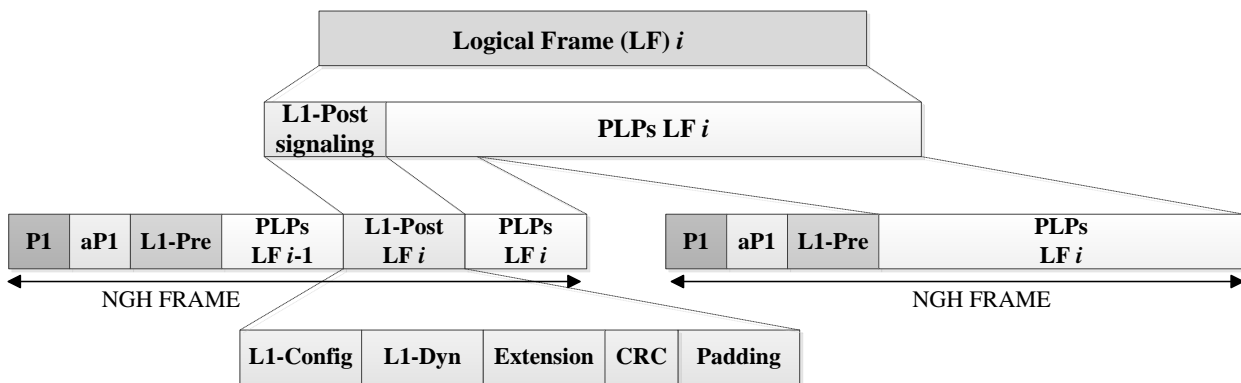


Figure 32: L1 signaling structure in DVB-NGH. The aP1 symbol is only transmitted in the MIMO and hybrid profiles.

From a L1 signaling overhead point of view, in DVB-NGH the L1-post signaling field does not need to be transmitted in every (physical) NGH frame, but only in the first NGH frame that carries the logical frame. One logical frame can span across several NGH frames, thus reducing the L1 signaling overhead. The overhead reduction is achieved at the expense of a larger zapping time because receivers may need to wait for more than one frame to start decoding the data PLPs. However, if the NGH frames are transmitted frequently, the impact can be negligible.

1.6.1.3 L1-Configurable Overhead Reduction

In DVB-T2, the L1 signaling allows each PLP to have completely independent parameters [16]. However, in realistic scenarios, there will be only a very limited number of different PLP configurations. This means that several PLP would use exactly the same settings. For this reason, DVB-NGH has changed the L1 signaling paradigm for multiple PLPs, categorizing PLPs with the same features and reducing the signaling overhead of the L1 configurable field. The adopted solution allows for a totally general case, with up to 255 unique PLP settings, but in typical scenarios with few configurations of PLPs the required amount of signaling information is radically reduced.

Another improvement to reduce the L1-config overhead in DVB-NGH is the introduction of flags to signal the availability of some optional features which are not commonly used. The L1-config signaling format for DVB-T2 is very generic, and supports a lot of features, such as TFS, auxiliary streams, reserved for future use fields, etc. The amount of required signaling information can be significant in some cases. However, in practical use cases only a few of these features may be used, and thus the corresponding fields could be removed. In DVB-NGH, at the beginning of the L1-config field one bit flags are introduced for some optional features to indicate whether the features are available or not.

The L1-config signaling cannot be divided into n blocks of the same size because the frame configuration (e.g., T2 frame length, FEF length) would not be known until the reception of n frames. Compared to n -periodic L1-pre transmission, the adopted approach for L1-config provides a flexible trade-off between overhead reduction and zapping delay, and consists on transmitting the PLP configurations in L1-config not in every frame but in a carousel like manner with controllable delay. The delay is controllable on a PLP basis, so that PLPs which cannot tolerate any delay can be sent with zero delay. This way, zero delay can be guaranteed for the constant signaling information which cannot tolerate any delay. The amount of L1-config information transmitted per frame is constant and self-decodable, but the signaling overhead is reduced because all the information of all PLPs is not transmitted in every frame.

1.6.2 Increased Physical Layer Signaling Capacity in DVB-NGH

DVB-NGH has improved the capacity of the physical layer signaling compared to DVB-T2 in two different aspects. On one hand, the adoption of an additional preamble P1 symbol has doubled the P1 capacity from 7 bits to 14 bits. On the other hand, the L1-post signaling capacity has been increased because it is not constrained to the preamble P2 symbol(s).

1.6.2.1 Additional Preamble aP1 OFDM Symbol for the Terrestrial MIMO and Hybrid Profiles of DVB-NGH

In DVB-T2, the P1 symbol provides seven signaling bits that define some essential transmission parameters such as the preamble format, the FFT size, and the guard interval. The preamble format, and hence the frame type, is signaled with three bits. These three bits are not sufficient to signal all profiles of DVB-T2, T2-Lite, and DVB-NGH. Therefore, additional bits are required. DVB-NGH has introduced an additional preamble P1 (aP1) symbol to identify the terrestrial MIMO and the hybrid terrestrial-satellite SISO and MIMO profiles. The presence of the aP1 symbol is signaled in the P1 symbol. For the basic profiles of DVB-NGH, as well as for DVB-T2 and T2-Lite, there is no aP1 symbol. The three bits of the P1 symbol used to identify the preamble format are used in the following way:

- Two combinations are used for DVB-T2 (SISO and MISO).
- Two combinations are used for T2-Lite (SISO and MISO).
- One combination is used for non-T2 applications (e.g., identification of transmitters in single frequency networks).

- Two combinations are used for the terrestrial SISO and MISO profiles of DVB-NGH.
- One combination is used as escape code to signal the presence of the aP1 symbol. This is used for the terrestrial MIMO and for the hybrid SISO and MIMO profiles of DVB-NGH.

The aP1 symbol provides seven signaling bits, and with this information the receiver is able to receive the preamble P2 symbols and access the L1 signaling. The aP1 has the same structure than the P1 symbol, and hence the same properties of the P1 symbol: robust signal discovery against false detection and the resilience to continuous interference. But in order to avoid interferences with the P1 symbol, the aP1 is scrambled with a different pseudo-random sequence, uses a different frequency offset value for the prefix and postfix, and employs a different set of carriers, see Figure 33.

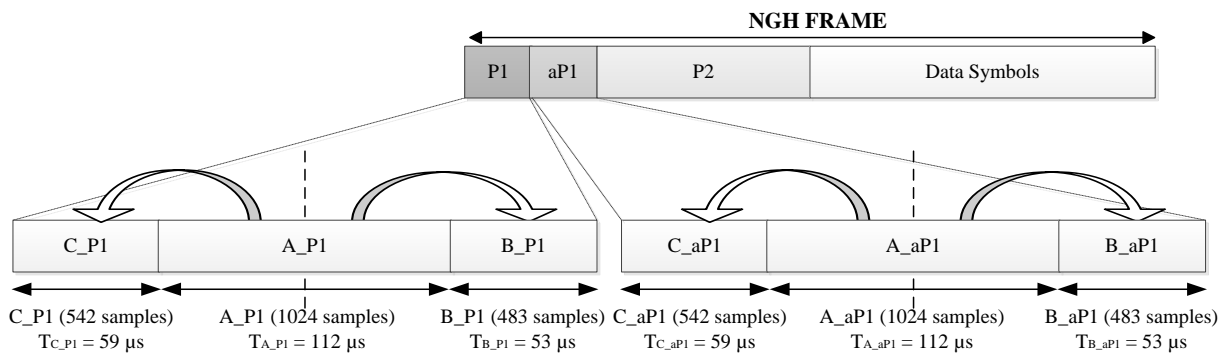


Figure 33: Preamble P1 and aP1 symbol in DVB-NGH.

The three design parameters mentioned above were carefully chosen to make aP1 have same performance as P1 in both detection and decoding performance in the receiver side. Compared to DVB-T2, the aP1 symbol improves the performance of detecting and correcting frequency and timing synchronization in the receiver side.

1.6.2.2 L1-post Signaling Capacity

DVB-T2 allows up to 255 PLPs to be used per multiplex. However, the maximum number of PLPs is in practice lower because the L1 signaling capacity is limited to the preamble P2 symbols. The L1 signaling capacity, and hence the maximum number of PLPs that can be used, is limited by the FFT size, the modulation used for the L1-post, and whether L1-repetition is used or not. For example, for any FFT size other than 32K, BPSK modulation, and with L1-repetition, the maximum number of PLPs is limited to 14 [16].

DVB-NGH has improved the L1-post signaling capacity compared to DVB-T2 because the L1-post is no longer constrained by a fixed number of preamble P2 symbol(s). The new logical frame structure allows transmitting the L1-post signaling outside the P2 symbol(s), see Figure 32. In DVB-NGH, only the L1-pre signaling is transmitted within the P2 symbol(s) with a fixed length, modulation and coding. The L1-post signaling may be transmitted after the L1-pre in the P2 symbol(s), but it can expand to the data symbols if needed.

1.6.3 Improved L1 Signaling Robustness in DVB-NGH

DVB-NGH adopts a similar L1 signaling structure than DVB-T2, and keeps the possibility of using L1-repetition, but it introduces three new mechanisms to improve the L1 robustness:

- 4k LDPC codes.

- Additional Parity (AP).
- Incremental Redundancy (IR).

1.6.3.1 4k LDPC Codes

The L1 signaling information of DVB-T2 does not generally fill one 16k LDPC codeword. Hence, codewords need to be shortened and punctured, which degrades the performance. For this reason, DVB-NGH adopts for L1 signaling new 4k LDPC codes of size 4320 bits. The reduced size of 4k LDPC codes is more suitable for L1 signaling, as the amount of shortening and puncturing can be significantly reduced, see Table 9. The LDPC code rates adopted for L1-pre and L1-post in DVB-NGH are 1/5 and 1/2, respectively. The modulation schemes used for L1-pre is always a BPSK modulated, whereas for L1-post is configurable between BPSK, QPSK, 16-QAM, and 64-QAM, as in DVB-T2.

Table 9: 4k LDPC codes in DVB-NGH vs. 16k LDPC codes in DVB-T2 for L1 signaling.

L1 Signaling	LDPC Code	Code Rate	Information Bits	Parity Bits	Signaling Bits	Padded Bits	Punctured Bits
L1-pre	4k	1/5	1080	3240	280	800	2120
	16k	1/5	4000	12000	200	3200	11200
L1-post	4k	1/2	2160	2160	640	1520	1520
	16k	4/9	7200	9000	640	6560	8200

4k LDPC codes have been created with similar parity check matrix structure than the 16k LDPC in order to efficiently share the hardware decoder chain at the receivers. Namely, a quasi-cyclic structure in the information part and a staircase structure in the parity part is used. 4k LDPC codes have a parallel factor of 72 (i.e., number of parallel computations to get the input from the memory for processing of the bit node and check node by the decoder), which is a divisor of the number used for 16k LDPC codes (360) to enable efficient sharing of the memory access. The maximum number of degrees of the parity check matrix, related at the decoder to the number of input values for variable node and check node processor, is also smaller than the one in 16k LDPCs.

Due to its lower size, 4k LDPC codes generally perform worse than 16k LDPC codes without padding and puncturing. This performance degradation depends on the code rate and the channel (i.e. it is larger for higher code rates and multipath fading channels), but it is less than 1 dB. However, for L1 signaling 4k LDPC codes outperform 16k LDPC codes in the order of 1-2 dB because of the reduced size of the L1 signaling information. This performance improvement is also translated into a lower number of iterations and hence lower power consumption and faster convergence. Other advantages of 4k LDPC codes are lower complexity and higher efficiency at the receivers, reduced latency, and finer granularity when choosing the code rate.

1.6.3.2 Additional Parity (AP)

The additional parity technique consists of transmitting punctured LDPC parity bits of the L1-post in the previous NGH frame. This technique improves the time diversity of the L1 signaling in a similar way than L1-repetition without affecting the zapping time, but it obtains a better performance because instead of just repeating the information the effective code rate is reduced.

DVB-NGH employs optimized puncturing patterns for L1 in a similar way than in DVB-T2 [16]. The code rate for L1-pre is fixed and equal to 1/5. For L1-post, the mother code is 1/2, but a code rate control is also

applied like in DVB-T2 to compensate the LDPC decoding performance degradation due to padding and puncturing such that the coverage does not depend on the amount of signaling information.

AP allows transmitting the punctured parity bits in the previous frame. Figure 34 shows the structure of the LDPC codeword with AP. The amount of additional parity bits is determined by the configuration parameter AP_RATIO, whose possible values are 0 (i.e., AP is not used), 1, 2, or 3. The proportion of additional parity bits transmitted in the previous frame is increased by a factor of 35% for each AP block. That is, AP1, AP2, and AP3 imply 35%, 70%, and 105% more parity bits.

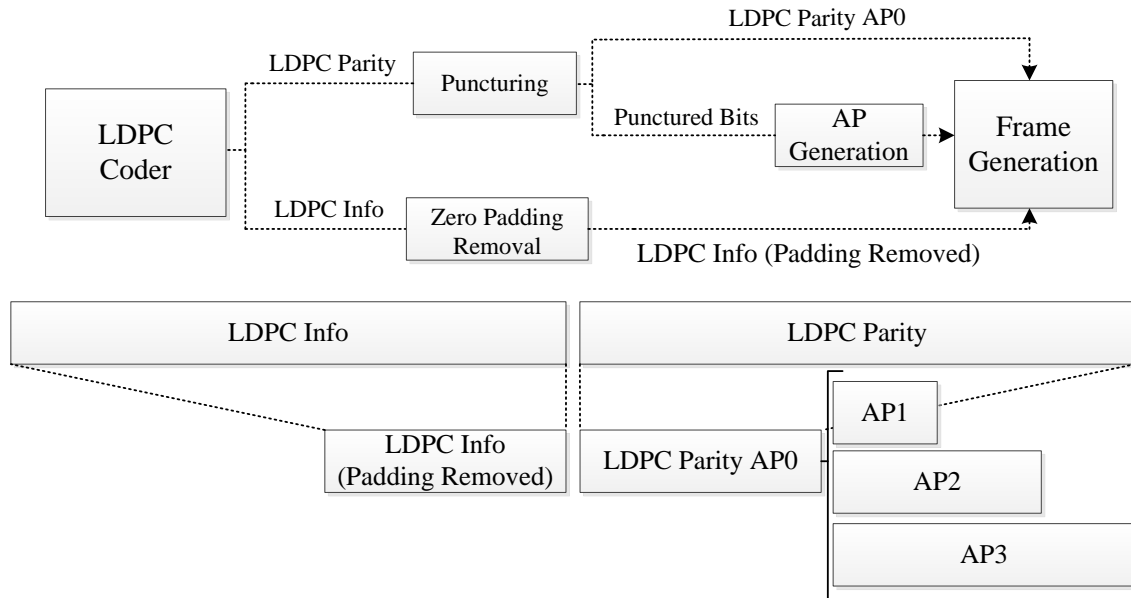


Figure 34: The resulting LDPC code word with additional parity bits.

Figure 35 shows the effective code rate for L1-post in DVB-T2 and in DVB-NGH with AP. We can see how the effective code rate decreases as the signaling information decreases (for DVB-NGH, the minimum value is 1/4 and the maximum 1/2). The main limitation of AP is the available number of punctured bits. In some cases, some AP configuration cannot be applied because there are not enough punctured bits. For this reason, the technique incremental redundancy was adopted.

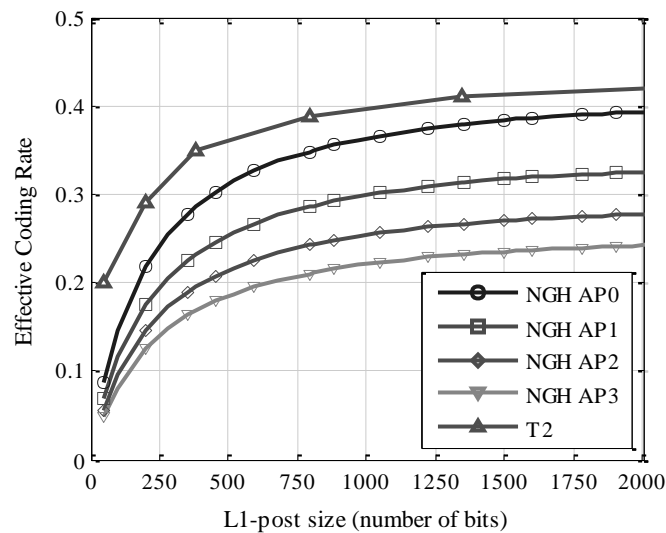


Figure 35: Effective code rate for L1-post in DVB-T2 and DVB-NGH with additional parity.

1.6.3.3 Incremental Redundancy (IR)

The technique incremental redundancy allows generating additional parity bits for AP when the amount of punctured bits is not enough for the selected AP configuration for L1-post. IR extends the 4k LDPC codeword into an 8k LDPC codeword, yielding an effective code rate of 1/4. The resulting codeword has two parts: the first part corresponds to the basic 4k LDPC codeword, and the second part corresponds to the additional IR parity bits, see Figure 36.



Figure 36: Extended 8k LDPC codeword with incremental redundancy. K_{LDPC} 2160 bits, N_{LDPC} 4320 bits, M_{IR} 4320 bits.

Figure 37 shows the structure of the IR parity check matrix. It can be noted that the parity check matrix of the 4k LDPC code is maintained.

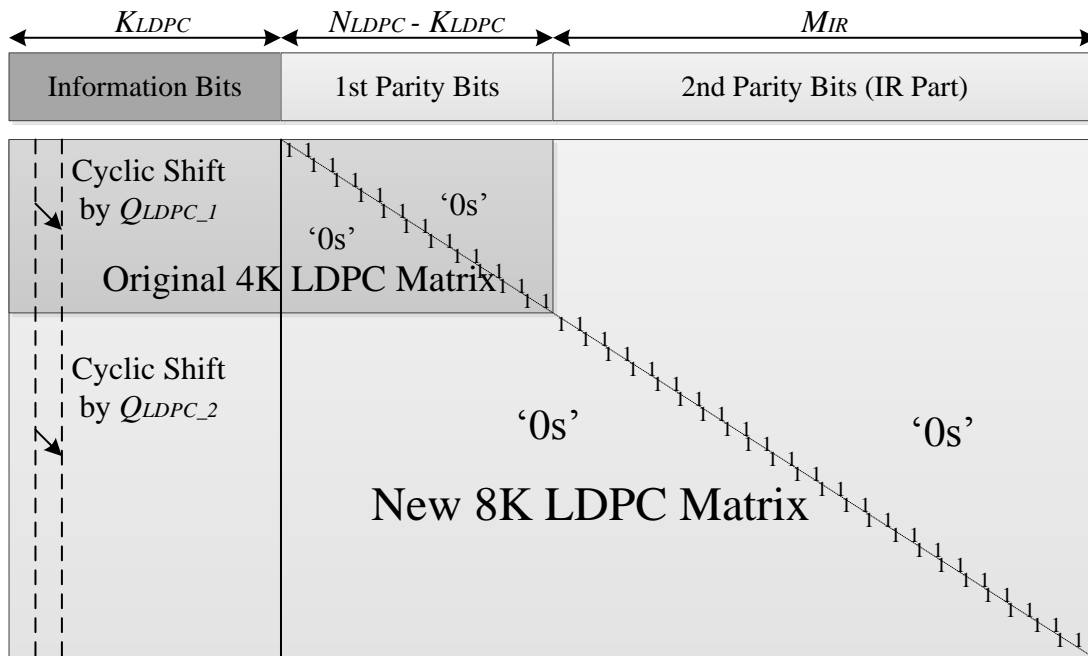


Figure 37: 8k LDPC parity check matrix with incremental redundancy.

The use of IR is determined by the code rate control mechanism depending on the AP configuration and the length of the L1-post signaling information. In particular, IR is applied when the amount of required parity bits is larger than the original 2160 bits generated by the 4k LDPC 1/2 code.

1.6.3.4 L1 Signaling Robustness Comparison in DVB-T2 and DVB-NGH

Figure 38 compares the robustness of the L1-post signaling in DVB-T2 and DVB-NGH. The performance has been evaluated with physical layer simulations for the mobile channel TU6 (6-Tap Typical Urban) for a Doppler frequency of 80 Hz. The modulation is QPSK, bandwidth is 8 MHz and the FFT size is 8K. The size of the L1-pre is representative for 8 PLPs. In the figure, it can be noted that DVB-NGH considerably improves the robustness of the L1-post compared to DVB-T2. The gain due to the use of 4k LDPC (i.e. without repetition and without additional parity) is around 1 dB. The difference in SNR between the most robust configurations in DVB-T2 and DVB-NGH is around 4 dB.

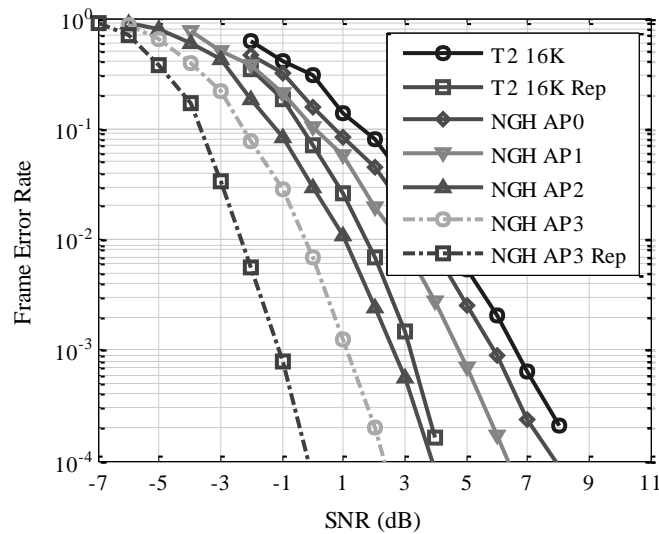


Figure 38: Robustness comparison of the L1-post in DVB-T2 and DVB-NGH. Modulation is QPSK. TU6 channel with 80 Hz Doppler. Bandwidth 8 MHz, FFT 8K.

1.6.3.5 L1 Signaling Robustness Performance Evaluation

The main objective in this section is to investigate the robustness of the DVB-NGH signaling path in terrestrial channels. As it has been explained before, it is important that the signaling path is transmitted at least 3 dB more robust than the data path in order to ensure the correct reception of the services. In DVB-T2, the data path with the most robust MODCOD QPSK 1/2 can be more robust than the L1 signaling path in mobile channels due to the short time interleaving of the L1 signaling. The use of L1-repetition can improve the robustness of the transmission (although recall that it is not useful in the reception of the first frame), but is not sufficient to ensure a 3 dB advantage for the L1-post signaling when the data path is transmitted with QPSK. In this case, the advanced decoding technique described next is needed.

1.6.3.5.1 Advanced Decoding of L1-post

Advanced receivers can improve the robustness of the L1 signaling by re-using the information that has been decoded successfully in previous frames and that is also transmitted in the current frame when decoding the LDPC codewords. This is the case of the L1-config part, which generally remains the same from frame to frame. If L1-repetition is used, this technique can also be applied to the L1-dynamic part of the previous frame that is transmitted in the current frame.

This technique can be applied to both DVB-T2 and DVB-NGH. It should be pointed out that none of these techniques improves the robustness of the L1 signaling during the reception of the first frame.

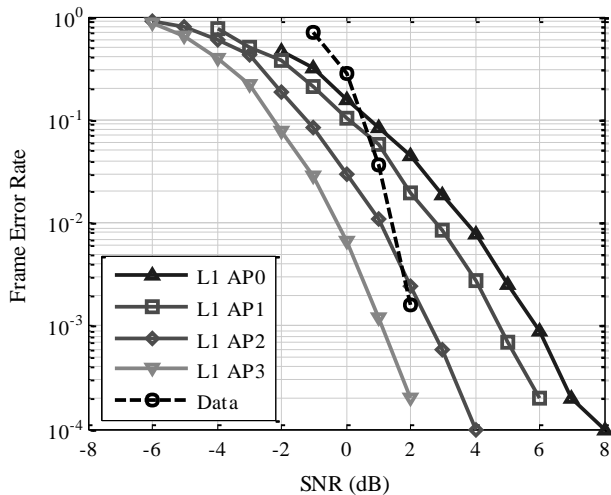
1.6.3.5.2 Simulation Results

Table 10 shows the simulation parameters for the terrestrial TU6 channel model. The data transmission mode is QPSK 1/3. The modulation assumed for the L1 signaling is BPSK. 8 PLPs have been considered to compute the L1 signaling information. The effective code rate depends on the configuration of the AP ratio: AP0, AP1, AP2, and AP3.

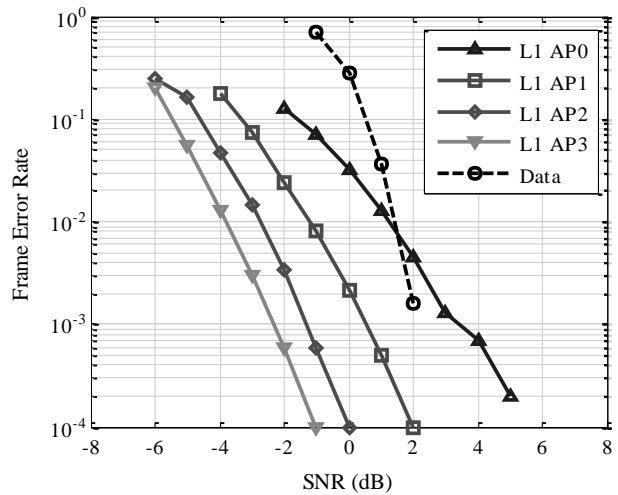
Table 10: Simulation parameters for the terrestrial profile of DVB-NGH.

Parameter		Value	Parameter		Value
OFDM	FFT Size	8192	Channel	Model	TU6
	BW	8 MHz		Doppler	33.3 Hz
	GI	1/4	Data	MODCOD	QPSK 1/3
	Pilot Pattern (PP)	PP1		Time Interleaver	Type 1 PLP
Time Slicing	NGH frame	50 ms	L1	Modulation	BPSK
	Cycle Time	300 ms		Nr. PLP	8 PLPs

Figure 39 shows the performance of the L1 signaling transmission in the terrestrial TU6 mobile channel with 4k LDPC, additional parity and incremental redundancy, with and without L1-repetition and advanced L1 decoding. The performance of the data path for QPSK 1/3 is also shown for comparison. The required SNR to achieve a frame error rate (FER) of 1% is 1.4 dB.



(a) Reference case without L1-repetition and without advanced L1 decoding.



(b) Advanced L1 decoding.

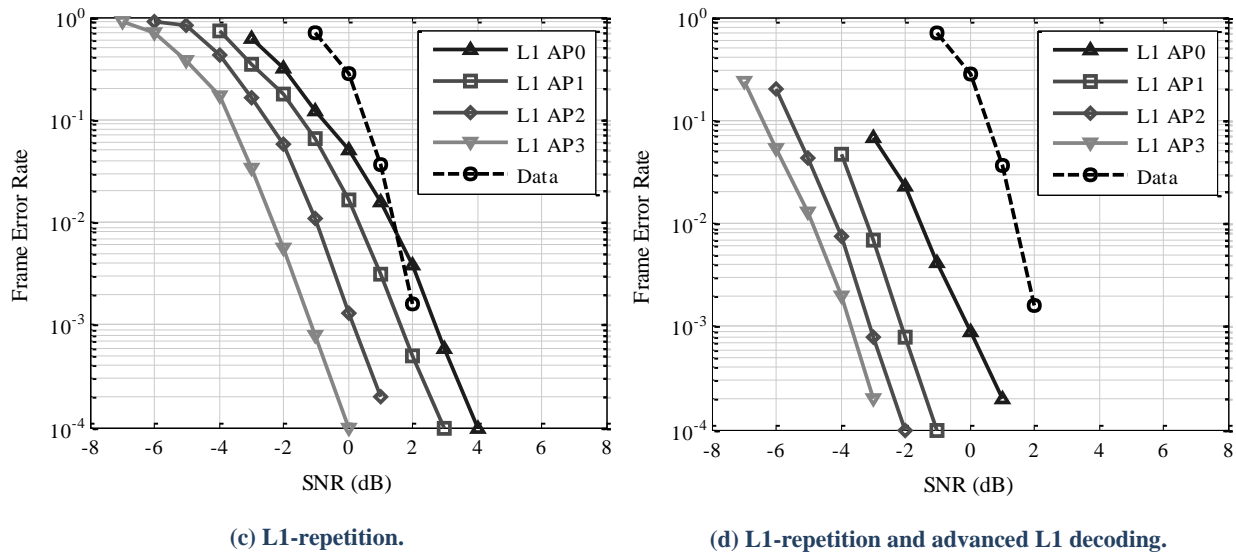


Figure 39: Robustness of the L1 signaling in the terrestrial TU6 mobile channel.

In Figure 39(a), we can see that without L1-repetition and without advanced L1 decoding, only the most robust AP3 configuration is more robust than QPSK 1/3 at FER 10^{-2} (and only 1.4 dB). Advanced L1 decoding provides a SNR gain between 2.2 dB and 3 dB, yielding together with AP2 and AP3, 2.5 dB and 4.5 dB more robustness than QPSK 1/3, respectively, see Figure 39(b). L1-repetition provides a similar gain than advanced decoding (between 2.5 dB and 3 dB), see Figure 39(c). The gain with both advanced decoding and repetition is in the order of 4 dB and 4.5 dB. In this case, AP0 is already 3 dB more robust than the data path. There is thus room for using the most robust MODCOD for the data path QPSK 1/5.

1.6.4 Conclusions

DVB-NGH has enhanced the physical layer signaling of DVB-T2 in three aspects: reduced overhead, higher capacity, and improved robustness. The overhead improvements allow reducing the signaling overhead and increasing the system capacity between 1% and 1.5% without affecting the system performance. The capacity enhancements allow signaling all five profiles of DVB-NGH (sheer terrestrial SISO, MISO, and MIMO; and hybrid terrestrial-satellite SISO and MIMO) without any restriction on the number of PLPs used in the system. Finally, the robustness improvements allow supporting extremely robust MODCODs for the data path such as QPSK 1/5 for both terrestrial and satellite mobile channels.

2 SCALABLE VIDEO CODING IN DVB-T2 AND DVB-NGH

2.1 SVC in Mobile Broadcasting DVB Systems

Current commercial DVB-H offerings mainly employ the H.264/AVC video codec with QVGA (Quarter Video Graphics Array) resolution [4]. However, a promising development as far as video coding is concerned is the extension of the H.264/AVC standard known as Scalable Video Coding (SVC), recently adopted within the DVB toolbox. SVC is an amendment to the H.264/AVC standard to provide efficient scalability functionalities on top of the high coding efficiency of H.264/AVC. SVC encodes the video information into a base layer and several enhancement layers [19]. While the base layer is compliant with H.264/AVC, and ensures backwards-compatibility with existing devices, the enhancement layers bring additional information that increases video quality, resolution, and/or frame rate.

SVC presents a great potential to achieve a more efficient and flexible provisioning of mobile TV services in DVB-H/SH systems. Compared to using a simple simulcast approach, SVC reduces the overall data rate required to cope with heterogeneous receivers' capabilities (e.g., screen size, processing power), by

distributing different service qualities within a single scalable stream. SVC also enables a more efficient usage of the allocated bandwidth, since it provides more flexibility for statistical multiplexing algorithms [20].

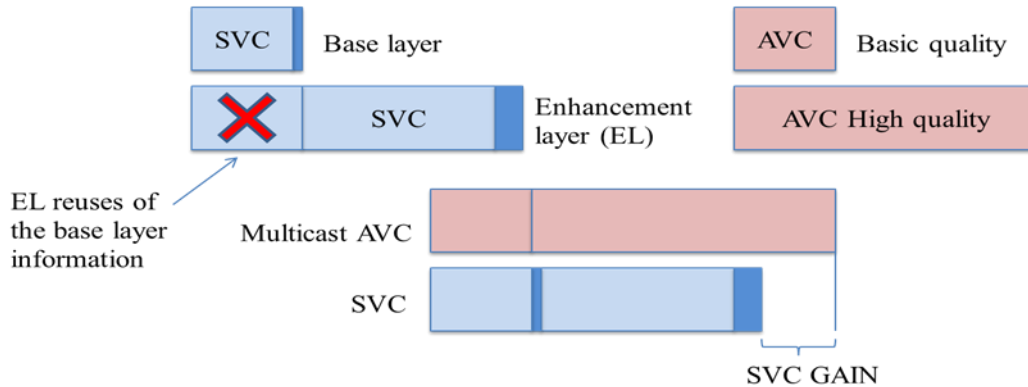


Figure 40: Diagram comparing multicast and scalable video coding (SVC) solutions.

SVC does not only provide benefits in terms of bandwidth savings, but potentially also in terms of improved coverage. SVC can provide a graceful degradation of the received service quality when suffering strong channel impairments by protecting more heavily the SVC base layer.

Scalable coding is very attractive in mobile broadcasting applications because it allows simple rate and format adaptation and efficient support for heterogeneous receiving devices and varying network conditions. A video stream is called scalable if it can be truncated in such a way that the resulting sub-streams can still be decoded providing lower reconstruction quality or resolution than the original stream.

SVC is a scalable extension of H.264/AVC that provides temporal, spatial, and quality scalability (and any combination of those). Its stream has a layered structure consisting of a base layer that can be decoded by H.264/AVC decoders (ensuring backwards compatibility), and one or more enhancement layers.

2.1.1 Spatial scalability

Spatial scalability involves generating two or more layers with different spatial resolutions from a single video source. The base layer is encoded at a low resolution and the enhancements layers make possible to increase the resolution of the video. In the following figure it can be seen an example of spatial scalability. Also it is shown the GOPs of the base layer (this GOP is consisted of frames red and blue) and the enhancement layer (GOP is consisted of frames red, blue and green).

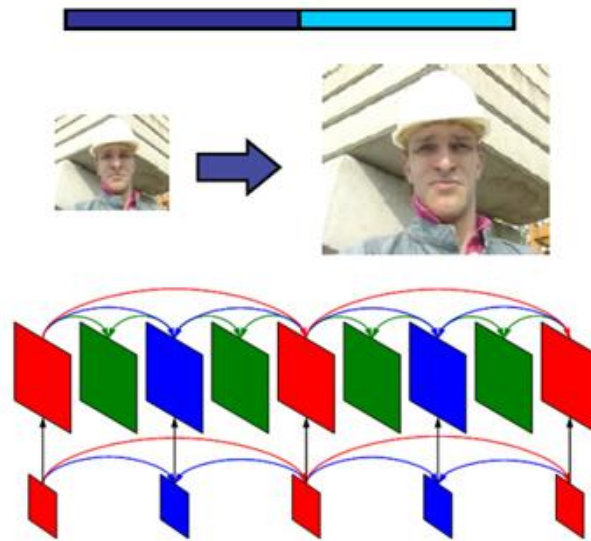


Figure 41: Spatial scalability.

2.1.2 Temporal scalability

Temporal scalability involves partitioning of video frames into layers, in which the base layer is coded to provide the basic frame rate and the enhancement layer(s) is coded with temporal prediction with respect to the base layer. In the Figure 42 it is shown the part of GOP transmitted by the base layer (frames painted red, green and blue) and the part transmitted by the enhancement layer (yellow frames). The base layer generates a video with bit rate B and the combination of base and enhancement layers generates a video with bit rate $2B$.

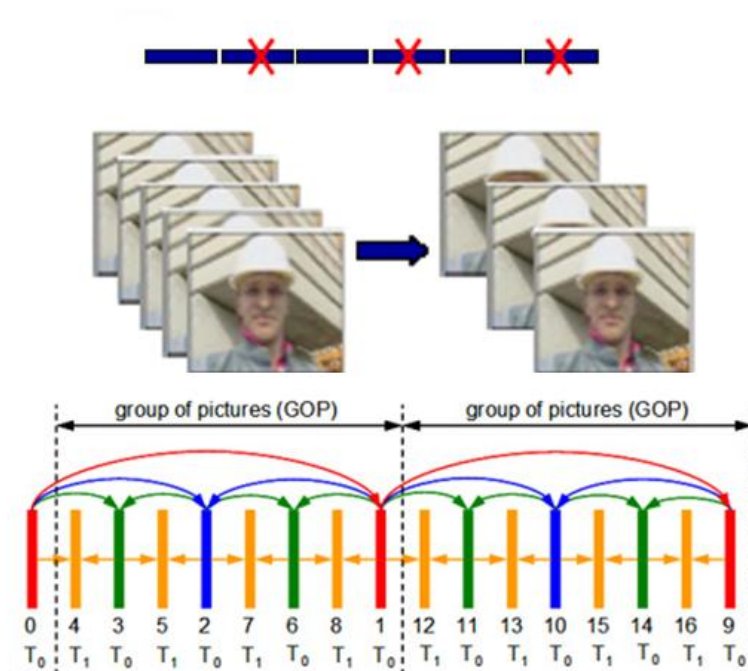


Figure 42: Temporal scalability

2.1.3 SNR scalability

Unlike the spatial and temporal scalability, in the SNR scalability all layers have the same resolution and frame rate. The difference between the layers is the quality, typically quantified by PSNR method. In following figure it can be seen an example of SNR scalability. The blue flow and red flow, which are shown in Figure 43, are corresponded to base layer and enhancement layer respectively.

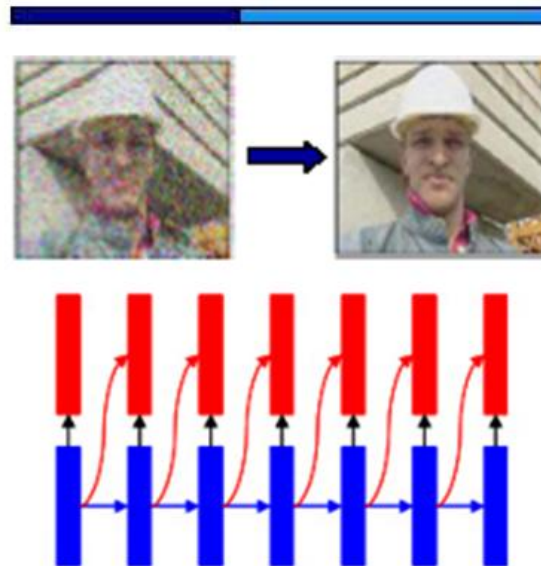


Figure 43: SNR scalability.

By this way, the more enhancement layers the receiver decodes the higher the reconstruction video quality. An overview of SVC broadcasting in mobile DVB systems is presented in [19].

2.2 SVC Delivery in DVB-T2

2.2.1 SVC Delivery Using Multiple PLPs

The support for multiple PLPs in DVB-T2 is ideal for broadcasting scalable video, due to the possibility to use different coding and modulation parameters for the various SVC layers. The base layer may then be broadcast in a robust PLP, while the enhancement layer(s) may be broadcast in less robust PLPs with higher spectral efficiency.

In order to simulate realistic reception conditions, we based our simulations on field measurements using regular DVB-T USB sticks (Hauppauge WinTV Nova-T) connected to a laptop. The USB sticks were only used to read variations in carrier-to-noise (C/N) ratios to be used in simulations. The measured C/N ratios were input into a DVB-T2 physical layer simulator, where the DVB-T2 performance at the desired modulation and coding settings was simulated. From the DVB-T2 simulator we obtained baseband frame error traces, which were converted into TS packet error traces. The TS error traces were, in turn, converted into SVC packet error traces giving us information on which layers of video were lost.

When analyzing the SVC packet error traces, we assumed that if one frame of an SVC layer inside a group of pictures (GOP) was lost, that layer and any layer dependent upon it was not decodable for the entire duration of the GOP. In reality, a good SVC decoder would be able to more or less effectively conceal some errors, depending on which frame in a GOP is lost. Furthermore, we ignored the possible impact of some packet headers resulting from encapsulation of SVC video in an MPEG-2 TS stream, but instead we assumed that the raw NAL (Network Abstraction Layer) packets of the SVC stream were directly encapsulated in TS packets.

Preliminary simulations were based on a 750-second field measurement. We simulated the use of two PLPs, where one PLP used a 16-QAM configuration with $\frac{1}{2}$ code rate, while the other was set to 64-QAM, $\frac{1}{2}$ -rate. An SVC video clip was encoded, where the base layer was coded in 640x360 resolution at 25 frames per second (fps), and the enhancement layer resolution was 1280x720 at 50 fps. The average bitrates of the base layer and enhancement layer were 2048kbps and 7168kbps, respectively. The GOP size for the enhancement layer was 16 frames (8 frames for the base layer).

Figure 44 shows the results from these preliminary simulations. The figure shows the measured C/N ratios, the average bit error rate in a simulated TI-block, as well as which SVC layers were successfully recovered per GOP (0 means no layers, 1 means base layer only, and 2 means both base and enhancement layers were recovered).

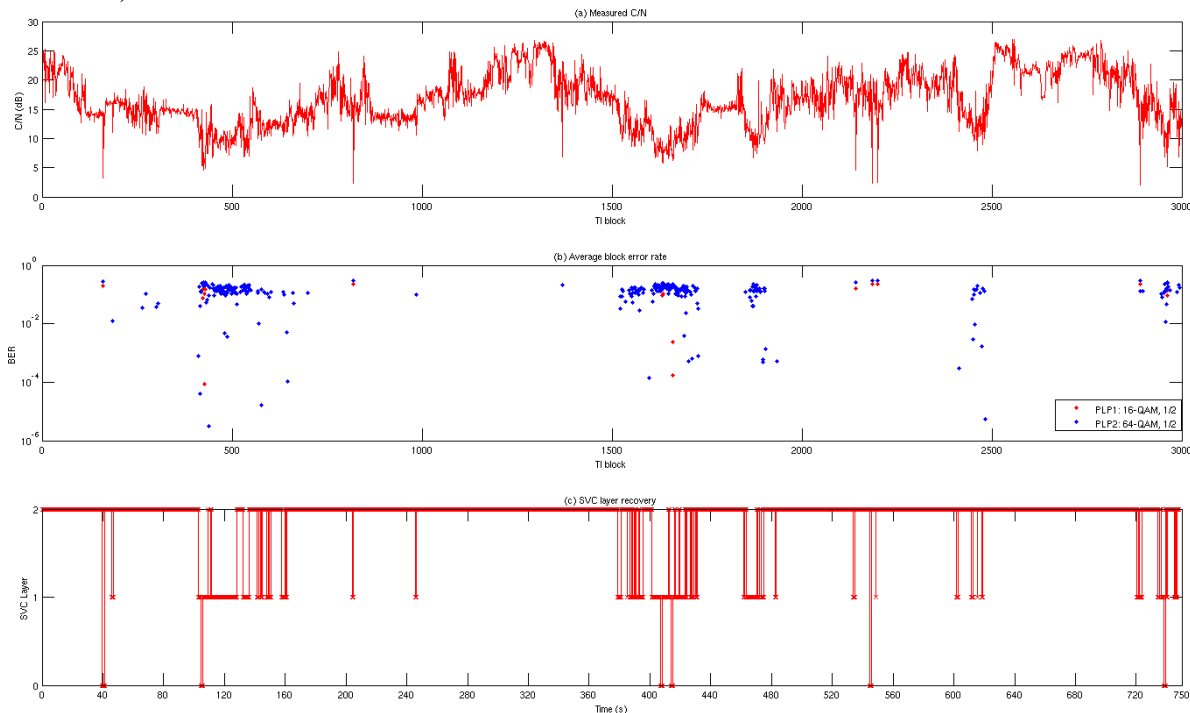


Figure 44: (a) The measured C/N ratios over the 750-second (3000 TI-blocks) field measurement round. (b) The average BER in each simulated TI-block for both PLPs. (c) The number of recovered SVC layers per GOP.

With this configuration, we found that the ESR5(20) (at most 1 erroneous second in a 20-second segment) criterion was fulfilled in about 49% of the 20-second segments for the enhancement layer, while the criterion was fulfilled 84% of the time for the base layer. From Figure 44, we can see that loss of the base layer is often caused by short sudden drops in signal quality. These losses could perhaps be avoided by using for example upper layer FEC coding for longer time interleaving. In some cases, however, the sudden drops in quality may also be a result of an incorrectly read or calculated C/N value from the receiver, rather than actual channel conditions.

2.2.2 Field Measurement Based SVC Performance Analysis over DVB-T2 Lite

In this section, broadcasting of SVC in a DVB-T2 Lite system is explored. Given equal bandwidth utilization and video quality constraints, the broadcasting of SVC video is compared to the simulcasting of separately coded H.264/AVC video streams. The study is based on a time series of real world measured signal strengths combined with DVB-T2 Lite physical layer simulations, and the results indicate that broadcasting of SVC provides an overall better end-user experience as compared to simulcasting of AVC video.

In order to simulate realistic reception conditions, the simulations were based on a field measurement campaign performed in the city of Turku, Finland (the field measurements were performed by Turku

University of Applied Sciences). These field measurements were performed by measuring the signal strength (in dBm) of DVB-T transmissions while going by bike around the city. Signal strength measurements were performed using a Rohde&Schwartz TSM-DVB test receiver. GPS coordinates were also logged for each measurement point. The measured signal strength values, which were sampled 20 times per second, were converted to Carrier-to-Noise Ratios (CNR) assuming a constant noise level of -70 dBm. With this assumption data series with realistic CNRs were obtained.

Using a DVB-T2 physical layer simulator, DVB-T2 baseband frame error rates were generated at CNR values 0.1 dB apart for all desired modulation and coding settings. These generated CNR to frame error rate tables were then used as lookup tables to estimate the DVB-T2 physical layer performance given the time series of CNR values obtained from field measurements. This use of lookup tables instead of inserting the measurement-based CNR values directly into the DVB-T2 simulator, gave the possibility to rapidly estimate the DVB-T2 performance in very long time series for all desired configurations. The channel model employed in all simulations is the time-variant FIR-filter based model described in [21]. The FIR-filter based model mimics the channel conditions experienced during a DVB-T2 channel sounding campaign carried out in Helsinki, Finland in 2010.

From the estimated baseband frame error probabilities, baseband frame error traces were produced, which were analyzed to determine when video packets would have been lost. While in reality, video would be transported in containers, such as MPEG-2 TS packets or GSE (Generic Stream Encapsulation) packets, the assumption was that the raw H.264 NAL (Network Abstraction Layer) packets were transported directly in the baseband frames.

2.2.2.1 DVB-T2 parameterization

A scenario in which a DVB-T2 Lite broadcaster would like to fit 6 video services into a single standard 8 MHz channel is considered. Consequently, only a small fraction of the available bandwidth is used for transmission of this service. The service bandwidth is further split onto two PLPs, with the physical layer parameters shown in Table 11.

Table 11: DVB-T2 Lite PLP Configuration

	Fraction of bandwidth	Modulation	FEC Rate	
			SVC	AVC
PLP1	0.5	16QAM	1/2	1/2
PLP2	0.5	64QAM	1/2	3/5

As seen in the table, each of the PLPs consumes 50% of the available service bandwidth. PLP1 is used for transmitting either the SVC base layer stream or the low quality AVC stream. Consequently, the physical layer code rate is chosen to the most robust one in DVB-T2, i.e. to 1/2. The modulation is also chosen to a sufficiently low order to obtain reasonable transmission rates, while not compromising the robustness significantly. On the other hand, PLP2 allows the use of a lower code rate for the SVC enhancement layer stream as compared to the high quality AVC stream, under the assumption that the complete AVC and SVC streams (low quality and high quality) require an equal bandwidth. According to the DVB-T2 Lite profile, the LDPC code lengths are all 16200 bits. With these settings, the number of FEC frames within each time interleaver (TI) frame is 29 and 44, for PLP1 and PLP2 respectively. In this study a time interleaving length of 250 ms was assumed. The division of the video streams into PLPs under these assumptions is conceptually visualized in Figure 45. In the following subsection, we motivate the choice of different code rates for PLP2 between the SVC and AVC cases, which follows directly from the SVC video coding gain versus simulcasting of AVC.

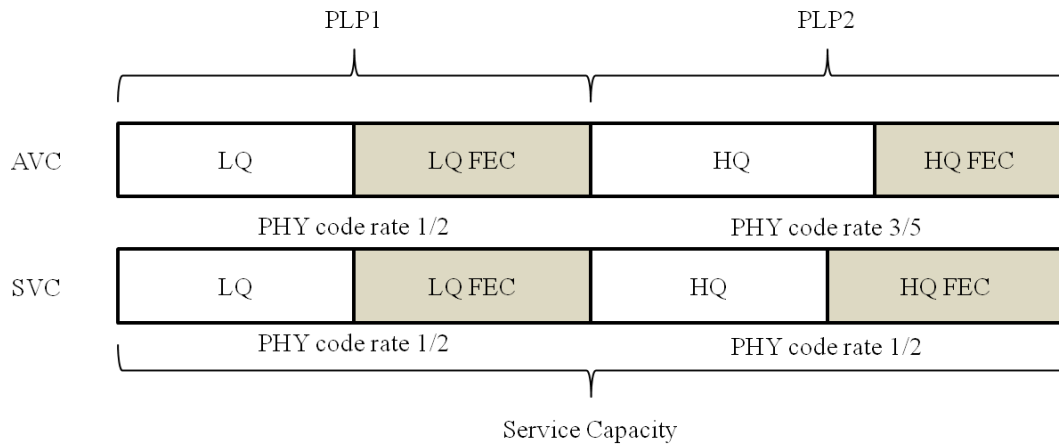


Figure 45: Division of the low and high quality (LQ and HQ) AVC and SVC services into PLPs for a fixed service capacity. A fraction of each PLP, equal to 1 - PHY code rate, is used for transmission of parity (FEC) data.

2.2.2.2 Video Coding

With SVC, the base and enhancement layers are transmitted in the two different PLPs, and the assumption is that both PLPs are required to be received without errors in order to reconstruct the enhancement layer. When simulcasting using AVC, independent single-layer streams are broadcasted within the two PLPs. In this study, only quality scalability is used, i.e. frame rate and spatial resolution is kept constant across layers. The encoder employed for both single-layer AVC and dual-layer SVC streams was the Joint Scalable Video Model (JSVM) version 9.19. JSVM is the reference software for SVC. In all encodings, the group of picture (GOP) size was set to 16 frames (this was also the intra period), and fast motion search was enabled. Video bit rate and quality were varied by modifying the basis quantization parameter of the encoder. The video clip used for encoding was *pedestrian_area*. The spatial resolution of the video was 960×544 (which is close to the native display resolution of several popular modern smart phones, and one quarter of full HD resolution), and the frame rate was 25 frames per second (fps).

For coding of the SVC stream, 16-QAM modulation with 1/2 code rate was used for the first PLP, and 64-QAM, 1/2-rate for the second. These settings imply a useful bitrate of $BR_1 = 791$ kbps for the base layer, and $BR_2 = 1199$ kbps for the enhancement layer. Once the maximum useful bitrates of the two PLPs were determined, one dual-layer SVC clip was first encoded, where the base layer was limited to a maximum bitrate of BR_1 and both layers together were limited to a maximum bitrate of $BR_1 + BR_2$. The mean PSNR (peak signal-to-noise ratio) of the luma component of these two layers were measured. Two single-layer AVC clips were also encoded, where the PSNR values were closely matched to the PSNR values of the two SVC layers, in order to keep video quality equal in both the SVC and AVC scenarios. The resulting bitrates and PSNR values of the encoded SVC layers and AVC streams are shown in Table 12. The cumulative bitrate is the total bitrate required for both sub-services in each case.

Table 12: Properties of the coded video sequences

Type	Bitrate (kbps)	Cumulative bitrate	PSNR (dB)
SVC BL	791	791	37.73
SVC EL	1199	1990	41.29
AVC LQ	796	796	37.84
AVC HQ	1573	2367	41.21

It can be observed from Table 12 that the bitrate of the AVC high quality stream is significantly higher than BR_2 , and would not fit into the 64-QAM 1/2-rate PLP specified earlier. The code rate has to be raised to 3/5 to fit that stream into the second PLP, given the same overall channel capacity constraints.

2.2.2.3 Simulations

From two different measurement routes, a baseband frame error trace was produced as described earlier. This was done for all the used modulation and code rate configurations, i.e. 16-QAM, 1/2-rate, and 64-QAM 1/2-rate and 3/5-rate. The properties of the measurement routes are shown in Table 13. Note that the suburban route 1 is significantly shorter than the urban route 2.

Table 13: Properties of signal strength measurement routes

Route	Environment	Number of samples	Samples per second
1	Suburban	27270	20
2	City center	192038	20

Figure 46 shows the CNR ratios as well as baseband frame error rates within T2 frames for all three combinations of modulation and code rate chosen earlier. It is quite apparent that route 2 as shown in Figure 46b is more varying in terms of CNR values than route 1 (Figure 46a). It can also be seen that especially the 64-QAM configurations suffer from several quite long bursts of high baseband frame error rates.

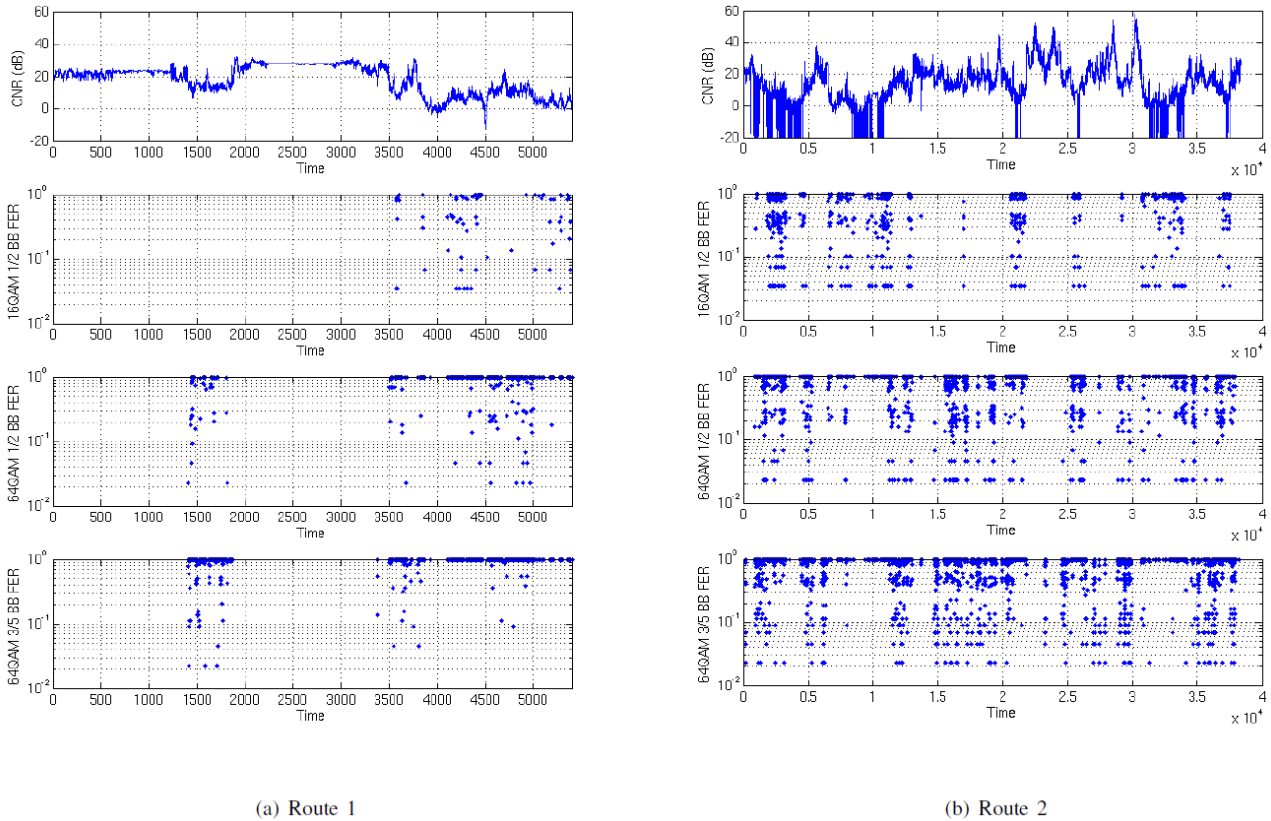


Figure 46: CNR measures, as well as baseband frame error rates per DVB-T2 frame for measurement routes 1 and 2. The x-axis of the figures is time measured in the number of T2 frames, where one frame has a duration of 250 ms.

When analyzing the baseband frame error traces, the assumption was that if one or more baseband frames of an SVC layer or an AVC stream was lost within the duration of one group of pictures (GOP), that layer and any layer dependent upon it was not decodable for the entire duration of the GOP. In reality, a good video decoder would be able to more or less effectively conceal some errors, depending on which frame in a GOP is lost. The duration of one GOP in this case is $16/25 = 0.64$ seconds.

Table 14 shows the GOP Recovery Rates (RR) as well as ESR 5% (erroneous second ratio 5%) fulfillment for the various streams. The GOP recovery rate is expressed as the percentage of full GOPs that are received error-free. The ESR 5% criterion usually corresponds to 1 second of errors over a 20 second observation period, and has shown to be highly correlated with the subjectively perceived reception quality [22]. In this

paper, we modify the criterion slightly to mean that no more than 2 GOPs per 40 consecutive GOPs may be lost. The ESR 5% fulfillment ratio thus expresses how often we fulfilled this criterion on the measured routes.

Table 14: GOP Recovery Rates (RR) and ESR 5% fulfillment for the two measured routes.

Layer	Route 1		Route 2	
	GOP RR	ESR 5%	GOP RR	ESR 5%
SVC BL/AVC LQ	96%	83%	95%	73%
SVC EL	80%	60%	77%	52%
AVC HQ	70%	55%	60%	36%

By analyzing Table 14, it can be seen that the base layer and AVC low quality stream is significantly more robust than the high quality SVC and AVC streams. Roughly 5% of the low quality GOPs on both measurement routes is not received correctly. The large variations in CNR ratios of route 2 can be seen as a lower ESR 5% fulfillment compared to route 1. When comparing the SVC enhancement layer and AVC high quality stream, a clear improvement in performance is observed when using SVC, due to the possibility of using a lower code rate. SVC provides approximately 14% and 28% improvement in GOP recovery rate compared to the AVC single-layer case on routes 1 and 2, respectively. Likewise, ESR 5% fulfillment is improved by 9% and 44%, respectively, in favor of SVC.

The large differences in performance between the three combinations of code rate and modulation is further explained by Figure 47, which shows simulated DVB-T2 bit error rates over a range of CNR values over the FIR-filter based channel model for all three configurations used in this study. From the figure, it can be seen that in order to achieve quasi error free reception with 64-QAM 3/5-rate, an almost 4.5 dB higher CNR ratio is required as compared to 64-QAM 1/2-rate. This means that when making use of SVC, the transmitter power could be reduced by this amount, or the area within which high quality reception is possible will be larger than when using single-layer simulcast. The difference of around 5dB between 16-QAM and 64-QAM 1/2-rate is also very significant, providing a much more robust low quality stream compared to the high quality versions, which is confirmed by the analysis in Table 14.

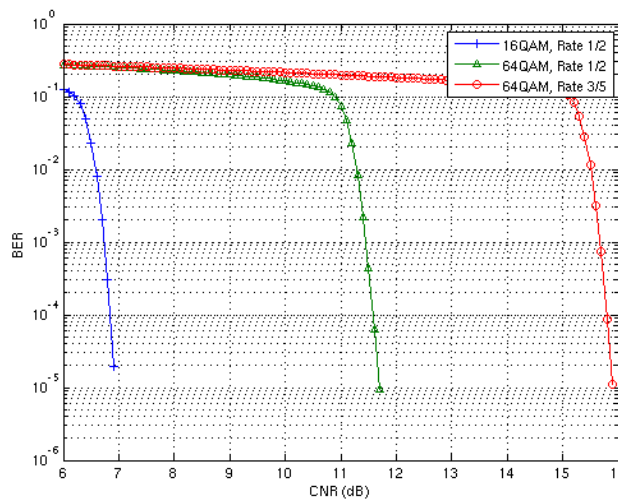


Figure 47: Simulated BER vs CNR for the three example combinations of modulation and code rate.

2.2.3 SVC Delivery Over Multiple Channels

The following section designs a demonstrator for the delivery of video using Scalable Video Coding (SVC) standard simultaneously over multiple (fixed) channels: over DVB-T2 networks and over high-speed Internet. We pursue the two following objectives:

- To improve bandwidth usage in DVB-T2 and optimize network planning

- To ensure the coverage of advanced video services for population distant to broadcast infrastructure or living in unfavourable signal-propagation areas
- To verify the inherent benefits of SVC in terms of scalability and adaptivity of the systems

As we see in the following section, the approach proposed is to send the full-quality video content over T2 using a multi-PLP configuration, splitting the video into a base layer and several enhancement layers. These enhancement layers will also be streamed simultaneously over high speed Internet. The content can consist of either a high-definition video or a 3D video. The base layer will offer a basic version of the HD video (either a SD or a more basic HD mode) in the first case and a 2D version in the second case.

2.2.3.1 IP encapsulation for DVB-T2 transport

DVB-T2 provides two main encapsulation protocols, the MPEG-2 TS packetization, which has been the classical encapsulation scheme for DVB services, and the Generic Stream Encapsulation (GSE), which was designed to provide appropriate encapsulation for IP traffic.

The standard ways to carry IP datagrams over MPEG2-TS are Multiprotocol Encapsulation (MPE) and Unidirectional Lightweight Encapsulation (ULE). However, their design was constrained by the fact that DVB protocol suite used MPEG2-TS at the link layer. MPEG-2 TS is a legacy technology optimized for media broadcasting and not for IP services. Furthermore, the MPE/ULE encapsulation of IP datagrams adds additional overheads to the transmitted data, thus reducing the efficiency of the utilization of the channel bandwidth.

An alternative to MPEG2 TS is GSE which was design mainly to carry IP content. GSE is able to provide efficient IP datagrams encapsulation over variable length link layer packets, which are then directly scheduled on the physical layer BB frames. Using GSE to transport IP datagrams reduces the overhead by a factor of 2 to 3 times when compared to MPEG-TS transmission.

For simplicity reasons, we will consider the traditional MPE technique in the demonstrator, since the IP encapsulation choice does not have a decisive influence on the pursued results.

2.2.3.2 Demonstrator architecture

The following figure illustrates the functional blocks of the communication infrastructure of SVC content delivery demonstrator through DVB-T2 and IP networks in mobile scenario. The upper part of the figure represents the SVC Server, which handles the raw video to convert it in SVC streaming in the proper format for the transmission. The bottom part of the figure shows the modules in charge of the reception and decoding of the content. The schema is general enough to allow the testing with different video standards, such as H.264/MPEG-4-AVC y its SVC extension.

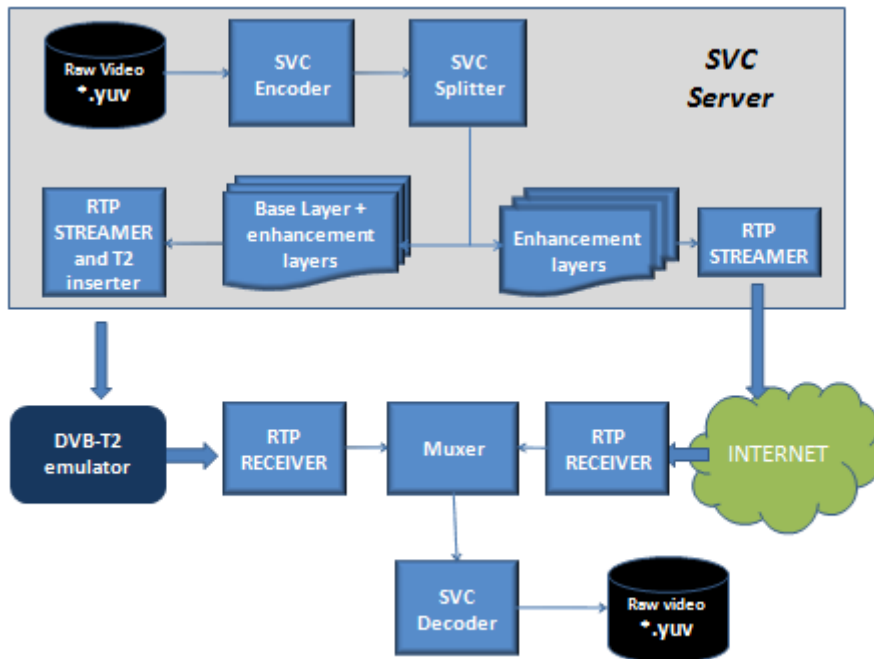


Figure 48: Block diagram of demonstrator

The modules above are programmed in C++ and currently they are in development stage. Next, we present a description of the main blocks.

The SVC ENCODER allows video coding operations according to SVC standards (ISO/IEC 14496-10 / Amd.3 Scalable video coding) and AVC/H.264 (MPEG-4 Part 10 AVC, ISO/IEC 14496-10). As SVC coder, it can scale the video in the three dimensions specified by the standard: temporal, spatial and quality domain. In case of temporal scalability, the coder only allows 3 scalability layers. Finally, the module requires raw video as input that has to be previously stored in one of the following formats: YUV 4:0:2, YUV 4:2:2, YUV 4:4:4, RGB 24 bits.

The SVC coding of high definition video content for the tests will consist of taking the standard definition version of the video as the base layer and one or more enhancement spatial layers providing the extended resolution.

The encoder naturally supports scalable coding of stereo (3D) video by sequential interleaving of right and left views using the present SVC MCTF structure without update steps. It has already been shown that the coding efficiency with hierarchical B pictures (MCTF without updates) and a closed-loop control is higher or similar to that of the MCTF-based coding.

The SVC SPLITTER module allows splitting the original SVC video in several files that contains the different base and enhancement layers that will be transmitted over the two targeted communication channels.

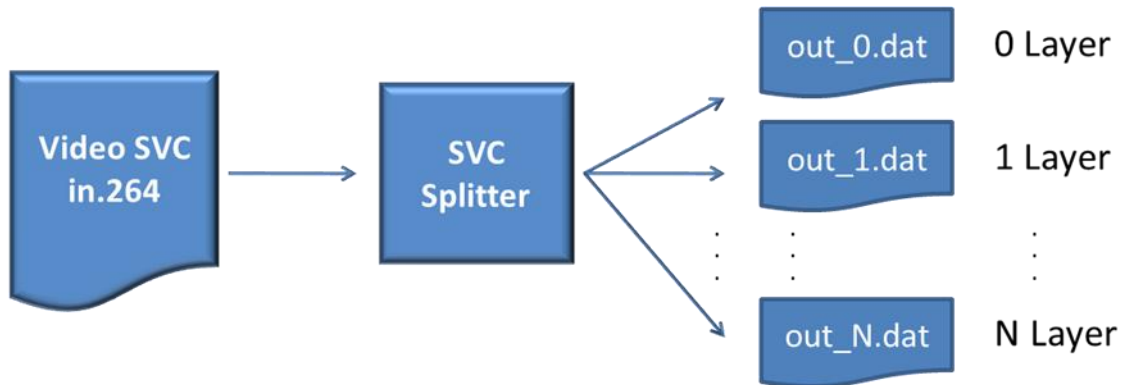


Figure 49: Block diagrams of SVC Splitter

This module receives an elemental SVC streaming and splits it in several sub-streaming. Each NALU (Network Abstraction Layer Unit) represents the unique structure of data which is possible to find in each SVC video streaming. There are 31 types of NALU. Each NALU is associated to a DTQ (Dependency, Temporal y Quality) which describes the essential parameters of SVC layer. Therefore the Splitter is a like a “NALU multiplexor” that analyzes the input video and forward the different NALUS to output sub-streaming according to the layer of such NALU. The following table summarizes a trace file of NALU with information of its associated layer.

i_Nalu	Type	Nalu_Size	Spatial	Temporal	Quality	Nº Layer
16.	14	9	X	X	X	0
17.	1	1837	X	X	X	0
18.	20	59	1	1	0	1
19.	20	82	2	1	0	2
20.	20	2749	1	2	0	1
21.	20	1210	2	2	0	2
22.	20	290	1	2	0	1

Annotations in the table: A red arrow points from the '0' in row 16 to 'Base layer'. Blue arrows point from the '1' in row 18 and '2' in row 19 to 'Layer 1'. Red arrows point from the '2' in row 21 to 'Layer 2'.

Figure 50: SVC Splitter

The SVC splitter also routes the different SVC layers to the targeted communication channel, this is different PLPs in the DVB-T network and the high speed Internet channel. The PLP destined to transport the enhancement layers will have a high efficient modulation scheme, requiring a very high C/N. This means that only areas close enough to the transmitter will be able to receive the enhancement layers. On the other hand, the PLP bearing the base layer will be configured with a highly robust MODCOD, so that a large area can be served with a minimum service quality.

The RTP STREAMER module encapsulates and transmits the RTP/IP streaming of the base layer, which is one of the outputs of the SVC Splitter. The encapsulation is done according to the H.264 / MPEG-4 AVC payload format, since this format is compliance with SVC standard. The output RTP streaming is broadcasted in DVB-T2 network. The streaming is received by the RTP Receiver that processes it and generates the base layer of SVC video.

The MUXER module rebuilds the SVC video from the layers generated in the SVC Splitter. The main feature of this module is to build the SVC video with the available layers while discarding if needed selected layers or layer segments due to detected errors or end user terminal limitations. One of the most critical problems to solve in the muxer is the synchronization between the different received layers.

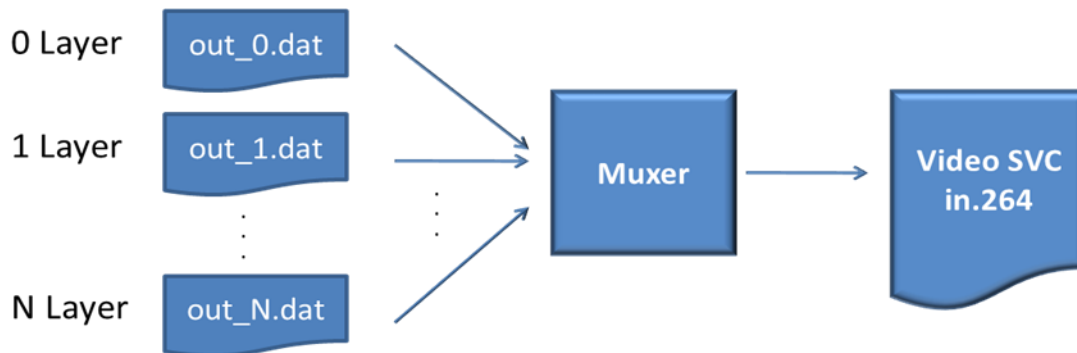


Figure 51: Block Diagrams of Muxer

The RTP SVC streamer module encapsulates the local SVC video in RTP/IP streams according to standard H.264/MPEG-4 SVC and transmits the video in unicast mode. This tool offers several functionalities related to the transport of the NALUs payload in RTP format for H.264 and SVC, such as SNU, STAP, MTAP and FU as specified by IETF and reflected in the above figure. The RTP module will take into account the fact that the base layer on the one hand and the enhancement layers on the other hand will be delivered using transmission bearers with different capacity and reliability characteristics.

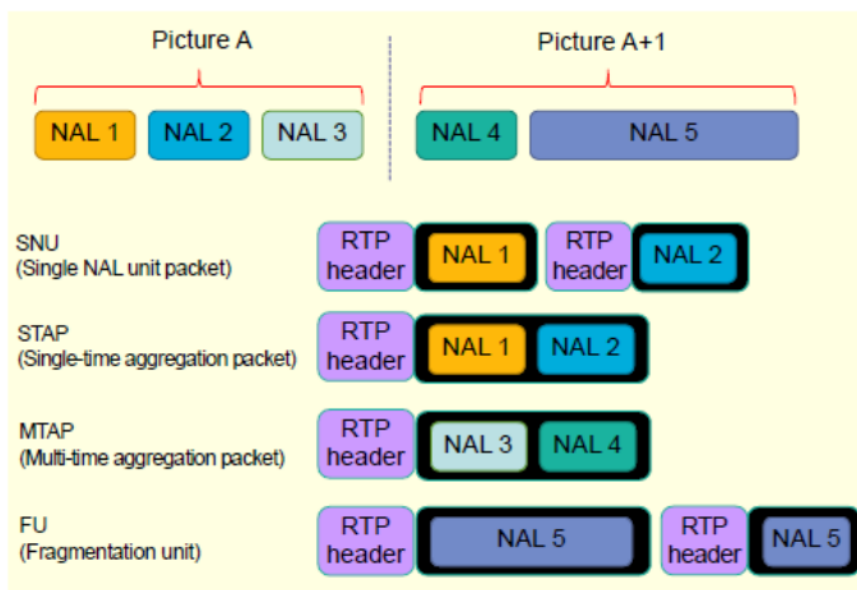


Figure 52: Basic RTP packets for SVC

It is for further study which RTP technique will be used for in the DVB-T2 bearer, taking into account both overhead minimization and interleaving features at the RTP layer.

The SVC decoder receives the RTP/SVC streaming (from RTP SVC), decodes it and creates a file with the raw video. It allows video decoding according to SVC (ISO/IEC 14496-10 / Amd.3 Scalable video coding) and AVC/H.264 (MPEG-4 Part 10 AVC, ISO/IEC 14496-10) standards. The output file can be customized to different versions of YUV format (YUV 4:0:2, YUV 4:2:2, YUV 4:4:4).

The DVB-T2 emulator is in charge of emulating in real time the DVB-T2 transmission channel, including propagation effects. An open source event-based network simulator named NCTUNs will be used for that purpose. In brief, three main components will be developed:

- a DVB-T2 gateway module featuring the T2 link layer at the transmitter side;

- a physical layer module (representing both the transmitter and the receiver) hosting performance profiles of the T2 physical layer under different propagation conditions (Gaussian noise, multipath, mobile etc.) and according to the received signal level at the receiver
- an RF module in charge of calculating the time-variant signal level received by the terminal according to the establish propagation scenario
- A DVB-T2 link-layer receiver module

The following configuration is preliminary proposed for the DVB-T2 PLPs to transport both the base and enhancement layers. The two first configurations are destined to test SD/HD services, and the third one will test 2D/3D services

Configuration	MODCOD		Bitrate		Content	
	PLP#1	PLP#2	PLP#1	PLP#2	PLP#1	PLP#2
#1	64QAM, FEC rate 4/5, GI 1/128, 32k, 56 blocks	256QAM, rate 4/5, GI 1/128, 32k, 127 blocks	13,2	30,5	SD (3-4 programmes)	720p+1080p (3-4 programmes)
#2	64QAM, FEC rate 5/6, GI 1/128, 32k, 80 blocks	256QAM, rate 5/6, GI 1/128, 32k, 99 blocks	19,2	24,6	720p (3-4 programmes)	1080p (3-4 programmes)
#3	64QAM, FEC rate 5/6, GI 1/128, 32k, 80 blocks	256QAM, rate 5/6, GI 1/128, 32k, 99 blocks	19,2	24,6	Several 2D (right channel reference)	Several 3D (left channel)

2.2.3.3 Conclusions

This section reports the current status of demonstrator that will be used to verify the delivery of broadcast video using Scalable Video Coding (SVC) over two different channels (DVB-T2 and high speed Internet) that complement each other in order to serve a coverage area with varying reception conditions: over DVB-T2 networks and over Internet.

2.3 SVC Delivery in DVB-NGH

The standardization process of the new mobile broadcasting system, known as DVB-NGH (next generation handheld), started at the end of February 2010. The main goal is to provide an efficient, flexible, and robust mobile broadcasting system to accompany the digital switch-over and the convergence of fixed and mobile services. One of the main commercial requirements of DVB-NGH is that it should allow transmission of scalable video content with UEP [20]. It is expected that DVB-NGH will be largely based on DVB-T2, the second generation standard for terrestrial television broadcasting [23]. Another commercial requirement is that DVB-T2 and DVB-NGH should be able to share a single multiplex in a time division manner, which can be achieved through the use of the DVB-T2 Future Extension Frames (FEF). Hence, DVB-NGH will have a discontinuous transmission scheme, such as those in DVB-H/SH. For the sake of discussion, we briefly review DVB-T2 and then point out the technical enhancements that are currently under consideration for DVB-NGH.

For the delivery of scalable video content with UEP in DVB-NGH, practical implementation and signalling issues are being evaluated for the cases of assigning one service to multiple PLPs, or having different modulations and code rates within a single PLP. Regarding MIMO, different schemes for the SVC base layer and enhancement layers are also being considered. While the MIMO schemes for the SVC base layer aim to increase the spatial diversity for improved coverage, the MIMO schemes for the SVC enhancement layers aim to increase the capacity with spatial multiplexing techniques [24]. Layer-aware FEC schemes are also being considered as a generic approach for UEP (both at the physical layer and the upper layers).

2.3.1 Multiple PLP solution

The input interface to the NGH system is one or more syntactically correct MPEG-2 TS or IP flows. Each contains one or more services with all service components. A service component is a flow that carries video, audio or any other information. For example, for the case when using the TS profile, a MPEG-2 TS may carry several SVC TV programs and each TV program requires two or more service component, one for audio and the others for the different SVC video layers. Hence MPEG-2 TS that must be transmitted requires different protection to different layers of SVC video, high robustness to base layer and audio and high efficiency to enhancement layers. The way to obtain this, it is using the multiple PLP solution.

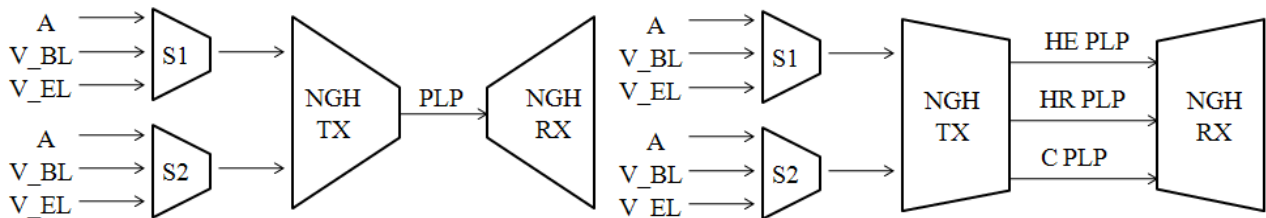


Figure 53: Example of transmission of two SVC programs for the single PLP case (left) and multiple PLP case (right).

This solution permits to transmit contents asymmetrically protected. Some PLP may be defined like PLP of high robustness (HR PLP), and therefore, the physical parameters of these PLP are selected to supply robustness. Others PLPs are used like PLP of high efficiency (HE PLP). These PLPs are capable of carrying more information in exchange for losing robustness. In the Figure 53 is shown an example of Multiple PLP transmission. In this example where it is transmitted two SVC TV services, the Common PLP (C PLP) is used to carry information common to several services, like PSI-SI signalling information or ESG. High Robustness PLP (HR PLP) is used to carry data of audio, base layer of video and radio. Finally, High Efficiency PLP (HE PLP) transmits enhancement video layers.

Moreover, two types of PLP have been defined for M-PLP mode, these types are named: anchor PLP and associated PLP. Common PLP, High Robustness PLP and High Efficiency PLP are associated PLP because they carry information of services but do not carry signalling information. Instead, Anchor PLP is responsible for transporting in-band signalling information for its service component and also for the associated service components.

The Task Force of Signalling and Upper Layers (SUL) has been working on different aspects as synchronization between PLP and SVC signalling services.

2.3.2 PLPs Synchronization

The synchronization between PLP that carry the different layers of the several NGN services is a critical aspect. The synchronization depends on the chosen profile. In DVB-NGH are defined two profiles, TS profile and IP profile.

The protocol stack of TS profile is shown in Figure 54. In this profile the multimedia contents are directly encapsulated over MPEG2 Transport Stream (MPEG2-TS). Transport stream specifies a container format encapsulating packetized elementary streams (video, audio and other information), with error correction and stream synchronization features for maintaining transmission integrity when the signal is degraded. The synchronization mechanism used in TS profile is Input Stream SYNchronizer (ISSY). ISSY is a BBHeader

field which carries the value of a counter clocked at the modulator clock rate and can be used by the receiver to regenerate the correct timing of the regenerated output stream.

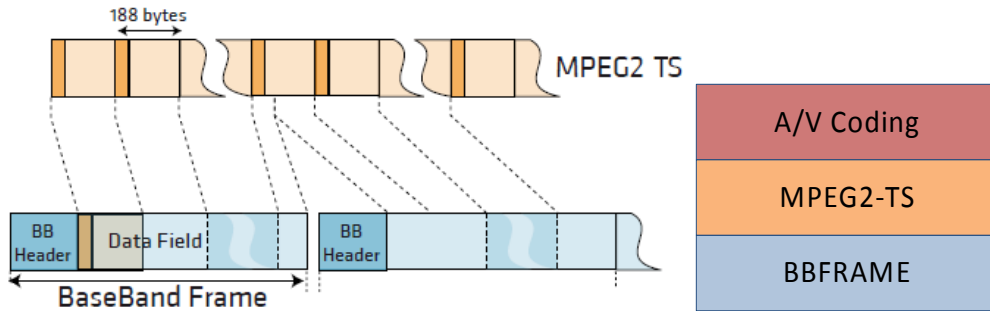


Figure 54: Protocol stack of TS profile and example of MPEG2-TS encapsulation on BBFrames.

ISSY field may carry three values:

- ISCR (Input Stream Time Reference), loaded with the LSBs of the counter content at the instant the relevant input packet is processed. ISCR shall be transmitted in the third ISSY field of each Interleaving Frame for each PLP.
- BUFS maximum size of the requested receiver buffer to compensate delay variations BUFS shall be transmitted in the second ISSY field of each Interleaving Frame for each PLP.
- TTO provides a mechanism to manage the de-jitter buffer in DVB-T2. TTO shall be transmitted in the first ISSY field of each Interleaving Frame for each PLP in High Efficiency Mode, and in the first complete packet of the Interleaving Frame in Normal Mode.

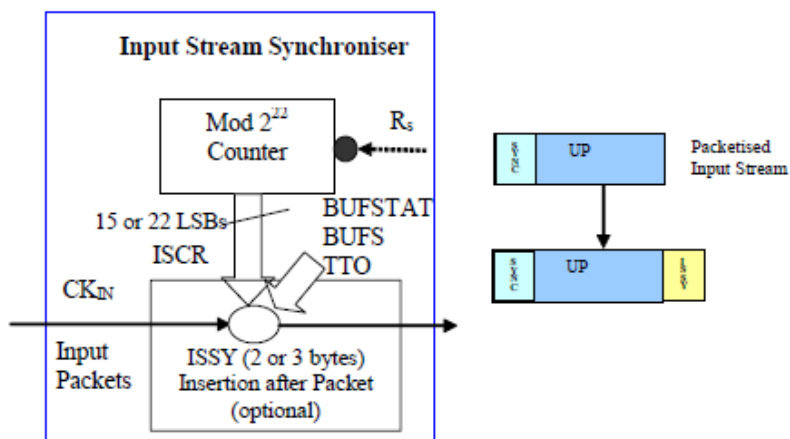


Figure 55: Input Stream Synchronizer block diagram.

Each Interleaving Frame for each PLP shall carry a TTO, a BUFS and at least one ISCR field.

ISSY solution could be a basis for DVB-NGH synchronization model:

- Delays between PLPs transmitting service components of the same service.
- Each operation point may require different initial buffering delay.
- A receiver before processing of data PLPs should know buffering time and required memory to decide whether it is capable of processing the data or not.

The other profile is the profile IP, in the Figure 56 is shown the protocol stack of this profile. The RTP protocol provides the necessary mechanism to synchronize the different multimedia streams, the timestamp is the main field for this purpose. Moreover, ISSY also is used in this profile to synchronize different PLPs.

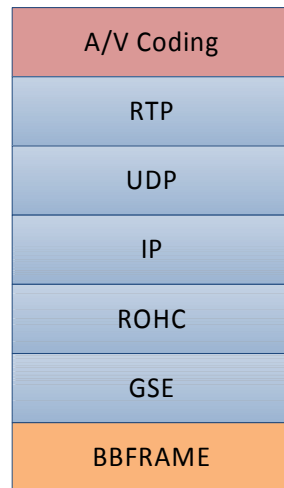


Figure 56: Protocol stack of IP profile.

2.3.3 SVC Signalling

The input interface to the NGH system is one or more syntactically correct MPEG-2 Transport Stream (TS), and each of these TS carry only one service (normal or SVC). The solution adopted by NGH forum consists in the introduction of a new descriptor in the PSI/SI signalling. The new descriptor is named NGH delivery system descriptor and it is carried by Network Information Table (NIT).

NGH_delivery_system_descriptor(){	
descriptor_tag	8 uimsbf
descriptor_length	8 uimsbf
descriptor_tag_extension	8 uimsbf
ngh_system_id	16 uimsbf
stream_id	8 uimsbf
outer_loop_length	
for (i=0;i<N,i++){	
service_id	16 uimsbf
inner_loop_length	
for (i=0;i<N,i++){	
component_tag	8 uimsbf
plp_id	8 uimsbf
anchor_flag	1 uimsbf
reserved_for_future_use	7 uimsbf
}	
}	
}	

Figure 57: Fields of NGH delivery system descriptor.

As shown in the Figure 57, each service_id entry in the outer loop contains an inner loop with all service components of the service_id, as indicated by the component_tag, and the plp_id where the service component is transmitted. One of these plp_ids is marked as an anchor PLP and contains at least PAT/PMT and SDT actual. With the information provided by this descriptor, the receiver can identify which streams are transmitted on the network and how to access them.

3 UPPER LAYER FEC IN DVB-T2 AND DVB-NGH

3.1 Expanding Window Fountain Coded Scalable Video Broadcasting

The Expanding Window Fountain (EWF) codes [20][23] are a class of rateless codes, providing Unequal Error Protection (UEP). These codes are especially suitable for Scalable Video Coding (SVC) having unequally important data layers. The EWF codes are used for transmitting scalable video in mobile channels. The channel is characterized by field measurements in a DVB-H network. The EWF code parameters are tuned to achieve real-time transmissions of SVC video. If some latency in the video is acceptable, then EWF codes can be used for real-time transmissions [25].

3.1.1 EWF Code Design

The EWF [20][23] codes are rateless codes, meaning that they can produce a potentially infinite stream of encoded symbols. The UEP property of the code, which is achieved through a windowing approach, allows a receiver to recover some codeword symbols with a higher probability than other codeword symbols. Because EWF codes are rateless, potentially an infinite stream of encoding symbols can be generated, and each encoding symbol is a random linear combination of some information symbols.

Let the subsets s_1, s_2, \dots, s_r determine the partitioning of the set of source symbols x_1, \dots, x_k into importance classes, such that $\sum_{j=1}^r s_j = k$, and s_j contains source symbols that are more important than those in s_i if $j < i$. The i -th window will contain the first $k_i = \sum_{j=1}^i s_j$ source symbols. Thus the first window contains the most important symbols, and the r -th window contains the entire source message, as illustrated in Figure 58. Compactly, this division can be described as $\prod(x) = \sum_{i=1}^r \prod_i x^i$, where $\prod_i = \frac{s_i}{k}$. Encoding symbols are generated for each window according to the standard LT encoding process [24]. That is, the i -th window is assigned a degree distribution $\Omega^{(i)}(x) = \sum_{d=1}^{k_i} \Omega_d x^d$, where Ω_d is the probability that the encoded symbol is a combination of d source symbols, i.e., that it has degree d .

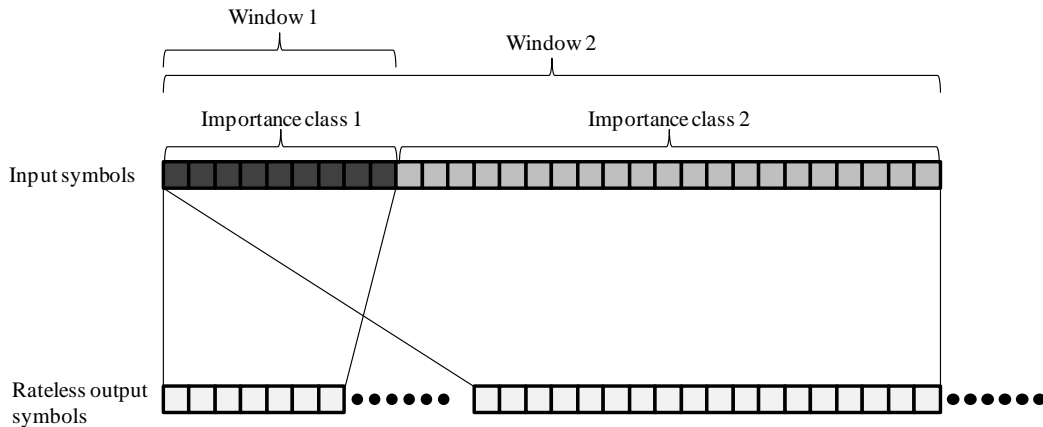


Figure 58: Division of importance classes into windows. Encoded symbols are generated based on random windows.

At the encoder, each encoding symbol is assigned to a randomly chosen window with respect to the window selection distribution $\Gamma(x) = \sum_{i=1}^r \Gamma_i x^i$, where Γ^i is the probability that window i is chosen. Using the degree distribution of the corresponding window $\Omega^{(i)}(x)$, the degree of the encoding symbol is sampled, and a number of symbols equal to the degree, which are randomly chosen from the set k_i , are combined to form the encoding symbol. Note that if $r = 1$, the code is identical to the LT code [24].

3.1.2 Measurement Setup

For measuring the performance of the EWF code, field measurements were carried out using the DVB-H test network in Turku, Finland. A laptop connected to a USB DVB-T device was used for gathering the transmitted data. Since DVB-H builds upon the DVB-T standard and adds additional functionalities on the link and application layers, the link and application layers were implemented in software, effectively obtaining a DVB-H receiver. The IP error traces were recorded and the EWF decoding was performed on these traces.

The performance of the EWF code was measured in terms of the reception overhead required for complete reconstruction of the information symbols. If the number of received symbols at the time when the information symbols are recovered is denoted as $n' = (1 + \varepsilon)k$, then ε is the reception overhead. However, since SVC is a layered video coding technique, and each layer incrementally improves the video quality, reception overheads were measured separately for each SVC layer as

$$n'_{BL} = (1 + \varepsilon_{BL})k$$

$$n'_{EL(i)} = (1 + \varepsilon_{EL})k$$

where ε_{BL} and ε_{EL} are the reception overheads for the SVC base layer and enhancement layer i respectively.

3.1.3 SVC Coding Parameters

The SVC coded video material used for the measurements was encoded using the JSVM (Joint Scalable Video Model) reference encoder. The video was encoded into blocks of 64 frames each. The average bit rate of each such block was constrained to 295 kbps maximum (-4% deviation allowed). In the three-layer stream, the base layer bit rate (again calculated as the average over a block) was constrained to 90 kbps ($\pm 2\%$), and the combined bit rate of the base layer and first enhancement layer was constrained to 170 kbps ($\pm 2\%$). The base layer of the video was coded in QCIF (Quarter Common Interchange Format) resolution, while both enhancement layers were coded in CIF resolution. The maximal frame rate of each layer was 25 frames per second (fps). The frame rate implied that each 64 frame block represented 2.56 seconds of video.

Table 15 summarizes the properties of the video layers. The video clip used was "Rush-hour". The table includes the average PSNR (peak signal-to-noise ratio) of the luma component of the frames in the coded video sequence. The base layer Y-PSNR value was calculated by comparing the decoded and up converted (to CIF resolution) base layer frames to the original frames in CIF resolution, in order to make the value directly comparable to the PSNR values of the enhancement layers.

Table 15: SVC layer properties

Layer	Resolution	Framerate fps	Bit rate kbps	Y-PSNR dB
BL	QCIF	25	90	31.5
EL1	CIF	25	170	34.3
EL2	CIF	25	295	36.1

Each 64-frame block would then be separately coded using EWF. The choice of block length was a compromise between channel zapping time and time diversity. The bit rate constraints set on the three layers meant that the base layer specific data would occupy less than, although nearly, 32% of a data block. Similarly, the base layer and first enhancement layer together would account for less than 60% of the data. This resulted in the window division distribution for the EWF code being $\Pi(x) = 0.32x + 0.28x^2 + 0.40x^3$.

The IP packet payload size used in the DVB-H test network was 1472 bytes. The 295 kbps bit rate constraint on the video stream implied that each 2.56-second video block would require up to 94400 bytes. Because of this, each video block was padded (if necessary) to exactly 94400 bytes.

3.1.4 EWF Code Parameterization

In this section we go through in detail how suitable EWF code parameters were determined. The transmission rate in the network was 452 kbps and since the SVC bit rate was approximately 295 kbps, the EWF code rate had to be at least $r=2/3$ or higher, corresponding to a maximal reception overhead of $\varepsilon_{MAX}=0.5$ in error free receptions. Because of the properties of linear codes, a symbol size of 8 bytes was chosen in order to get a sufficiently long code, implying 184 encoding symbols per IP packet, $k = 11800$ source symbols per block, and $n'_{MAX} = 17700$. The degree distributions $\Omega(x)$ for all windows was the Robust Soliton distribution [24]. Following [23], the procedure for selecting window selection probability distributions can be summarized into the following steps:

1. For all possible window selection probability distributions, analyze the asymptotic EWF performance for a sufficiently large range of reception overheads.
2. Based on the asymptotic performances, and the source block length, analyze the finite length performance.
3. Define desired reception overheads for complete recovery of each importance class.
4. For the defined reception overheads and from the finite length analysis, find the subset of window selection probability distributions that satisfies these requirements with a high probability.

Using these 4 steps, the layer-wise probabilities of recovery as function of window selection probability distribution and reception overhead were analyzed (see [25] and [23] for more details).

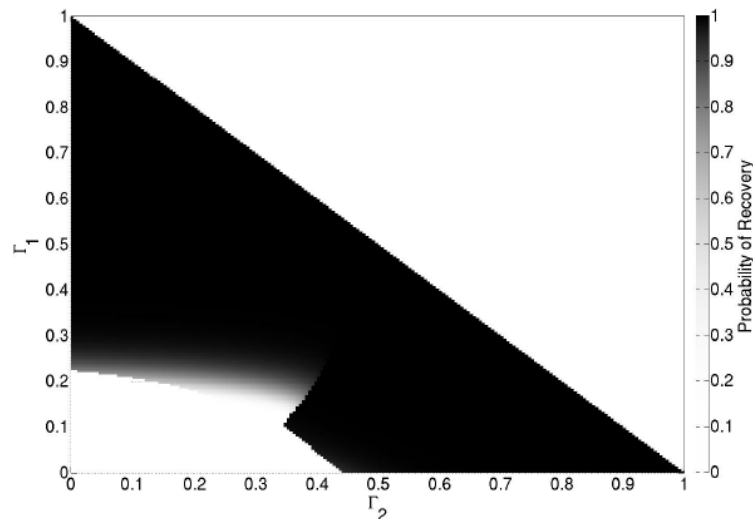


Figure 59: Probability of recovery of the base layer at $\varepsilon = 0$ with $k = 11800$.

Figure 59 illustrates the probability of recovery of the base layer at $\varepsilon = 0$ for the scalable video clip for the finite length analysis. When Γ_1 and Γ_2 are sufficiently large and at this reception overhead, the probability of recovery of the base layer is close to 1. However, increases in Γ_1 and Γ_2 imply increased reception overheads for enhancement layer 2 because Γ_3 is reduced. Figure 59 also indicates that window selection probabilities chosen from within the region limited by $\Gamma_1 < 0.22$ and $\Gamma_2 < 0.43$ will not produce negative reception overheads for the base layer. However, as will be detailed below, a negative reception overhead is desirable.

In the third step, desired reception overheads for each importance class are defined. The reasoning behind our choice of these overheads is the following. A major advantage of EWF codes is their potential to provide negative reception overheads for the most important classes. Under the assumption of an almost error free reception, the smaller the reception overhead the shorter is the channel zapping time, since it is highly unlikely that when changing channels, the receiver will receive all data belonging to the block. Rather, the reception will on average begin in the middle of the block. Suppose the required reception overhead for

successful reconstruction of the base layer is $\varepsilon_{BL} = -0.15$. This means that a number of symbols equal to 0.85k is needed for the reconstruction. In a rate 2/3 transmission, this corresponds to the requirement of receiving approximately 56.7% of the encoding symbols in a block. An ideal Equal Error Protection (EEP) code would require 66.7% of the symbols for the reconstruction under the same circumstances. Thus, it is more likely that a code with a negative reception overhead will be able to reproduce at least the base layer more quickly than an ideal EEP code. Also, in a DVB-H network the IP packet error rates should be low on average. Therefore, one can choose to have high reception overheads on the least important classes. Note that the choice of reception overheads is related to the IP packet error rate (IP PER) tolerances for each importance class, i.e., a high reception overhead implies a small IP PER tolerance and vice versa.

For the chosen reception overheads, a subset of window selection probability distributions were found that maximized the probability of recovery of all layers. Finally, from this subset the possible choices of window selection probability distributions can be further narrowed down for example by selecting those that maximize the average PSNR in the scalable video [23]. Choosing any $\Gamma(x)$ from this set is arbitrary with respect to the video quality.

Since the IP error trace was recorded and decoding was performed separately, three different window selection probability distributions were chosen with different properties. Common to all chosen $\Gamma(x)$ was the requirement on a negative reception overhead for the base layer. An overall robust performance was also desired, and finally a separation between the reception overheads of the enhancement layers was desired. The chosen window selection probability distributions are listed in Table 16.

Table 16: Chosen window selection probability distributions.

Name	$\Gamma(x)$
Code 1	$0.31x + 0.07x^2 + 0.62x^3$
Code 2	$0.28x + 0.17x^2 + 0.55x^3$
Code 3	$0.205x + 0.205x^2 + 0.59x^3$

3.1.5 Measurement Results

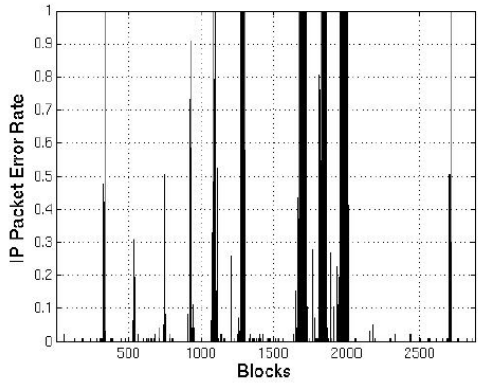
Figure 60 illustrates the reception overhead results from the measurements along with the block-wise IP PER. As can be seen in Figure 60(a), the overall IP PER remains very low over time, but with a few occasional burst losses. Additionally, there are some longer periods of outages where the receiver was completely shadowed from the available transmitters, most notably in the approximate region of blocks 1600-2000. As can be seen from the remaining figures, none of the codes could cope with these outages, and only if the code length had been significantly longer had the EWF codes managed with the outages.

Figure 60(b) shows the results for Code 1, where the window selection probability distribution was chosen such that the base layer could be decoded with a very low reception overhead. This had the benefit of having an EWF code that could successfully decode the base layer even at IP PERs as high as 48%. Moreover, the negative reception overhead would improve the average channel zapping time. On the other hand, in order to achieve an overall robust behavior the selection probability for window 3 had to be large, resulting in a very small selection probability for window 2. In Figure 60(b), this can be seen as practically no separation between the reception overheads of enhancement layer 1 and 2.

For Code 2, illustrated in Figure 60(c), the window selection probabilities for windows 1 and 3 were slightly reduced, to obtain a separation of the reception overheads for the enhancement layers. The chosen window selection probability distribution resulted in an increased average reception overhead for the base layer and enhancement layer 2, while decreasing the reception overhead for enhancement layer 1, as desired. However, the decrease in the selection probability for window 3 resulted in a reception overhead that was too close to the maximal reception overhead ε_{MAX} , which can be seen as occasional failures in decoding enhancement layer 2 at IP PERs close to zero.

The results for Code 3 are illustrated in Figure 60(d), and with this code an attempt to find a balance between Codes 1 and 2 was made. The results show an overall robust reception overhead performance, albeit with

large fluctuations in the reception overheads for the base layer and enhancement layer 1. A negative side effect of this $\Gamma(x)$ was that the requirement on a negative reception overhead for the base layer had to be relaxed. The result of this is clearly visible in Figure 60(d), as the reception overhead for the base layer is fluctuating around zero. An interesting thing to note is that the average reception overhead for enhancement layer 2 is slightly lower than for Code 1, although the selection probability for window 3 is smaller in Code 3 than in Code 1.



(a) Measured IP PERs

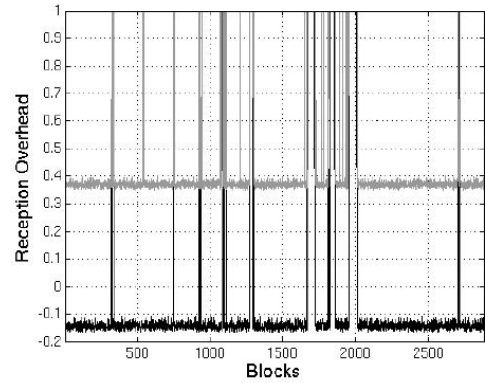
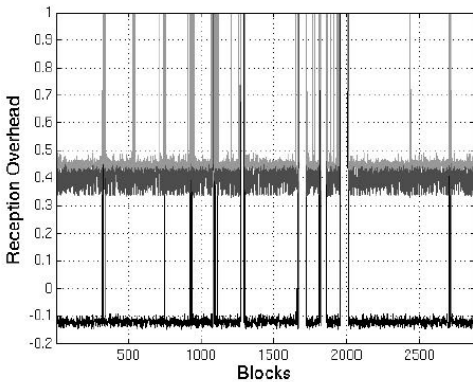
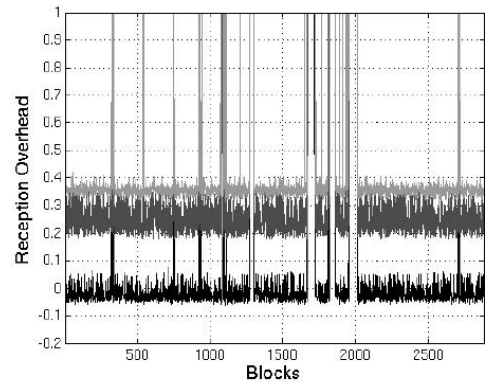

 (b) Code 1: $\Gamma(x) = 0.31x + 0.07x^2 + 0.62x^3$

 (c) Code 2: $\Gamma(x) = 0.28x + 0.17x^2 + 0.55x^3$

 (d) Code 3: $\Gamma(x) = 0.205x + 0.205x^2 + 0.59x^3$

Figure 60: Measurement results for various $\Gamma(x)$ for the EWF codes. The reception overhead of the base layer is illustrated with black, enhancement layer 1 with dark gray, and enhancement layer 2 with light gray.

3.1.6 Video Quality Analysis

To evaluate the Quality of Service (QoS), two quality measures were used. The ESR5(20) and the average PSNR in the scalable video was measured. Table 17 lists the fraction of the time that the codes meet the ESR5(20) criterion separately for each video layer and the average PSNR when using the codes.

Table 17: Scalable video quality analysis.

Code	ESR5(20)			Avg. PSNR
	BL	EL 1	EL 2	
Code 1	88.0%	83.7%	83.4%	33.36
Code 2	88.0%	82.1%	81.0%	33.29
Code 3	87.7%	85.3%	84.0%	33.24

As can be seen from Table 17, the ESR5(20) results are all close to each other. The reason to not fulfilling the ESR5(20) follows mostly from the outage areas. A comparison of the ESR5(20) results reveals that Code 2 meets the ESR5(20) criterion as often as Code 1 does for the base layer (BL), but has a worse performance

than Code 1 with respect to the enhancement layers (EL) . Moreover, it is evident that the BL is notably more robust than the EL for all codes. On average, Code 3 has the most robust performance although it suffers from a slight degradation in robustness for the BL as compared to the other codes. On the other hand, when observing the average PSNRs, Code 3 produces the lowest PSNR. The difference to the other codes is however negligible.

3.1.7 Conclusions

The possibility of transmitting scalable video in real-time over a DVB-H network has been explored. The video has been encoded with the Expanding Window Fountain (EWF) codes with carefully chosen code parameters to achieve this goal. The results are based on field measurements, obtained by using a DVB-H test network in Turku, Finland. Our results demonstrate that real-time transmission of scalable video can be achieved with a subjectively perceived good quality when using EWF codes. This is confirmed by assessing the fraction of the time that the overall performance meets the ESR5(20) criterion and measuring the average PSNR in the scalable video. The reason to the occasional failures in meeting the ESR5(20) criterion follows from extremely high IP packet error rates.

3.2 Receiver-Controlled Parallel Fountain Codes

An upper layer unequal error protection (UEP) FEC scheme for distribution of SVC content over multiple parallel paths to receivers is presented, which is referred to as Receiver-Controlled Parallel Fountain (RCPF) codes [26]. Unlike previously proposed UEP fountain codes, where the UEP performance is controlled by the fountain code design at the transmitter side, this solution allows receivers to tailor their own set of received fountain coded packets thereby controlling the UEP performance. By selecting which parallel broadcast channels to connect to, each receiver independently controls the encoded data collection process according to its device capabilities, reception conditions and the desired video quality. The RCPF code design is motivated by the second generation DVB standards employing multiple PLPs for transmission of data. When using RCPF coding, each PLP can be viewed as a transmission path to receivers. Thus receivers collect data from a number of PLPs and decode the collected data jointly, allowing for a flexible and robust coding scheme.

3.2.1 RCPF Code Design

The RCPF codes are rateless codes, meaning that they can produce a potentially infinite stream of encoded symbols. The UEP property is achieved through a windowing approach, identical to that of the EWF codes [20][23].

The main difference between EWF codes and RCPF codes is that the encoded symbols are not generated based on random windows when using RCPF codes. Rather, encoded symbols are simultaneously produced from different windows and streamed in parallel over different broadcast channels. The encoded symbols of window i are transmitted over channel i , where channel i has a bit-rate R_i . If the total transmission rate over all parallel channels is R , then the relative transmission rates can be expressed as $\Phi(x) = \sum_{i=1}^r \Phi_i x^i$, where $\Phi_i = \frac{R_i}{R}$. The receivers obtain symbols from each channel separately, which are then jointly decoded. This transmission scenario is illustrated in Figure 61. In the context of DVB-T2 and DVB-NGH, each path from the encoder to the decoder in Figure 61 can be considered as the transmission and reception of a PLP. Receiver devices can control the level of UEP simply by connecting to a number of parallel channels, according to their needs and capabilities.

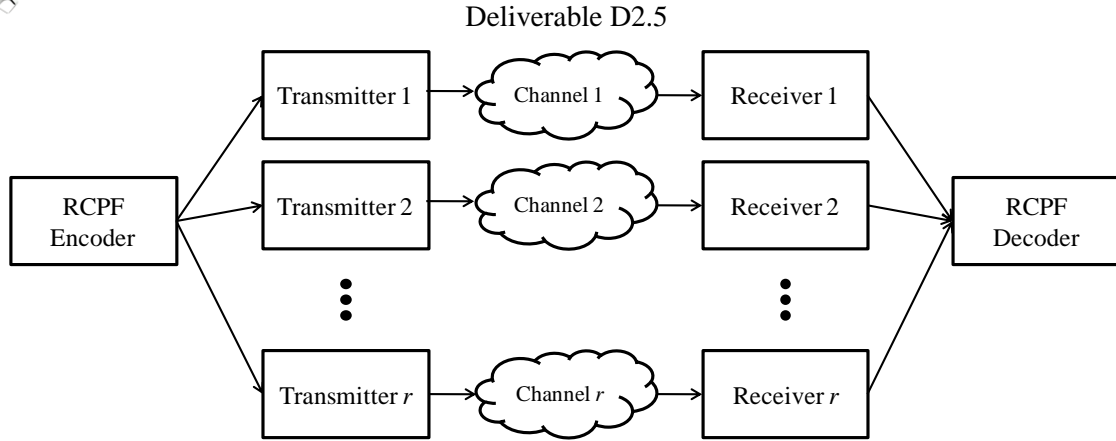


Figure 61: Transmission scheme using RCPF coding.

3.2.2 Analysis of RCPF Coding Scheme

Following a similar analysis approach as in [20], the probability of error while decoding iteratively an RCPF encoded message can be determined as follows [26]. Let an RCPF code be applied over an r -layer source message with division into importance classes defined by $\Pi(x)$, where the set of degree distributions $\{\Omega^1, \dots, \Omega^r\}$ is defined over the set of r windows. The encoded symbols from the r different windows are streamed over the set of r parallel broadcast channels with parameters (R_i, p_i) , $1 \leq i \leq r$, respectively, where p_i is the symbol erasure probability in channel i . The number of received encoded symbols of size L bits the receiver has obtained from the i -th broadcast channel at time t is on average equal to

$$n_i(t) = \lfloor \frac{R_i \cdot t}{L} \rfloor (1 - p_i)$$

Using $n_i(t)$, the expected received window selection distribution $\Gamma_R(x)$, i.e., the distribution on the fraction of received encoding symbols generated from different windows, is obtained as

$$\Gamma_R(x) = \sum_{i=1}^r \Gamma_{R,i} x^i = \sum_{i=1}^r \frac{n_i(t)}{n(t)} x^i$$

where $n(t) = \sum_{i=1}^r n_i(t)$ is the total number of received encoded symbols from all the parallel channels until time instant t . The excess number of encoded symbols over the source message length, $n(t) - k$, normalized by the length of the source message k , is called the average reception overhead $\epsilon(t) = (n(t) - k)/k$. Given $\Gamma_R(x)$ at time instant t , and assuming a sufficiently large length k of the source message, we can obtain asymptotic (as $k \rightarrow \infty$) probabilities of decoding source symbols from different importance classes after receiving $n(t) = (1 + \epsilon(t))k$ encoded symbols (c.f. [20]). The probability $y_{l,j}$ that a source symbol of the j -th importance class is not recovered after l iterations of the iterative message-passing decoding algorithm at time instant t is equal to

$$y_{0,j}(t) = 1$$

$$y_{l,j}(t) = e^{\left(-(1+\epsilon(t)) \sum_{i=j}^r \frac{\Gamma_{i,R}}{\sum_{l=1}^i \Pi_l} \Omega^{(i)} \left(1 - \frac{\sum_{m=1}^i \Pi_m y_{l-1,m}(t)}{\sum_{l=1}^i \Pi_l} \right) \right)}$$

Figure 62 illustrates the asymptotic BER versus the reception overhead $\epsilon(t)$ for a scenario with two importance classes. The RCPF encoder applies the Robust Soliton degree distribution [24] over both windows, where the first importance class contains the most important bits (MIB) and the second contains the least important bits (LIB). The three different pairs of curves show how the erasure rates of broadcast channels influence the BER when the receiver connects to both parallel channels. The waterfall regions of

the MIB and LIB curves correspond well to the simulation results presented in Section 3.2.3, with respect to required reception overhead for successful recovery.

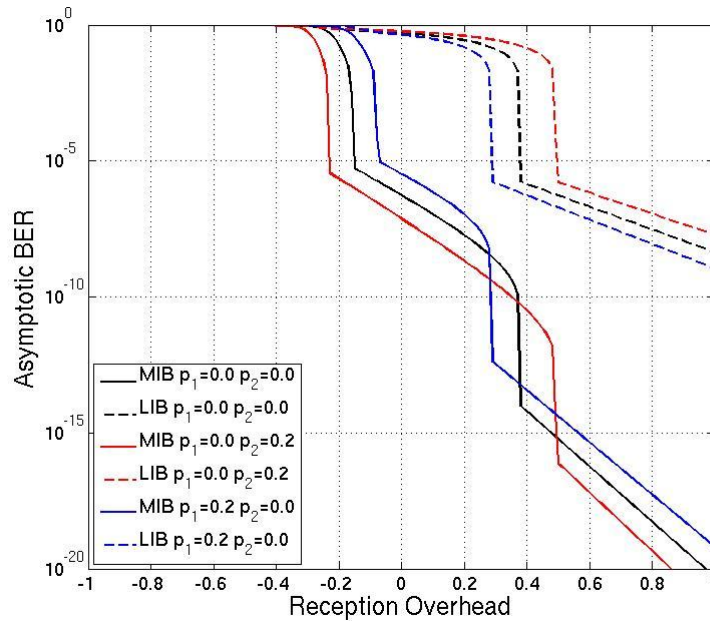


Figure 62: Analysis of asymptotic BER versus reception overhead ε for $\Pi(x)=0.3x+0.7x^2$, $\Phi(x)=0.33x+0.67x^2$, for some sample erasure rates p_1 and p_2 .

3.2.3 Simulation Results

The RCPF codes are analyzed in terms of required reception overhead $\varepsilon(t)$ for successful recovery of the source data with the following simulation settings. The source data contains two importance classes and $k=3000$. The division into windows is $\Pi_1=\{0.1, 0.2, 0.3, 0.4\}$ and $\Pi_2=1-\Pi_1$. The information in the first importance class contains the most important bits (MIB) and the information in the second importance class contains the least important bits (LIB). Encoding symbols from window 1 (covering the MIB) are transmitted over channel 1 and encoding symbols from window 2 (covering both the MIB and the LIB) are transmitted over channel 2. The code rate is 1/2, and the degree distribution for each window is the Robust Soliton distribution [24]. Since the code rate is 1/2, if the reception overhead $\varepsilon(t) > 1$, a decoding failure is declared. The relative transmission rates are $\Phi(x)=0.33x+0.67x^2$, i.e., one encoding symbol is transmitted over channel 1 during the same time interval as two encoding symbols are transmitted over channel 2. The channels are modeled as binary erasure channels (BEC), each with erasure rates 0-100%.

Figure 63 illustrates the required reception overheads for successful recovery of the MIB and the LIB. On the left in Figure 63, the erasure rate over channel 1 is set to zero, while the erasure rate over channel 2 is allowed to vary. The opposite case is illustrated on the right in Figure 63. It can be seen that the reception overhead for the MIB decreases with increasing erasure rates over channel 2. This follows from the fact that the reception overhead increases for each received encoded symbol from both channels, but since we assume channel 1 is error free, the increase in erasure rate over channel 2 decreases the number of encoded symbols received from channel 2, thus leading to the MIB reception overhead decrease. A similar but opposite trend is visible on the right in Figure 63. It is noteworthy that as long as either one of the two channels has a relatively small erasure rate, the MIB are always successfully recovered, either by recovery of the first or the second expanding window.

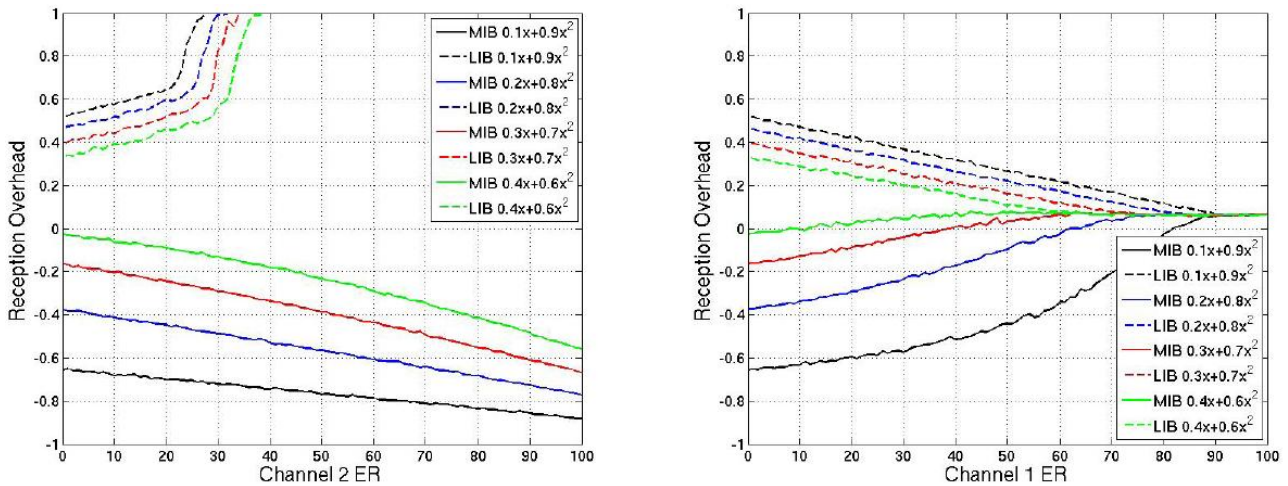


Figure 63: Reception overheads for the simulation scenario, with zero erasure rate over channel 1 (left) and zero erasure rate over channel 2 (right).

Figure 64 shows the decoded BER for the same scenario, with increasing erasure rates over channel 2. It is readily seen that the error tolerance of the RCPF code increases with increasing MIB fractions of the message under the assumption that channel 1 is error free. Note that for all the applied values of Π_1 , when channel 1 is error free, the MIB are always successfully recovered (i.e., the decoded BER is equal to 0). In the opposite case, when channel 2 is error free and channel 1 is erroneous, both the MIB and LIB are successfully recovered, which was already seen in Figure 64.

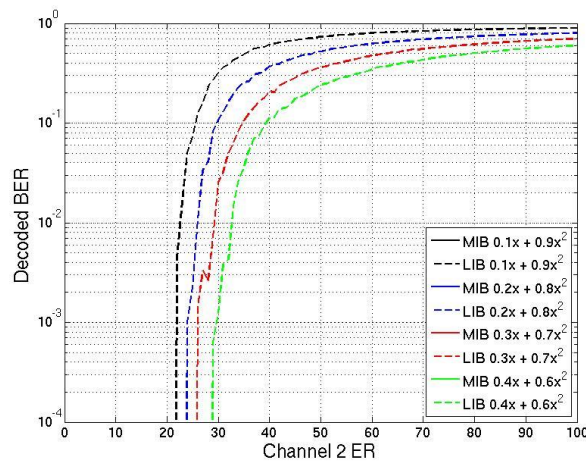


Figure 64: Decoded BER with zero erasure rate over channel 1.

Figure 65 shows the reception overheads required for the recovery of window 1 and window 2 respectively with increasing erasure rates over both channels for the window division distribution $\Pi(x)=0.3x+0.7x^2$. The black regions in the figures correspond to decoding failures. As can be seen on the left in Figure 65, the MIB are recovered for any erasure rates over channel 2 as long as the erasure rate over channel 1 is below 50%. When the erasure rate over channel 2 is below 20%, the MIB are recovered for any erasure rate over channel 1. The right part of Figure 65, which illustrates the reception overhead for the LIB, reveals that the LIB are recovered for erasure rates below 30% over channel 2, as long as the erasure rate over channel 1 is below 80%. Thus, the LIB are not as tolerant against transmission errors as the MIB are, but are still easily recovered under normal reception conditions with this setup. By changing the window division distribution $\Pi(x)$, the code rate, or the relative transmission rate $\Phi(x)$, more or less robust performances are obtainable. For instance, if $\Pi(x)=0.1x+0.9x^2$, the MIB are even more robust at the expense of less protection for the LIB. This is evident from Figure 65. However, as can be seen in Figure 65, a reduction in the MIB fraction does not significantly reduce the robustness of the LIB.

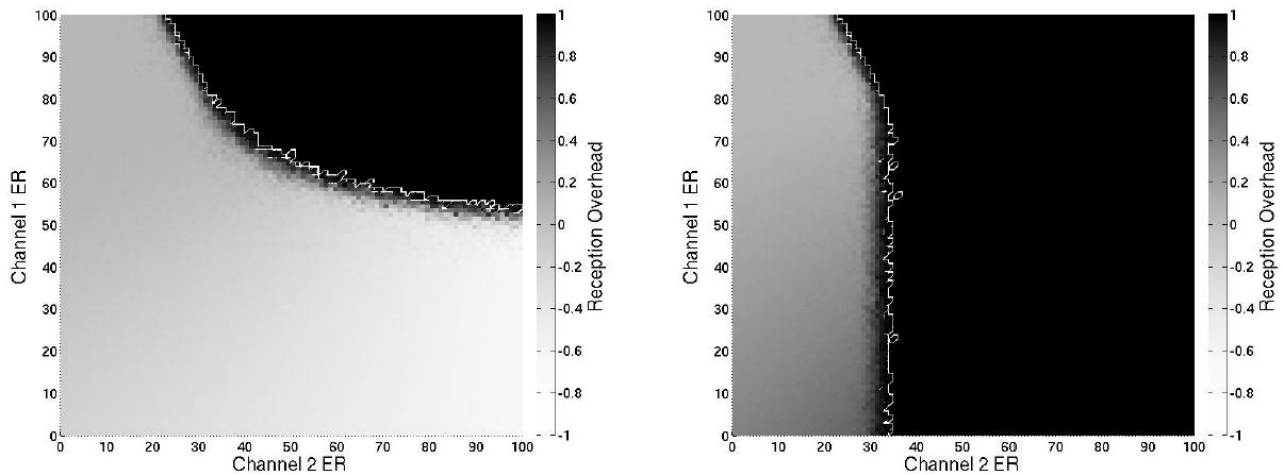


Figure 65: Reception overheads for $\lambda(x)=0.3x+0.7x^2$ for successful recovery of the MIB (left) and the LIB (right) for various channel erasure rates. The black regions correspond to decoding failures.

3.2.4 Conclusions

We have presented the Receiver-Controlled Parallel Fountain (RCPF) coding scheme for transmission over parallel communication channels. The RCPF codes provide Unequal Error Protection (UEP) to layered source and allow receivers to control the layer decoding performance. This is achieved through a windowing approach, identical to that of the Expanding Window Fountain (EWF) codes. Using RCPF codes, receivers collect data from a number of parallel broadcast channels according to their needs and capabilities. If the RCPF codes are used to protect scalable video, receivers may collect data from a number of channels according to the desired video quality of the end-user. The proposed coding scheme additionally allows receivers to adapt to varying reception conditions and thus allows receivers to recover at least the most important layer in the source, even while experiencing poor reception conditions. The RCPF codes have been analyzed both analytically and through simulations. We have shown that the RCPF codes can effectively protect layered source while providing a robust decoding performance.

3.3 Fading Margin Reduction due to Inter-Burst Upper Layer FEC in Terrestrial Mobile Broadcast Systems

In wireless communications mobile users typically experience signal fading effects due to the superposition of multiple propagation paths between transmitter and receiver. In general, it can be distinguished between slow or long-term fading due to local shadowing effects, commonly known as shadowing, and fast or short-term fading due to the coherent superposition of the signals reaching the terminal, commonly known as fast or multipath fading [22]. Shadowing implies significant variations of several dB over distances of several tens of meters (comparable to the widths of buildings in the region of the mobile), whereas fast fading involves variations on the scale of a half-wavelength and frequently introduces variations as large as 35 to 40 dB.

Signal fading can be compensated with forward error correction (FEC) with a time interleaving large enough to essentially average out the fading statistics. FEC mechanisms rely on the transmission of redundant repair information (parity data) such that the receiver can correct errors occurred during the transmission. For the FEC code to be efficient, the different code symbols should ideally experience uncorrelated fading. In this case, it is possible to cope with erasure rates as large as the inverse of the code rate. Otherwise, the efficiency of the FEC mechanism is reduced.

In case of fast fading, a relatively short time interleaving is usually required to eliminate it (in the order of few to several milliseconds, depending on the user velocity and operating frequency). This is traditionally done at the physical layer as part of the radio interface for wireless communication systems.

This is typically not a feasible way to cope with shadowing due to memory and latency constraints. The memory requirement is directly proportional to the service data rate, the interleaving duration, the proportion of parity data transmitted, and the interleaver profile. On the other hand, terminals should in principle wait and store all data jointly encoded before decoding. The traditional approach to cope with shadowing consists in adding an extra fading margin of several dB to the link budget, in order to assure a reliable communication with a given probability at the cell edge. Nevertheless, for mobile users it is in principle possible to reduce the required fading margin exploiting the time diversity of the mobile channel using a FEC scheme spanning a sufficiently long time. Recent advances in FEC make this possibility a reality.

Digital video broadcasting standards such as DVB-H (Handheld) [27] and DVB-SH (Satellite to Handhelds) [28], define FEC schemes with long time interleaving profiles to exploit the time diversity of the mobile channel. These mobile broadcasting technologies are characterized by a discontinuous transmission technique, known as time-slicing, where data is periodically transmitted in so-called bursts. Hence, these FEC schemes are usually referred to as inter-burst FEC. For file download services, both DVB-H and DVB-SH adopt application layer FEC (AL-FEC) using Raptor coding [29]. For streaming services, in DVB-SH it is possible to provide long time interleaving together with fast zapping support either at the physical layer or at the link layer. The physical layer FEC outperforms the link layer FEC at the expense of higher memory requirements [30]. The link layer FEC mechanism is known as multi protocol encapsulation inter-burst FEC (MPE-iFEC) [31], and it specifies two coding schemes: one mandatory using sliding Reed-Solomon encoding (SRSE) and another optional using Raptor coding.

On the other hand, in the new generation of DVB standards such as DVB-T2, UL-FEC methods are also interesting. Due to the limited amount of TDI (time de-interleaving) memory available in DVB-T2 receivers (approx. 2^{19} cells), long interleaving durations (i.e. several seconds) cannot be provided for typical mobile TV data rates. In addition, the time interleaver included in the physical layer of DVB-T2 does not support fast zapping, and long time interleaving cannot be used with tolerable channel change times. In order to overcome these limitations, UL-FEC protection can be used in DVB-T2 to provide long time interleaving at upper layers with fast zapping support. If fast zapping is enabled, receivers in good reception conditions can start to display the service before the reception of all the information and parity data. Depending on the UL-FEC implementation, it may be still possible to achieve full protection (e.g. the entire information and parity data is available for decoding) later on by means of parity recovery techniques [32].

Here it is described a theoretical framework to evaluate the shadowing fading margin reduction that can be achieved in a generic terrestrial broadcast system with inter-burst upper layer FEC (UL-FEC, i.e. either link or application layer [33]).

3.3.1 Problem description

A generic terrestrial mobile broadcast system with time-slicing, where the different services are transmitted at the same frequency but in different time slots (bursts). Without loss of generality, we assume that the cycle time between bursts of the same service is constant. The system is characterized by a receiver sensitivity, which is the minimum signal level at which reception is possible. Fast fading is assumed to be eliminated at the physical layer with some form of FEC and short time interleaving during the burst duration.

Shadowing is assumed to remain constant during this time. It is worth to note that these assumptions are commonly accepted in DVB-H and DVB-SH. Their physical layer FEC have a brick-wall characteristic that corrects above a certain signal to-noise ratio (SNR) threshold whereas fails below; and the burst duration is in the order of few hundreds of milliseconds. The variations of the shadowing in dB are described by a zero-mean Gaussian random variable with standard deviation σ_l and correlation distance d_{corr} [22]. The shadowing standard deviation is known as the location variability, and it determines the spread of the signal field strength around the mean value. Values typically used for terrestrial outdoor broadcasting signals are 5.5 dB in the UHF band and 8 dB in the S band [34]. On the other hand, the spatial correlation is usually modeled as a first-order exponential model [35]:

$$\rho(d) = e^{-d/d_{corr}} \quad (1)$$

where d_{corr} is distance taken for the autocorrelation to fall by e^{-1} . Typical values range from 20 m to 100 m, depending on the environment surrounding the receiver [22].

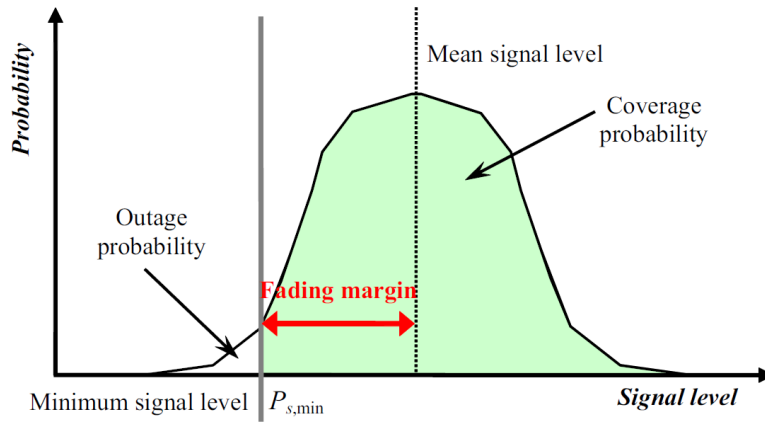


Figure 66: Shadowing fading margin concept.

Shadowing makes coverage prediction statistical, such that what is predicted is the signal availability rather than the signal level, see Figure 66. The *outage probability* at a single reception point with an average signal level \overline{SNR} , is equal to the probability that the shadowing increases the mean path loss by at least $\overline{SNR} - SNR_{th}$ (in dB), where SNR_{th} is the required SNR threshold for the system. The outage probability can be computed as:

$$\text{Outage Probability} = Q\left(\frac{\overline{SNR} - SNR_{th}}{\sigma_l}\right) \quad (2)$$

where the $Q(\bullet)$ function is the complementary cumulative normal distribution:

$$Q(x) = \frac{1}{\sqrt{2\pi}} \int_x^{\infty} e^{-t^2/2} dt. \quad (3)$$

The *shadowing fading margin* required to assure a reliable communication with a given probability, also known as correction location factor in broadcasting C_l [34], is usually expressed as the product of the shadowing standard deviation, σ_l , and a correction coefficient, μ :

$$C_l = \mu \cdot \sigma_l \quad (4)$$

The value of the correction coefficient μ depends only on the target coverage probability. It takes the value of 0 for 50%, 0.52 for 70%, 1.28 for 90%, 1.64 for 95%, and 2.33 for 99% [34]. Typical coverage probability targets in DVB-H and DVB-SH (terrestrial) are 95% for good pedestrian reception and 99% for good vehicular reception. We consider an ideal systematic FEC erasure code operating above the physical layer that produces repair packets which are sent along with the original source packets to compensate for potential losses due to shadowing. The original multimedia stream is divided into *source blocks*, which are treated and encoded independently. The inter-burst UL-FEC configuration parameters are: the ratio of source information to the total amount of source and repair data transmitted, commonly known as *code rate* (CR), and the number of bursts jointly encoded, here denoted as *protection period* (PP). An illustrative example is depicted in Figure 67.

Deliverable D2.5

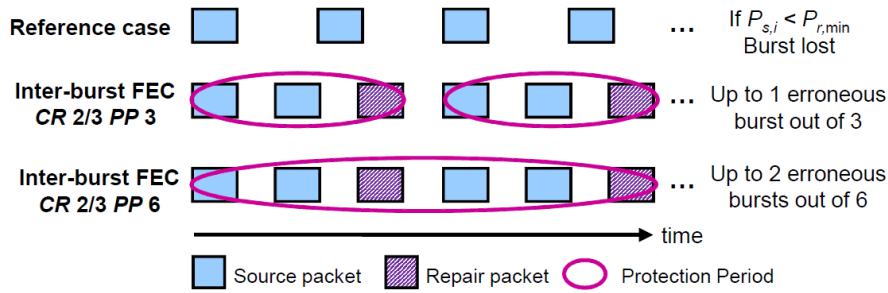


Figure 67: Inter-burst UL-FEC concept in a generic mobile broadcast system with time-slicing. Under our assumptions, if the received signal strength is lower than the receiver sensitivity the burst (slot) is lost.

The error correction capability of inter-burst UL-FEC in terms of percentage of erroneous bursts that can be corrected within each protection period depends only on the code rate. The more repair data is transmitted, the more robust the transmission (at the expense of a decreased system capacity). However, the transmission robustness depends also on the protection period. In general, the longer the interleaving depth, the more robust the transmission (at the expense of an increased latency and larger memory capabilities at the terminals). In practice, depending on the channel, the reception speed, and the code rate, there is a point where no visible gain is achieved by increasing the interleaving.

In the example shown in Figure 67, a code rate 2/3 can correct up to 33% errors, and thus it will be possible to recover from one erroneous burst out of three (for PP 3), two erroneous bursts out of six (for PP 6) and so on; as soon as all other bursts within the protection period are correctly received.

Inter-burst UL-FEC reduces the fading margin required to cope with shadowing because the probability of correctly receiving a burst, henceforth denoted as service availability, is higher than the coverage probability (percentage of covered locations with an average signal level higher than the receiver sensitivity). This gain stems from the time diversity of the mobile channel due to the mobility of the users. Therefore, for a given scenario and transmission configuration (code rate and protection period), the gain depends on the user trajectory and velocity [36].

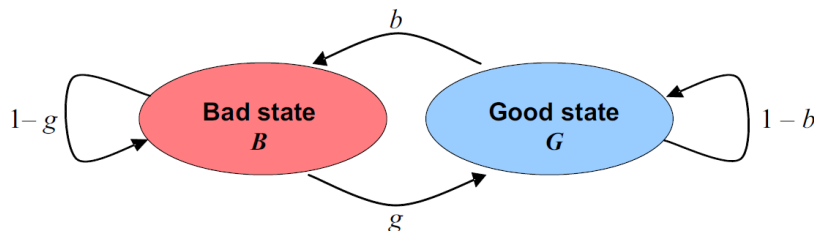


Figure 68: The Gilbert-Elliott channel.

In this case, the analysis can be easily derived analytically using the well-known Gilbert-Elliott (GE) channel model, see Figure 68. The GE model dates back to the early 60's [37]-[38]. In this model, the channel is assumed to be either in a good state where the error rate is small, or in a bad state where the error rate is large. The good and the bad states are denoted G and B respectively, and the probabilities that the channel changes from the good state to the bad state and vice versa b and g . We further assume that the probability of erasure is 1 in the bad state and 0 in the good state. The stationary probabilities that the channel is in the good state, $P^\infty(G)$, and in the bad state, $P^\infty(B)$, are:

$$P^\infty(G) = \frac{g}{g+b}; P^\infty(B) = \frac{b}{g+b} \quad (5)$$

3.3.2 Theoretical analysis for streaming delivery with uncorrelated shadowing

3.3.2.1 Analytical Framework

The maximum reduction of the shadowing fading margin occurs when there is no shadowing correlation between reception conditions of consecutive bursts. In this case, the GE channel is memoryless, and the probability of being in the good or bad state is independent of the previous state. The GE channel becomes memoryless when $g + b = 1$. Therefore, g and b are the coverage and outage probabilities respectively.

Under these conditions, if the GE channel is observed at n consecutive instants of time, the probability that the channel is in the bad state d times ($0 \leq d \leq n$), denoted as $P_n(d)$, is given by:

$$P_n(d) = \binom{n}{d} g^{(n-d)} \cdot (1-g)^d \quad (6)$$

With inter-burst UL-FEC, given the code rate, CR , and the protection period PP , the minimum number of bursts needed to decode a source data block, n_{min} , can be computed as:

$$n_{min} = \lceil CR \cdot PP \rceil, \quad (7)$$

where $\lceil \cdot \rceil$ is the ceiling function.

Finally, the service availability, S_{av} , defined as the probability of receiving a burst correctly after inter-burst UL-FEC decoding, can be computed using Eq. (6) as:

$$S_{av} = 1 - \sum_{i=PP-n_{min}+1}^{PP} P_{PP}(i) \cdot \left(\frac{i}{PP}\right) \quad (8)$$

Note that the second term in Eq. (8) covers all the cases where the inter-burst UL-FEC decoding is not successful.

3.3.2.2 Analytical Results

Figure 69 shows the service availability as a function of the coverage probability for inter-burst UL-FEC with code rate $2/3$ for different protection periods. The case without UL-FEC (CR 1, PP 1) is also shown for comparison. In this case, the service availability is equal to the coverage probability.

In the figure we can see how the service availability perceived by the users with inter-burst UL-FEC is considerably increased compared to the reference case, and that the improvement depends on the protection period and the coverage probability. It should be noted that increasing the interleaving depth (protection period) is only beneficial when the code rate is robust enough to correct the total number of errors (i.e., for coverage probabilities above 66% in the figure). Otherwise, the performance is reduced.

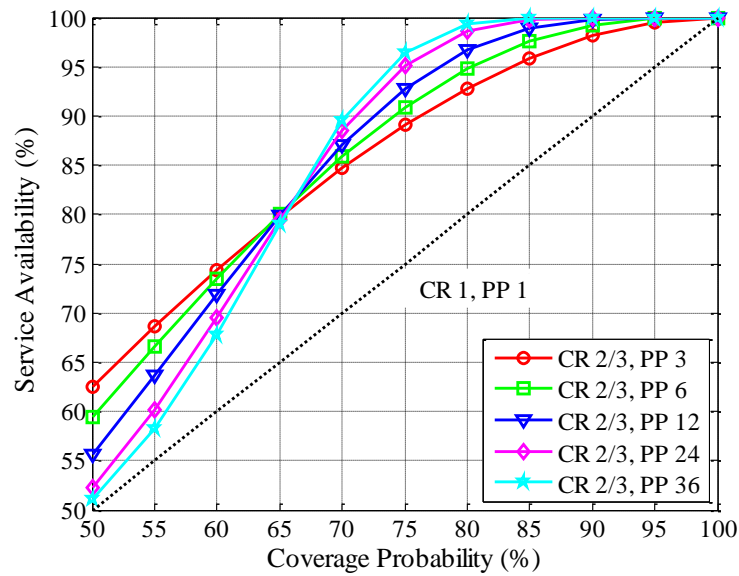


Figure 69: Service availability vs. Coverage probability. Uncorrelated shadowing.

From the results shown in Figure 69, it can be obtained a new distribution factor μ for computing the fading margin as in Eq. (4). Therefore, the fading margin reduction depends on the code rate, protection period and target service availability, and it is directly proportional to the standard deviation of the shadowing.

Figure 70 presents the fading margin reduction as a function of the protection period for different UL-FEC code rates (σ_l is 5.5 dB and the service availability 95%). In this case, the fading margin without inter-burst UL-FEC would be 9 dB. We can see that the reduction increases for more robust code rates and for larger protection periods. The potential gain is very significant, even for short interleaving depths, especially for code rates 1/2 and 2/3 (almost 5 dB and 4 dB reduction for protection periods of just 2 and 3 bursts, respectively). Finally, we want to point out that the reduction increases not only for larger values of the standard deviation of the shadowing (e.g., for σ_l 8 dB reductions are 45% larger than for 5.5 dB), but also for more demanding service probabilities. For example, for 99% service availability the reduction is between 1 dB and 3 dB larger than the values shown in Figure 70.

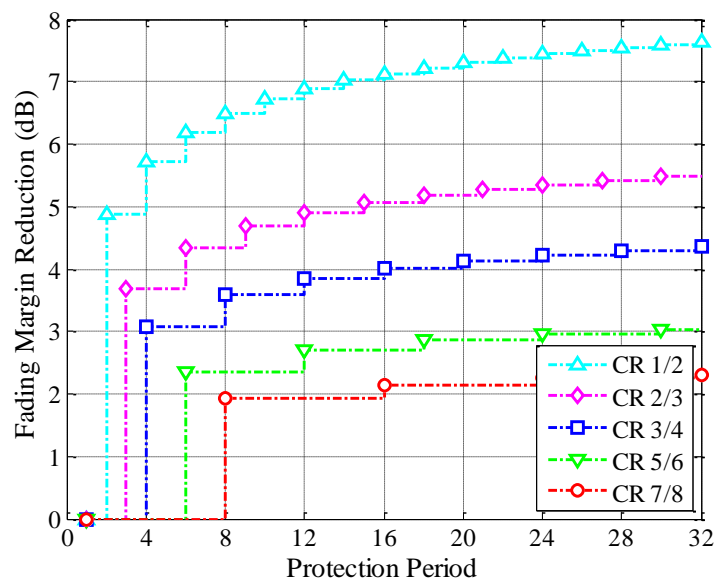


Figure 70: Shadowing fading margin reduction for 95% service availability vs. Protection period in burst units. Uncorrelated shadowing; $\sigma_l = 5.5$ dB, $d_{corr} = 0$ m.

3.3.3 Theoretical analysis for streaming delivery with correlated shadowing

The shadowing correlation between consecutive bursts depends on the shadowing correlation distance, the cycle time between bursts, and the user velocity, see Eq. (1). In general, the assumption that the shadowing is uncorrelated between consecutive bursts does not apply in most cases. Typical cycle time values for mobile TV streaming services in DVB-H/SH are in the range of one to few seconds. Therefore, only users with very high speeds experience uncorrelated shadowing between consecutive bursts, and the fading margin reduction is, in practice, smaller than the values presented in the previous section. The gain decreases for larger shadowing correlation distances, smaller user velocities, and cycle time values. Nevertheless, it should be clear that the maximum reduction does not depend on these parameters. These parameters basically determine the level of time interleaving depth required to achieve a target shadowing fading margin. Indeed, all three parameters can be combined into one: the ratio between the moved distance by the user during the cycle time and the shadowing correlation distance.

3.3.3.1 Analytical Framework

In case there is correlation between consecutive burst, the GE channel is no longer memoryless, and the probability of being in the good or the bad state depends on the previous state (i.e., $g + b \neq 1$). The parameters of the GE channel can be obtained taking into account that the GE has an exponential correlation function like the shadowing [39]. At time m , the correlation function of the GE channel, $\rho(m)$, equals to:

$$\rho(m) = (1 - b - g)^m \quad (9)$$

Comparing Eq. (1) and Eq. (9), it follows that:

$$(1 - b - g) = e^{-(vT_c)/d_{corr}}, \quad (10)$$

where v is the receiver velocity, and T_c is the time step used in the discrete time GE model (i.e., cycle time between bursts).

Comparing Eq. (2) and Eq. (5) we obtain:

$$\frac{b}{g+b} = Q\left(\frac{\sqrt{SNR} - SNR_{th}}{\sigma_t}\right). \quad (11)$$

Using Eq. (12) and Eq. (13), the GE parameters b and g are easily determined. Note that the ratio $b = (g + b)$ does not depend on the dynamics of the channel. It is also intuitively clear that the GE channel become closer to being memoryless for larger T_c or v , and for smaller d_{corr} .

For the correlated GE channel, the probability distribution for being in the bad state d times out of n , $0 \leq d \leq n$, is given by:

$$P_n(d) = \begin{cases} P^\infty(G)(1 - b)^{n-1} & d = 0 \\ P^\infty(G)(P_n(d|GG) + P_n(d|GB)) + P^\infty(B)(P_n(d|BG) + P_n(d|BB)) & 1 \leq d < n \\ P^\infty(B)(1 - g)^{n-1} & d = n \end{cases} \quad (12)$$

where $P_n(d|GG)$ is the conditional probability of being d times in the bad state out of n , conditioned on being in the good state both the first and the last instants of time. The other conditional probabilities are defined accordingly. They can be computed as (for details and demonstration, interested readers are referred to [16]):

$$P_n(d|GG) = \sum_{i=2}^{\min(d+1, n-d)} \binom{n-d-1}{i-1} \binom{d-1}{i-2} \cdot (1-b)^{n-d-i} b^{i-1} (1-g)^{d-i+1} g^{i-1} \quad (13)$$

$$P_n(d|GB) = \sum_{i=1}^{\min(d,n-d)} \binom{n-d-1}{i-1} \binom{d-1}{i-1} \cdot (1-b)^{n-d-i} b^i (1-g)^{d-i} g^{i-1} \quad (14)$$

$$P_n(d|BG) = \sum_{i=1}^{\min(d,n-d)} \binom{n-d-1}{i-1} \binom{d-1}{i-1} \cdot (1-b)^{n-d-i} b^{i-1} (1-g)^{d-i} g^{i-1} \quad (15)$$

$$P_n(d|BB) = \sum_{i=2}^{\min(d,n-d+1)} \binom{n-d-1}{i-2} \binom{d-1}{i-1} \cdot (1-b)^{n-d-i+1} b^{i-1} (1-g)^{d-i} g^{i-1} \quad (16)$$

3.3.3.2 Analytical Results

Figure 71 shows the fading margin reduction achieved with inter-burst UL-FEC with a code rate $2/3$ for the case of correlated shadowing (σ_l 5.5 dB), as a function of the interleaving depth for different $(v \cdot Tc) = d_{\text{corr}}$ ratios. The service availability is 95%. We can see how the reduction decreases when the correlation between consecutive bursts increases. It should be noted that there is no gain by performing an inter-burst UL-FEC protection of the transmission for fully static reception conditions (i.e., $(v \cdot Tc) = d_{\text{corr}} = 0$), as users either receive all content or nothing.

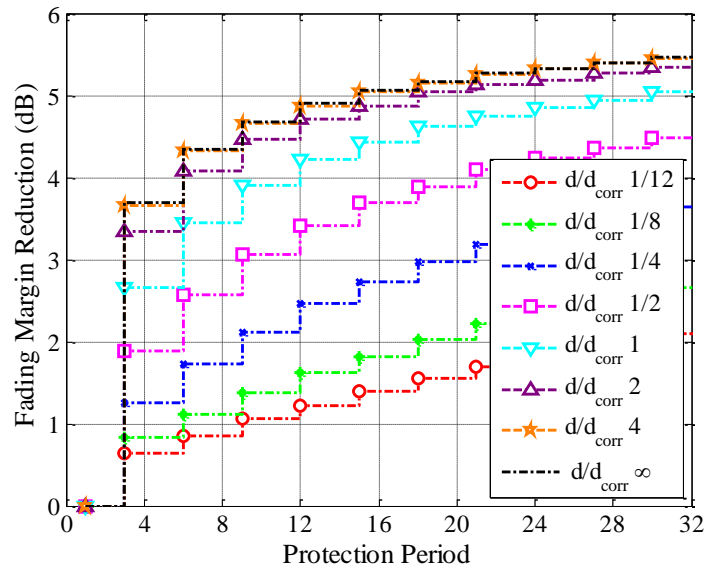


Figure 71: Shadowing fading margin reduction for 95% service availability vs. Protection period in burst units. Code rate $2/3$. Correlated shadowing: $\sigma_l = 5.5$ dB.

3.3.4 Validation results

3.3.4.1 DVB-H Results

Figure 72(a) compares the theoretical fading margin results shown in Figure 70 for uncorrelated shadowing (dashed lines) with laboratory measurement results for DVB-H (solid lines). The DVB-H transmission mode employed in the measurements is: FFT size 8K, guard interval $1/4$, modulation 16-QAM and code rate $1/2$; and for an ideal inter-burst UL-FEC code in the upper link or application layers (burst size is 2 Mb). The

channel model employed is the typical urban 6-tap TU6 channel model for 10 Hz Doppler (18 km/h at 600 MHz). This channel model is representative for DVB-H vehicular reception [27], and it includes the time variant small-scale fluctuations of the received signal due to receiver mobility (i.e., fast fading). The shadowing component is modeled adding to the mean SNR of every burst an uncorrelated lognormal component with 5.5 dB standard deviation.

In the figure, we can see that the laboratory DVB-H measurement results resemble to some extent the theoretical results (the maximum difference is about 1 dB). The differences are due to the fact that fast fading is not completely eliminated at the DVB-H physical layer because there is no time interleaver [27]. Hence, the inter-burst UL-FEC code copes not only with completely erroneous bursts due to shadowing, but also with partial received bursts due to fast fading [31]. As a consequence, some parity data is employed to repair partially received bursts, reducing the protection against shadowing.

However, inter-burst UL-FEC in DVB-H also reduces the fading margin required to cope with fast fading, and this reduction can even exceed the potential reduction of the fading margin due to shadowing. This occurs for high code rates, where the percentage of completely lost bursts that can be

recovered is rather small (e.g., for a code rate 7/8 only one out of eight bursts can be repaired if the remaining seven bursts are received without errors), and when the shadowing correlation between consecutive bursts is high. On the other side, for robust code rates such as 1/2, the potential reduction of the fading margin of only due to shadowing inter-burst UL-FEC is higher than the fading margin reduction obtained in DVB-H due to both fast fading and shadowing. The difference is larger for shorter interleaving depths, as the influence of receiving partially a burst is more significant.

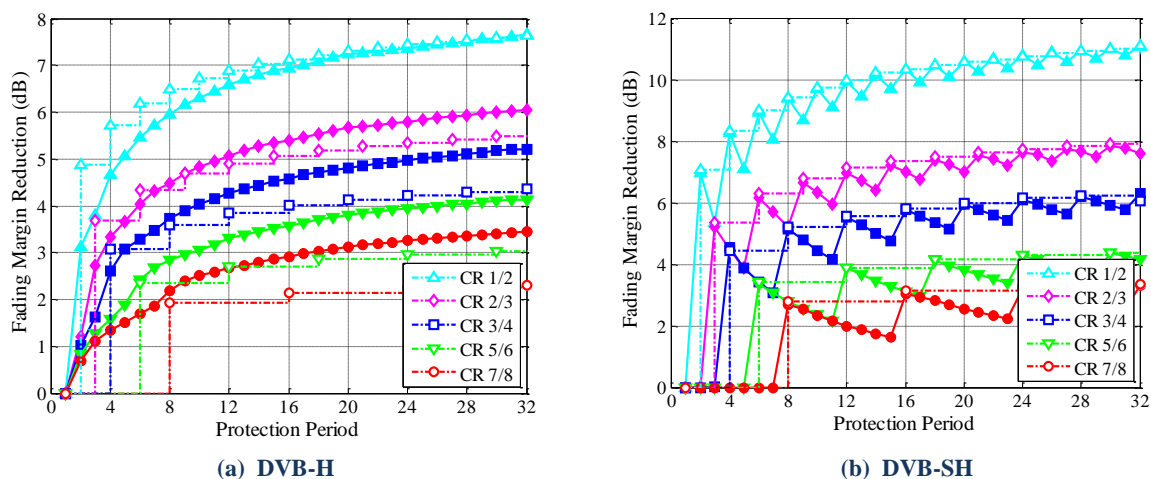


Figure 72: Fading margin reduction for 95% service availability vs. Protection period in bursts units. Uncorrelated shadowing; $d_{corr} = 0$ m.

3.3.4.2 DVB-SH Results

Figure 72(b) compares the theoretical fading margin results shown in Figure 70 for uncorrelated shadowing (dashed lines) with laboratory measurement results for DVB-SH (solid lines). The DVB-SH transmission mode employed in the measurements is: FFT size 2K, guard interval 1/4, modulation QPSK, code rate 1/3, and for a time interleaving depth of 210 ms at the physical layer (short uniform time interleaving profile), and MPE-iFEC with sliding Reed-Solomon encoding at the link layer (burst size is 2 Mb). The channel model employed is TU6 channel model for 40 Hz Doppler with uncorrelated shadowing with standard deviation 8 dB. In the figure, we can see that the laboratory DVB-SH measurement results coincide with the theoretical results. The reason is that the assumption that the fast fading is completely eliminated at the physical layer holds for DVB-SH. In the figure, we can also see that there are values for the protection period where the fading margin reduction is maximized. The reason is that the percentage of bursts that can be

recovered is maximum (and equal to the proportion of parity data transmitted) for values of the protection period that are multiple of n , being k/n the code rate.

3.3.4.3 DVB-T2 Results

It has been investigated the use of time diversity in DVB-T2 by means of computer simulations. Table 18 shows the simulation parameters. We have selected the BB FER (Baseband Frame Error Rate) 1% as quality of service (QoS) criterion at the physical layer, whereas we have selected the IP PER (IP Packet Error Rate)

Table 18: Simulation Parameters

System Parameters	Value
Bandwidth	8 MHz
FFT mode	8K
Guard interval	1/4
Input mode	B
FEC word length	16200
Code rate	1/2
Channel estimation	Perfect
QAM demapping	Optimum soft maximum a posteriori (MAP)
Channel model	TU6 SFN TU6 TU6 + shadowing
QoS criterion	BB FER 1%

1% in the case of UL-FEC. Bit error ratios (BER) were used to evaluate the system performance in the standardization process of DVB-T2. More specifically, the QoS criterion followed was a BER of 10^{-7} after LDPC (Low Density Parity Check) decoding [16]. However, BER criterions only indicate the percentage of erroneous bits and are not a proper indicator of the QoS seen by upper layers.

In order to investigate the influence of shadowing, we have assumed a user moving at constant velocity across a log-normal carrier-to-noise (CNR) map with mean of 0 dB defined by its standard deviation σ and correlation distance d_{corr} . The user velocity is given by the Doppler frequency f_d and the carrier frequency f_{rf} . In the simulations we have used Doppler frequencies of 10 Hz and 80 Hz with a carrier frequency of 600 MHz, which correspond to user velocities of 18 km/h and 144 km/h respectively. The shadowing model outputs CNR values that are used in the TU6 simulations as the average CNR over time. This way it is possible to combine the presence of fast fading and shadowing in the received signal.

In Figure 73 we show the performance of DVB-T2 when UL-FEC is used to provide long time interleaving. In particular, we have consider the protection of IP packets by means of MPE-iFEC. We have used this as an example of how UL-FEC protection could be implemented in DVB-T2 in order to validate the performance of the system. For the simulations we have used a configuration of 16QAM, code rate 1/2 and maximum sub-slicing.

From the figures we can see that in this case the gain depends not only on the interleaving duration but also on the code rate used for UL-FEC. According to the results, similar gains than those achieved at the physical layer can be obtained with an UL-FEC code rate of 1/2. It must be noted that the use of code rate 1/2 for UL-FEC with 16QAM and code rate 1/2 at the physical layer results in an spectral efficiency of 1 bit per cell (bpc). This is similar to the spectral efficiency obtained with QPSK and code rate 1/2 at the physical layer without UL-FEC protection. For example, with 10 seconds of interleaving, a configuration of 16QAM and

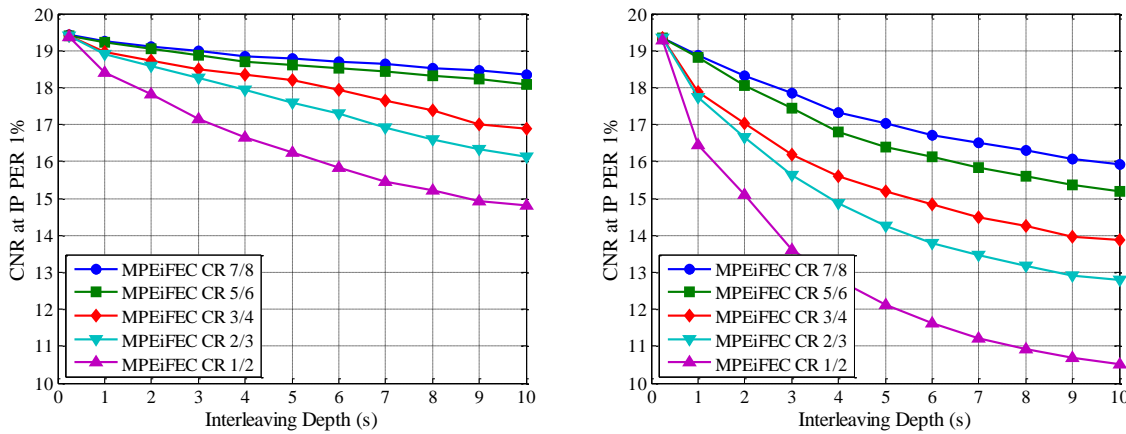


Figure 73: CNR at IP FER 1% for different configurations of MPEiFEC. DVB-T2 physical layer with 16QAM, code rate 1/2 and maximum sub-slicing. Reception scenario with $d_{corr} = 20m$, $\sigma = 5.5$ dB, $f_d = 10$ Hz (left) and $f_d = 80$ Hz (right).

code rate 1/2 at the physical layer with UL-FEC code rate 1/2 can achieve reception at IP PER 1% with 10.5 dB of CNR. A configuration of QPSK and code rate 1/2 at the physical layer without UL-FEC requires approximately 14.5 dB of CNR.

On the contrary, UL-FEC may not provide any gain for the same spectral efficiency in low diversity scenarios. If we perform the same comparison as before, we can see that in the case of 10 Hz of Doppler, the configuration with UL-FEC requires approximately 15 dB of CNR, which is 0.5 dB higher than the case with no UL-FEC.

3.3.5 Discussion file download services

File download services consist on the delivery of a finite amount of data that is stored into the terminals as a file. Typically, an error-free reception of the files is required, as even a single bit error can corrupt the whole file and make it useless for the receiver. Hence, file delivery in a generic timesliced mobile broadcast system without inter-burst UL-FEC implies that all bursts where the file is partitioned must be correctly received. Large files spanning several bursts are thus more difficult to deliver, as it is more likely to lose at least one burst.

In the following, we extend the theoretical framework to file download services for the case of uncorrelated shadowing. Interested readers are also referred to [39]. Assuming that each burst experiences uncorrelated shadowing, the probability of successfully receiving the file, denoted as *file acquisition probability*, F_{acq} , can be computed as:

$$F_{acq} = P_{F_s}(0) = g^{F_s} \quad (17)$$

where g is the coverage probability and F_s is the file size in number of bursts. We can see that the acquisition probability decreases exponentially with the file size. In lossy environments the complete file may not be fully received by most users during the initial file transmission, since some bursts may be lost. In these cases one common approach is to repeatedly transmit the file in a carousel.

If the file is transmitted n times, the file acquisition probability becomes:

$$F_{acq} = (1 - b^n)^{F_s} \quad (18)$$

where b is the outage probability. The problem of transmitting the file in a carousel with repetitions is that users may receive duplicate packets which are useless. If a user misses a single packet, he must wait until that specific packet is retransmitted and correctly received, discarding in the meantime packets already received.

In contrast, with inter-burst UL-FEC if a single FEC code word is applied over the entire file all source and repair packets are useful. It makes no difference which packets are received and terminals never receive duplicate data. The file acquisition probability can be computed as:

$$F_{acq} = \sum_{i=0}^{PP-F_s} P_{PP}(i) \tag{19}$$

where $PP = F_s/CR$ the total number of source and repair bursts transmitted.

Figure 74 shows the file acquisition probability as a function of the coverage probability for different file sizes for several delivery cases. In particular, it is shown the reference case without inter-burst UL-FEC and without retransmissions, the case with one file retransmission, and the case with interburst UL-FEC with 1/2 code rate.

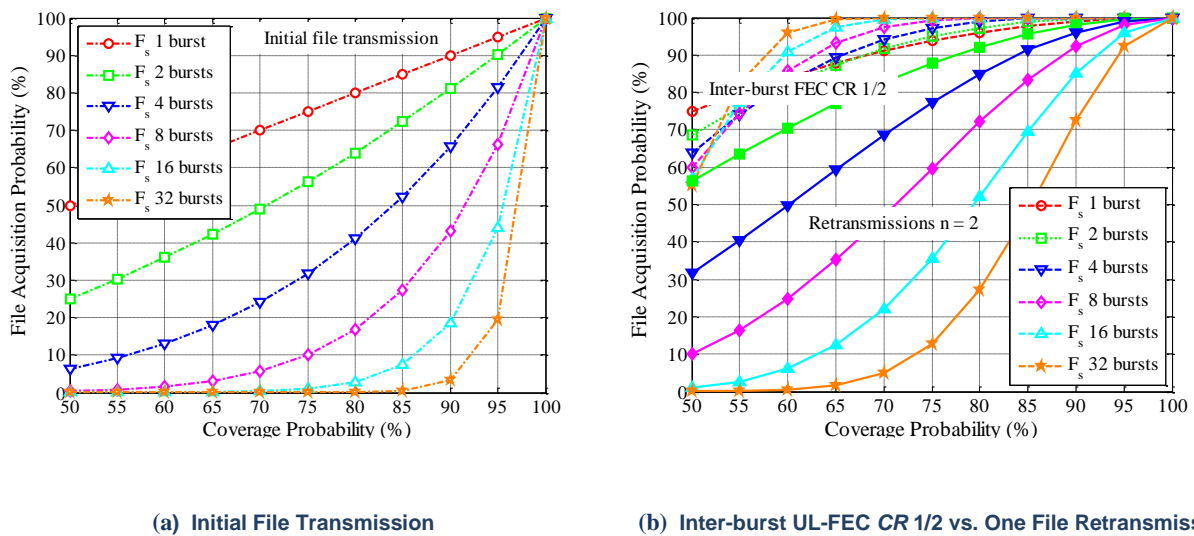


Figure 74: File acquisition probability vs. Coverage probability. File size in bursts units.

In Figure 74(a) we can see that without inter-burst UL-FEC and without repetitions an efficient file delivery is only possible within the service area where the coverage probability is close to one. Hence, for this delivery case larger fading margins are required than for conventional streaming services.

When retransmitting the file once, the acquisition probability increases, see Figure 74(b). However, the performance is still poor for large file sizes and/or for not so high coverage probabilities. Compared to retransmissions, inter-burst UL-FEC results in a much more efficient delivery of files because all correctly received packets are useful to the receivers. The gain can be translated into a reduction of the transmission time, being possible to deliver more content (files) with the same bandwidth, or into a reduction of the required fading margin.

The effect of correlated shadowing when inter-burst UL-FEC is employed is the same as for streaming services, see 3.2.3. That is, the performance (acquisition probability) decreases when the correlation increases. File retransmissions also suffer a similar degradation. However, this is not true for the initial file transmission without inter-burst UL-FEC, as in this case the acquisition probability increases with the correlation towards the coverage probability.

3.3.6 Conclusions

In the previous sections it has analytically evaluated the potential reduction of the required fading margin to cope with shadowing that can be achieved with inter-burst UL-FEC in a generic time-sliced terrestrial mobile broadcast system. Results have been validated with DVB-H/SH laboratory measurements and DVB-T2 computer simulations. Inter-burst UL-FEC exploits the time diversity of the mobile channel to recover from temporary losses, increasing the service availability compared to the coverage probability. Hence, for a target service availability level, the required coverage probability is reduced, which yields a lower shadowing fading margin. The gain increases for more robust code rates, for longer interleaving and for more demanding service availabilities, and it is directly proportional to the shadowing standard deviation. The potential gain is very significant even for short interleaving depths for robust code rates such as $1/2$ or $2/3$. But the gain depends on the statistical correlation of the shadowing between consecutive bursts. The lower the correlation, the higher the gain. For a given scenario and transmission configuration, the gain depends on the user velocity. Inter-burst UL-FEC is thus especially suited for vehicular users due to their high speeds, whereas lower gains can be expected for pedestrian users due to their reduced mobility. In any case, very important gains are feasible for background services where a relatively large latency is not an issue, as it is possible to encode large amounts of bursts jointly, or to reduce the correlation level between reception conditions of consecutive bursts by increasing the cycle time between bursts. File download services fall in this category of services, and they can in general fully exploit the benefits of interburst UL-FEC. On the other hand, for streaming services it is necessary to establish an adequate trade-off between the protection provided by inter-burst UL-FEC and the latency introduced in the system, as it may compromise the user experience.

4 REFERENCES

- [1] DVB Commercial Module sub-group on Next Generation Handheld, "Commercial Requirements for DVB-NGH," CM-1062R2, June 2009.
- [2] DVB Technical Module sub-ground on Next Generation Handheld, "NGH Study Mission Report," TM-H 411, June 2008.
- [3] C. Bormann, *et al.*, "RObust Header Compression (ROHC): Framework and Four Profiles: RTP, UDP, ESP, and Uncompressed," IETF RFC 3095, July 2001.
- [4] H. Schwarz, D. Marpe, and T. Wiegand, "Overview of the Scalable Video Coding Extension of the H.264/AVC Standard," *IEEE Trans. Circuits and Systems for Video Technology*, vol. 17, no. 9, pp. 1103-1120, Sept. 2007.
- [5] C. Hellge, E. Guinea, David Gómez-Barquero, T. Schierl, and T. Wiegand, "HDTV and 3DTV Services over DVB-T2 using Multiple PLPs with SVC and MVC," *Proc. IEEE Broadcast Symposium*, Alexandria, USA, 2012.
- [6] ETSI EN 302 755 v.1.3.1, "Frame Structure Channel Coding and Modulation for a Second Generation Digital Terrestrial Television Broadcasting System (DVB-T2)," Nov. 2011.
- [7] ETSI EN 303 105 v.1.1.1, "Digital Video Broadcasting (DVB); Next Generation Broadcasting System to Handheld, Physical Layer Specification (DVB-NGH)," in press.
- [8] EN 302 755 v1.3.1, "Frame Structure Channel Coding and Modulation for a Second Generation Digital Terrestrial Television Broadcasting System (DVB-T2)," Nov. 2011.
- [9] ETSI TS 102 992 v1.1.1, "Structure and Modulation of Optional Transmitter Signatures (T2-TX-SIG) for use with the DVB-T2," Sept. 2010.
- [10] C.R. Nokes and O.P. Haffenden, "DVB-T2 Receiver Buffer Model (RBM): Theory & Practice," *BBC White Paper*, July 2012.
- [11] ETSI TS 102 606 v1.1.1 "Digital Video Broadcasting (DVB): Generic Stream Encapsulation (GSE) Protocol European" October 2007
- [12] IETF RFC 768 "User Datagram Protocol", J. Postel, August 1980; URL:<http://www.ietf.org/rfc/rfc768.txt>
- [13] IETF RFC 4815 "RObust Header Compression (ROHC): Corrections and Clarifications to RFC 3095", L-E. Jonsson *et al.*, February 2007; URL: <http://www.ietf.org/rfc/rfc4815.txt>
- [14] TM-NGH 352 "Header compression - new results", DVB TM-H System and Upper Layers, August, 2010;
- [15] TM-NGH 382 "Analysis of IP header compression proposals", DVB TM-H System and Upper Layers, August 2010
- [16] ISO/IEC 13818-1 "Information Technology - Generic coding of moving pictures and associated audio information: Systems," International Organization for Standardization, Geneva, Switzerland, 2007
- [17] ETSI TR 102 831 v1.2.1, "Implementation Guidelines for a Second Generation Digital Terrestrial Television Broadcasting System (DVB-T2)," 2012.
- [18] G. Liebl, *et al.*, "Study of the Performance Of Scalable Video Coding Over a DVB-SH Satellite Link," *Proc. IEEE ICME 2010*, Singapore, 2010.
- [19] D. Gómez-Barquero, K. Nybom, D. Vukobratović, and V. Stanković, "Scalable Video Coding over Mobile Broadcasting DVB Systems", in *IEEE International Conference on Multimedia & Expo (ICME2010)*, Singapore, July, 2010.
- [20] D. Sejdinović, D. Vukobratović, A. Doufexi, V. Senk, and R. Piechocki. "Expanding Window Fountain Codes for Unequal Error Protection", *IEEE Trans. on Communications*, 57(9):2510-2516, September 2009.
- [21] D. Vukobratović, V. Stanković, D. Sejdinović, L. (Fagoonee) Stanković, and Z. Xiong. "Scalable Video Multicast Using Expanding Window Fountain Codes", *IEEE Trans. on Multimedia*, 11(6):1094-1104, October 2009.
- [22] J. Björkqvist, K. Nybom, J. Rinne, and A. Hazmi, "Performance Evaluation of a DVB-T2 System Using a New Time-Variant FIR-Channel," *Proc. SDR'11 Technical Conference and Product Exposition*, 2011.

- [22] G. Faria, J. A. Henriksson, E. Stare, and P. Talmola, "DVB-H: Digital Broadcast Services to Handheld Devices," *Proc. of the IEEE*, vol. 94, no. 1, Jan. 2006, pp. 194-209.
- [23] K. Nybom, S. Grönroos, and J. Björkqvist, "Expanding Window Fountain Coded Scalable Video in Broadcasting", in *IEEE International Conference on Multimedia & Expo (ICME2010)*, Singapore, July, 2010.
- [24] K. Nybom and D. Vukobratović. "Receiver-Controlled Fountain Coding for Layered Source Transmission over Parallel Broadcast Channels", in *COST 2100*, Bologna, Italy, November 2010.
- [25] M. Luby. "LT Codes", in *Proc. 43rd Annual IEEE Symposium on Foundations of Computer Science*, pages 271-280, 2002.
- [26] S. R. Saunders, "Antennas and Propagation for Wireless Communication Systems," Wiley, 2003.
- [27] P. Kelley and C. Rigal, "DVB-SH – Mobile Digital TV in S band," *EBU Technical Review*, July 2007.
- [28] A. Shokrollahi, "Raptor Codes," *IEEE Trans. on Information Theory*, vol. 52, no. 6, pp. 2251-2567, June 2006.
- [29] B. Sayadi, Y. Leprovost, S. Kerboeuf, M. L. Alberi-Morel, and L. Roullet, "MPE-IFEC: An Enhanced Burst Error Protection for DVB-SH Systems," *Bell Labs Techn. J.*, vol. 14, no. 1, pp. 25-40, May 2009.
- [30] D. Gómez-Barquero, D. Gozávez, and N. Cardona, "Application Layer FEC for Mobile TV Delivery in IP Datacast over DVB-H Systems," *IEEE Trans. on Broadcasting*, vol. 55, no. 2, pp. 396-406, June 2009.
- [31] Harald Fuchs and N. Färber, "Optimizing channel change time in IPTV applications," *Proc. IEEE Broadband Multimedia Systems and Broadcasting*, Las Vegas, USA, 2008.
- [32] L. Roullet, D. Gómez-Barquero, C. Hellge, L. Ottavj, and T. Stockhammer, "Digital Video Broadcasting (DVB); Upper Layer Forward Error Correction in DVB," *ETSI TR 102 993*, DVB bluebook A148, March 2010.
- [33] J.-J. Delmas and P. Bretilon, "Mobile Broadcast Technologies – Link Budgets," *BMCO forum white paper*, Feb. 2009.
- [34] M. Gudmunson, "Correlation Model for Shadow Fading in Mobile Radio Systems," *Electronic Letters*, vol. 37, no. 23, pp. 2145-2146, Nov. 1991.
- [35] D. Gómez-Barquero, P. Unger, T. Kürner, and N. Cardona, "Coverage Estimation for Multiburst FEC Mobile TV Services in DVB-H Systems," *IEEE Trans. on Vehicular Technology*, vol. 59, no. 7, pp. 3491-3500, Sept. 2010.
- [36] E. N. Gilbert, "Capacity of a Burst-Noise Channel," *Bell System Technical Journal*, vol. 39, pp. 1253-1265, Sept. 1960.
- [37] E. O. Elliott, "Estimates of Error Rates for Codes on Burst-Noise Channels," *Bell System Technical Journal*, vol. 42, pp. 1977-1997, Sept. 1963.
- [38] L. R. Wilhelmsson, "Evaluating the Performance of Raptor Codes for DVB-H by using the Gilbert-Elliott Channel," *Proc. IEEE VTC Fall*, Baltimore, USA, 2007.
- [39] L. R. Wilhelmsson and L. B. Milstein, "On the Effect of Imperfect Interleaving for the Gilbert-Elliott Channel," *IEEE Trans. on Communications*, vol. 47, no. 5, pp. 681-688, May 1999.